

WCAP-8775

HEAVY SECTION STEEL TECHNOLOGY PROGRAM
TECHNICAL REPORT NO. 41

THE IRRADIATED DYNAMIC FRACTURE TOUGHNESS
OF ASTM A533, GRADE B, CLASS 1 STEEL
PLATE AND SUBMERGED ARC WELDMENT

Westinghouse Nuclear Energy Systems



WESTINGHOUSE CLASS 3

ORNL/SUB/3720-1
DIST. CATEGORY NRC-5

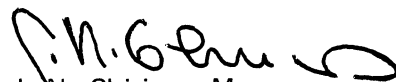
HEAVY SECTION STEEL TECHNOLOGY PROGRAM
TECHNICAL REPORT NO. 41

THE IRRADIATED DYNAMIC FRACTURE TOUGHNESS
OF ASTM A533, GRADE B, CLASS 1 STEEL
PLATE AND SUBMERGED ARC WELDMENT

J. A. Davidson
L. J. Ceschini
R. P. Shogan
G. V. Rao

October 1976

APPROVED:



J. N. Chirigos, Manager
Structural Materials Engineering

APPROVED:



A. G. Opitz
Project Engineer HSST Program
Development Contracts

Research performed under Subcontract No. 3720 for the Oak Ridge National Laboratory, operated by Union Carbide Corporation for the Energy Research and Development Administration.

This work funded by U.S. Nuclear Regulatory Commission under Interagency Agreements 40-551-75 and 40-552-75.

WESTINGHOUSE ELECTRIC CORPORATION
Nuclear Energy Systems
P. O. Box 355
Pittsburgh, Pennsylvania 15230

LEGAL NOTICE

This report was prepared as an account of Government sponsored work. Neither the United States, nor the Commission, nor any person acting on behalf of the Commission:

- A. Makes any warranty or representation, expressed or implied, with respect to the accuracy, completeness, or usefulness of the information contained in this report, or that the use of any information, apparatus, method, or process disclosed in this report may not infringe privately owned rights; or
- B. Assumes any liabilities with respect to the use, or for damages resulting from the use of any information, apparatus, method, or process disclosed in this report.

As used in the above, "Person acting on behalf of the Commission" includes any employee or contractor of the Commission, or employee of such contractor, to the extent that such employee or contractor of the Commission, or employee of such contractor prepares, disseminates, or provides access to, any information pursuant to his employment or contract with the Commission, or his employment with such contractor.

ABSTRACT

As a result of the Heavy Section Steel Technology Program (HSST), sponsored by the Nuclear Regulatory Commission, Westinghouse Electric Corporation conducted dynamic fracture toughness tests on irradiated HSST Plate 02 and submerged arc weldment material.

Testing performed at the Westinghouse Research and Development Laboratory in Pittsburgh, Pennsylvania, included 0.394T compact tension, 1.9T compact tension, and 4T compact tension specimens. Testing temperatures ranged from lower to upper fracture toughness shelf temperatures. Results were analyzed using the equivalent energy method, and test results were compared with unirradiated small and large specimen results.

This data showed that, in the transition region, dynamic test procedures resulted in lower (compared to static) fracture toughness results, and that weak direction (WR) oriented specimen data were lower than the strong direction (RW) oriented specimen results.

Irradiated lower-bound fracture toughness results of the HSST Program material were well above the adjusted ASME Section III K_{IR} curve. Large-thickness specimen test results showed that the irradiated fracture toughness shelf exceeded $220 \text{ MNm}^{-3/2}$ ($210 \text{ ksi } \sqrt{\text{in.}}$) for both plate and weldment material. The extent of irradiation for specimens tested in the program ranged from 2.5 to $4.5 \times 10^{19} \text{ n/cm}^2$ ($E > 1 \text{ Mev}$).

Westinghouse PWR Instrument Systems Development Group acoustically monitored an irradiated and a nonirradiated 4T-CT specimen during a fracture toughness test as a preliminary study to determine the effect of irradiation on the acoustic emission-stress intensity factor relationships in pressure vessel grade steel. The tests were performed at the Hanford Engineering Development Laboratory in Richland, Washington, under the HSST Program.

The results indicated higher levels of acoustic emission activity from the irradiated sample as compared to the unirradiated one at a given stress intensity factor (K) level. Also, the total acoustic emission counts (N) varied approximately as $K^{3.5}$ in the irradiated material while the emission from the nonirradiated one approximately follows the relationship $N \propto K^{7.3}$, indicating a shift in the mechanism of acoustic generation during the deformation of unirradiated and radiation embrittled microstructures.

ACKNOWLEDGMENTS

The work of the following authors, contributors and editors is hereby acknowledged.

WESTINGHOUSE RESEARCH AND DEVELOPMENT LAB

Materials Evaluation and Application — D. M. Moon

Materials Testing and Evaluation — W. T. Broush

Mechanics Department

W. K. Wilson

W. A. Logsdon

J. D. Landes

J. A. Begley

Reactor Core Material Group — J. R. Holland

WESTINGHOUSE PRESSURIZED WATER REACTORS DIVISION

Structural Materials Engineering

L. R. Singer

W. H. Bamford

J. N. Chirigos

S. E. Yanichko

T. R. Mager

Development Programs

A. G. Opitz

Instrument Systems Development

J. Craig

OAK RIDGE NATIONAL LABORATORY

G. D. Whitman

LIST OF RELATED REPORTS

This report is designated Heavy-Section Steel Technology Program Technical Report No. 41. Prior reports in this series are listed below.

1. S. Yukawa, "Evaluation of Periodic Proof Testing and Warm Prestressing Procedures for Nuclear Reactor Vessels," HSSTP-TR-1, General Electric Company, Schenectady, New York, July 1, 1969.
2. L. W. Loechel, "The Effect of Testing Variables on the Transition Temperature in Steel," MCR-69-189, Martin Marietta Corporation, Denver, Colorado, November 20, 1969.
3. P. N. Randall, "Gross Strain Measure of Fracture Toughness of Steels," HSSTP-TR-3, TRW Systems Group, Redondo Beach, California, November 1, 1969.
4. C. Visser, S. E. Gabrielse, and W. VanBuren, "A Two-Dimensional Elastic-Plastic Analysis of Fracture Test Specimens," WCAP-7368, October 1969.
5. T. R. Mager, F. O. Thomas, and W. S. Hazelton, "Evaluation by Linear Elastic Fracture Mechanics of Radiation Damage to Pressure Vessel Steels," WCAP-7328, Revised, October 1969.
6. W. O. Shabbits, W. H. Pryle, and E. T. Wessel, "Heavy Section Fracture Toughness Properties of A533 Grade B Class 1 Steel Plate and Submerged Arc Weldment, WCAP-7414, December 1969.
7. F. J. Loss, "Dynamic Tear Test Investigations of the Fracture Toughness of Thick-Section Steel," NRL Report 7056, U. S. Naval Research Laboratory, Washington, D.C., May 14, 1970.
8. P. B. Crosley and E. J. Ripling, "Crack Arrest Fracture Toughness of A533 Grade B Class 1 Pressure Vessel Steel," HSSTP-TR-8, Materials Research Laboratory, Inc., Glenwood, Illinois, March 1970.
9. T. R. Mager, "Post-Irradiation Testing of 2 T Compact Tension Specimens," WCAP-7561, August 1970.

10. T. R. Mager, "Fracture Toughness Characterization Study of A533, Grade B, Class 1 Steel," October 1970.
11. T. R. Mager, "Notch Preparation in Compact Tension Specimens," WCAP-7579, November 1970.
12. N. Levy and P. V. Marcal, "Three-Dimensional Elastic-Plastic Stress and Strain Analysis for Fracture Mechanics, Phase I: Simple Flawed Specimens," HSSTP-TR-12, Brown University, Providence, Rhode Island, September 1970.
13. W. O. Shabbits, "Dynamic Fracture Toughness Properties of Heavy Section A533 Grade B, Class 1 Steel Plate," WCAP-7623, December 1970.
14. P. N. Randall, "Gross Strain Crack Tolerance of A533-B Steel," HSSTP-TR-14, TRW Systems Group, Redondo Beach, California, May 1, 1971.
15. H. T. Corten and R. H. Sailors, "Relationships Between Material Fracture Toughness Using Fracture Mechanics and Transition Temperature Tests," T&AM Report No. 346, University of Illinois, Urbana, Illinois, August 1, 1971.
16. T. R. Mager and V. J. McLoughlin, "The Effect of an Environment of High Temperature Primary Grade Nuclear Reactor Water on the Fatigue Crack Growth Characteristics of A533 Grade B Class 1 Plate and Weldment Material," WCAP-7776, October 1971.
17. N. Levy and P. V. Marcal, "Three-Dimensional Elastic-Plastic Stress and Strain Analysis for Fracture Mechanics, Phase II: Improved Modeling," HSSTP-TR-17, Brown University, Providence, Rhode Island, November 1971.
18. S. C. Grigory, "Tests of Six-Inch-Thick Flawed Tensile Specimens, First Technical Summary Report, Longitudinal Specimens Numbers 1 through 7, HSSTP-TR-18, Southwest Research Institute, San Antonio, Texas, June 1972.
19. P. N. Randall, "Effects of Strain Gradients on the Gross Strain Crack Tolerance of A533-B Steel," HSSTP-TR-19, TRW Systems Group, Redondo Beach, California, June 1972.
20. S. C. Grigory, "Tests of Six-Inch-Thick Flawed Tensile Specimens, Second Technical Summary Report, Transverse Specimens Numbers 8 through 10, Welded Specimens Numbers 11 through 13," HSSTP-TR-20, Southwest Research Institute, San Antonio, Texas, June 1972.
21. Lee A. James and John A. Williams, "Heavy Section Steel Technology Program Technical Report No. 21, The Effect of Temperature and Neutron Irradiation Upon the Fatigue-Crack Propagation Behavior of ASTM A533, Grade B, Class 1 Steel," HEDL-TME 72-132, September 1972.

22. S. C. Grigory, "Tests of Six-Inch-Thick Flawed Tensile Specimens, Third Technical Summary Report, Longitudinal Specimens Numbers 14 through 16, Unflawed Specimen Number 17," HSSTP-TR-22, Southwest Research Institute, San Antonio, Texas, October 1972.
23. S. C. Grigory, "Tests of Six-Inch-Thick Tensile Specimens, Fourth Technical Summary Report, Tests of One-Inch-Thick Flawed Tensile Specimens for Size Effect Evaluation," HSSTP-TR-23, Southwest Research Institute, San Antonio, Texas, June 1973.
24. S. P. Ying and S. C. Grigory, "Tests of Six-Inch-Thick Tensile Specimens, Fifth Technical Summary Report, Acoustic Emission Monitoring of One-Inch and Six-Inch-Thick Tensile Specimens," HSSTP-TR-24, Southwest Research Institute, San Antonio, Texas, November 1972.
25. R. W. Derby, et al., "Test of 6-Inch-Thick Pressure Vessels, Series 1: Intermediate Test Vessels V-1 and V-2," ORNL-4895, February 1974.
26. W. J. Stelzman and R. G. Berggren, "Radiation Strengthening and Embrittlement in Heavy Section Plates and Welds," ORNL-4871, June 1973.
27. P. B. Crosley and E. J. Ripling, "Crack Arrest in an Increasing K-Field," HSSTP-TR-27, Materials Research Laboratory, Glenwood, Illinois, January 1973.
28. P. V. Marcal, P. M. Stuart and R. S. Bettles, "Elastic-Plastic Behavior of a Longitudinal Semi-Elliptic Crack in a Thick Pressure Vessel," HSSTP-TR-28 Brown University, Providence, Rhode Island, June 1973.
29. W. J. Stelzman, Characterization of HSST Plate 02 (To be published as HSSTP-TR-29).
30. D. A. Canonico, Characterization of Heavy Section Weldments in Pressure Vessel Steels (To be published as HSSTP-TR-30).
31. J. A. Williams, "The Irradiation and Temperature Dependence of Tensile and Fracture Properties of ASTM A533, Grade B, Class 1 Steel Plate and Weldment," HEDL-TME 73-75, August 1973.
32. J. M. Steichen and J. A. Williams, "High Strain Rate Tensile Properties of Irradiated ASTM A533 Grade B Class 1 Pressure Vessel Steel," HEDL-TME-73-74, July 1973.
33. P. C. Ricardella and J. L. Swedlow, "A Combined Analytical-Experimental Fracture Study of the Two Leading Theories of Elastic Plastic Fracture J-Integral and Equivalent Energy," WCAP-8224, October 1973.

34. R. J. Podlasek and R. J. Eiber, "Final Report on Investigation of Mode III Crack Extension in Reactor Piping," HSSTP-TR-34 Battelle Columbus Laboratories, Columbus, Ohio, December 1973.
35. T. R. Mager et al., "The Effect of Low Frequencies on the Fatigue Crack Growth Characteristics of A533 Grade B Class 1 Plate in an Environment of High-Temperature Primary Grade Nuclear Reactor Water," WCAP-8256, December 1973.
36. J. A. Williams, "The Irradiated Fracture Toughness of ASTM A533, Grade B, Class 1 Steel Measured with a Four Inch Thick Compact Tension Specimen," HEDL-TME 75-10, January 1975.
37. R. H. Bryan et al., "Test of 6-Inch-Thick Pressure Vessels, Series 2: Intermediate Test Vessels V-3, V-4, and V-6," ORNL-5059, November 1975.
38. T. R. Mager, S. E. Yanichko, and L. R. Singer, "Fracture Toughness Characterization of HSST Intermediate Pressure Vessel Material," WCAP-8456, December 1974.
39. J. G. Merkle, G. D. Whitman, and R. H. Bryan, "An Evaluation of the HSST Program Intermediate Pressure Vessel Tests in Terms of Light-Water Reactor Pressure Vessel Safety," ORNL-TM-5090, November 1975.
40. J. G. Merkle et al., Test of 6-Inch-Thick Pressure Vessels. Series 3: Intermediate Test Vessel V-7, ORNL/NUREG-1, Oak Ridge National Laboratory, Oak Ridge, TN, August 1976.

TABLE OF CONTENTS

Section	Title	Page
1	BACKGROUND	1-1
2	MATERIAL AND SPECIMENS	2-1
	2-1. RW and Weld 58 4T-Compact Tension Specimens and Heat Treatment	2-1
	2-2. Irradiation Procedure	2-7
	2-3. Capsule Dosimetry	2-12
3	DYNAMIC FRACTURE TOUGHNESS TESTING	3-1
4	TESTING EQUIPMENT AND PROCEDURE	4-1
	4-1. Test Machine	4-1
	4-2. Test Machine Operating Procedure	4-3
	4-3. Specimen Loading System	4-3
	4-4. Load Cell	4-4
	4-5. Temperature Control	4-5
	4-6. LVDT (Linear Variable Differential Transformer) Extensometer	4-5
	4-7. Load Cell Calibration	4-5
	4-8. LVDT Calibration	4-6
5	EQUIVALENT ENERGY METHOD	5-1
	5-1. Analysis	5-2
	5-2. Compliance Consideration	5-4
	5-3. Cleavage Controlled Fracture and Valid K_{1d} Tests	5-8
6	TEST RESULTS	6-1
	6-1. Fracture Toughness Test Results	6-1
	6-2. 0394T-Compact Tension Specimens	6-1

TABLE OF CONTENTS (cont)

Section	Title	Page
	6-3. 1.9T-Compact Tension (RW) Specimens	6-1
	6-4. 4T-Compact Tension Specimen Dynamic Test Results	6-1
	6-5. Previous Static Test Result for Irradiated 4T-CT Specimen W58-4	6-8
6-6.	Dosimetry Results	6-8
	6-7. 0.394T-Compact Tension Specimens	6-8
	6-8. 1.9T-CT (RW) Specimens	6-8
	6-9. 4T-CT Specimens	6-13
	6-10. 4T-CT Specimen W58-4	6-13
7	DISCUSSION OF RESULTS	7-1
	7-1. Upper Shelf and Transition Temperature Evaluation of K_{1d}	7-1
	7-2. Upper Shelf Evaluation	7-1
	7-3. Transition Temperature Dynamic Toughness K_{1d}	7-3
	7-4. Regions in the K_{1d} Versus Temperature Curve	7-3
	7-5. 4T-CT W58-1 and Subcritical Crack Growth Evaluation	7-7
	7-6. Shift in Fracture Properties	7-7
	7-7. HSST Plate 02 (RW Orientation)	7-7
	7-8. HSST Plate 02 (WR Orientation)	7-14
	7-9. HSST Submerged Arc Weldment W58	7-14
8	ACOUSTIC MONITORING OF 4-INCH-THICK COMPACT TENSION FRACTURE MECHANICS SPECIMENS	8-1
	8-1. Background	8-1
	8-2. Instrumentation and Test Setup	8-2
	8-3. Test Results and Discussion	8-3
9	CONCLUSIONS	9-1

LIST OF ILLUSTRATIONS

Figure	Title	Page
2-1	Location and Weld-Up Orientation of the Material for the RW, WR, and Weldment 4T-CT Specimens and the 0.394T-CT Small-Thickness Specimens	2-2
2-2	Location and Orientation of the RW and Weldment 4T-CT Specimens and the WR, RW, and Weldment 0.394-CT Specimens	2-3
2-3	Location and Orientation of the Four 1.9T-CT Specimens Machined from the Broken Halves of 4T-CT Specimen W58-4	2-4
2-4	Typical Dimension Relationships for Compact Tension Specimens Used in the Irradiation Program	2-5
2-5	Effect of Stress-Relief Time on Charpy-V Impact Properties (RW Orientation) of HSST Plate 02 (ASTM A533, Grade B, Class 1)	2-8
2-6	Dynamic Irradiated and Unirradiated Fracture Toughness Properties for HSST Plate 02, RW Orientated Material	2-9
2-7	Static Irradiated and Unirradiated Fracture Toughness Properties for HSST Plate 02, RW Oriented Material	2-10
2-8	4T Specimen Capsule Geometry	2-13
2-9	4T-CT Capsule Designation and Dosimetry Location	2-14
2-10	BRR Core Configuration for 4T Irradiations	2-15
2-11	Variation Influence Received by the 4T-CT Specimens Located in the Three Test Capsules Based on the Dosimetry Results	2-16
3-1	Yield Strength of Irradiated ASTM A533 Grade B Class 1 Plate and Submerged Arc Weld	3-3
4-1	Diagram of the Dynamic Test Machine	4-2
5-1	Typical Load-Displacement Curve for A Compact Tension Specimen Tested at a Temperature at which Elastic-Plastic Fracture Toughness Values are Evaluated	5-3
5-2	Typical Displacement Measuring Assembly Attached to a Compact Tension Specimen	5-6
5-3	Measurement Point Compliance of a Typical Dynamic Load Displacement Curve for a Compact Tension Specimen Tested at Upper Shelf Temperatures	5-7
5-4	Adjustment of the Measurement Point Compliance Line to the Point Where Deviation from Linearity is Presumed to Occur	5-7

LIST OF ILLUSTRATIONS (cont)

Figure	Title	Page
5-5	Modified Load-Displacement Curve Employing the Measurement Point Compliance as the Linear Region of the Curve	5-9
5-6	Load-Deflection Traces Typical of Upper Shelf Temperatures for Dynamically Performed Fracture Toughness Tests	5-9
5-7	Load-Deflection Traces Typical of Shelf Initiation Temperatures for Dynamically Performed Fracture Toughness Tests	5-9
5-8	Variation of K_{Icd} as a Function of Temperature and Thickness	5-11
6-1	Immersed and Unimmersed Conditions of the HSST Irradiated 4T-CT Specimens as Received in The Shipping Cask at the Westinghouse R&D Hot Cell Facility	6-5
6-2	Close-up Photograph of the Fatigue Precrack Tip Area on the Side of the Ubroken Irradiated Weldment 4T-CT Specimen W58-1 Tested Dynamically at 74°C (165°F).	6-6
6-3	Three Fracture Areas of W58-1 4T-CT Weldment Specimen After Break at -18°C (0°F). S.E.M. Photographs Illustrate Fracture Areas Characteristic of: A, Fatigue Precracking; B, Fatigue Precracking; C, Cleavage Failure	6-7
7-1	Irradiated Dynamic Fracture Toughness Results For HSST Plate 02 (WR, RW) and Weldment 58-A Material Showing the Extent of Cleavage Controlled Fracture As a Function of Temperature and Specimen Size	7-2
7-2	Dynamic Irradiated and Unirradiated Fracture Toughness Properties for HSST Plate 02, RW Orientated Material	7-4
7-3	Dynamic Irradiated and Unirradiated Fracture Toughness Properties for HSST Plate 02, WR Oriented Material	7-8
7-4	Dynamic Irradiated and Unirradiated Fracture Toughness Properties for HSST Weldment W58-A	7-9
7-5	Irradiated and Unirradiated Charpy V-Notch Impact Curves for HSST Plate 02 and Submerged Arc Weldment W58-A	7-10
7-6	Static Irradiated and Unirradiated Fracture Toughness Properties for HSST Plate 02, RW Oriented Material	7-11
7-7	Static Irradiated and Unirradiated Fracture Toughness Properties for HSST Plate 02, WR Oriented Material	7-12
7-8	Static Irradiated and Unirradiated Fracture Toughness Properties for HSST Weldment W58-A	7-13

LIST OF ILLUSTRATIONS (Cont)

Figure	Title	Page
8-1	Acoustic Test Instrumentation	8-4
8-2	Acoustic Emission From Flaw Growth In Irradiated and Unirradiated 4T-CT Samples, Plotted as a Function of Stress Intensity Factor "K" (Linear Plot)	8-5
8-3	Acoustic Emission From Flaw Growth in Irradiated and Unirradiated 4T-CT Samples, Plotted as a Function of Stress Intensity Factor "K" (Logarithmic Plot)	8-6

LIST OF TABLES

Table	Title	Page
2-1	Composition of HSST Plate 02 and Submerged Arc Weldment W58-A	2-6
2-2	Heat Treatment of HSST Plate 02 and Submerged Arc Weldment W58-A	2-6
2-3	Summary of Total Stress Relief of the Fracture Toughness Specimens	2-11
2-4	Type and Designation of the 0.394T-CT Specimens Located in the Cans in the 4T-CT Specimen Pin Holes	2-11
2-5	Capsule Internal Dosimetry	2-17
5-1	Finite Element Displacements on the Crack Surface of Compact Tension Specimens ($H/W = 0.6$)	5-4
6-1	Irradiated Dynamic Fracture Toughness Data Results for the Small-Thickness Compact Tension Specimens	6-2
6-2	Irradiated Fracture Toughness Data for the 1.9- and 4T-Compact Tension Specimens	6-3
6-3	Dosimetry Results of Cs^{137}	6-9
6-4	Co^{60} Dosimetry Results of the Al-Co Dosimeter Wires	6-9
6-5	Mn^{54} Dosimetry Results of Fe Dosimeter Wires	6-10
6-6	Co^{58} Dosimetry Results of Ni Dosimeter Wires	6-11
6-7	Fast Neutron [$E > 1.0$ Mev] Fluence Levels Derived from the 1.9T-CT Drilling Activities	6-12
6-8	Fast Neutron [$E > 1.0$ Mev] Fluence Levels Derived from the 4T-CT Drilling Activities	6-14
6-9	Irradiation Fluence of 4T-CT (101.6mm) Specimen W58-4, Irradiated at $287.8^{\circ}C$ ($550^{\circ}F$)	6-15
7-1	Shifts in the Fracture Toughness and RT_{NDT} for the HSST Plate 02 and Weldment W58 Material Due to Irradiation	7-5
8-1	General Test Data for the Irradiated Acoustic Test	8-7

SECTION 1

BACKGROUND

In 1967, the United States Atomic Energy Commission^[1] initiated a program to evaluate the overall material characteristics and structural reliability of heavy section structures used in light-water reactor installations. This program was designated the Heavy Section Steel Technology (HSST) Program, and encompasses research and development activities in the areas of both material properties and fracture characterization.^[2]

This report deals solely with irradiation effects on the fracture toughness properties of the HSST plate and weldment material, in particular, HSST Plate 02. The material was irradiated at Battelle Columbus Laboratories Research Reactor, and dynamic fracture toughness testing was conducted at the Westinghouse Research and Development hot cell facility in Pittsburgh, Pennsylvania with the majority of irradiated specimens. One large thickness (4T-CT) specimen was tested statically^[3] at the Hanford Engineering Laboratory in Richland, Washington. Results of the irradiated dynamic tests are compared with the static test in this report.

-
1. Now called the United States Nuclear Regulatory Commission
 2. "Heavy Section Steel Technology Program Semi-Annual Progress Report for the Period Ending August 31, 1967" ORNL-4176, January 1968
 3. Williams, J. A., "The Irradiated Fracture Toughness of ASTM A533, Grade B, Class 1 Steel Measured with a Four Inch Thick Compact Tension Specimen," HSST Program Technical Report No. 36, HEDL-TME 75-10, June 1975.

HSSTP-TR-41

SECTION 2

MATERIAL AND SPECIMENS

Heavy Section Steel Technology Program (HSST) Plate 02 is a 304.8-mm-thick quenched and tempered ASTM A533, Grade B, Class 1 steel plate, 3048 x 6591 mm, purchased specifically by Oak Ridge National Laboratory (ORNL) for evaluation in the HSST Program.^[1] A record of the entire plate history including the fabrication, heat treatment, and inspection is documented by Childress.^[2] Tables 2-1 and 2-2 summarize the chemistry and heat treatment for the plate 02 and weldment material. Shown in figures 2-1^[2,3] through 2-3 are the regions of the plate which were used to fabricate the Charpy thickness (0.394-inch) and the six 4-inch-thick compact tension (CT) specimens which were later irradiated. The specimens were oriented in both the strong (RW) and weak (WR)^[4] directions and are shown in these figures. Figure 2-4^[5] shows the general dimensions for standard compact tension specimens as outlined by ASTM E-399, "Plane-Strain Fracture Toughness of Metallic Materials." Throughout the text of this report, the compact tension specimen thickness will be given in inches. The equivalent standard international units are the following:

0.394T-CT = 10-mm-thick CT
1.9T-CT = 48.26-mm-thick CT
4.0T-CT = 101.6-mm-thick CT

2-1. RW AND WELD 58 4T-COMPACT TENSION SPECIMENS AND HEAT TREATMENT

The HSST Plate 02, as shown in table 2-2, received 40 hours of stress relief. Figures 2-1 through 2-3 illustrate the location of the RW 4T-CT and all 0.394T-CT specimen material

-
1. "Heavy Section Steel Technology Program Semi-Annual Progress Report for the Period Ending August 31, 1967," ORNL-4176, January 1968
 2. Childress, C. E. "Fabrication History of the First Two 12-Inch-Thick ASTM A533 Grade B, Class 1 Steel Plates of the Heavy Section Technology Program, Documentary Report 1," ORNL-4313, Feb. 1969
 3. Whitman, G. D. "HSST Program Quarterly Progress Report on Reactor Safety Programs Sponsored by the NRC Division of Reactor Safety Research," for April-June 1975, Vol. II, ORNL-TM-5021, September 1975
 4. Tiffany, C. F., Masters, J. N., "Applied Fracture Mechanics," in *Fracture Toughness Testing and Its Applications*, ASTM STP 381, pp. 249-277, Am. Soc. Testing Materials, 1965
 5. "Standard Method of Test for Plane-Strain Fracture Toughness of Metallic Materials," ASTM-E399-74, Part 10, *Metals - Physical, Mechanical and Corrosion Testing*, pp. 432-451, Am. Soc. for Testing and Materials, 1974

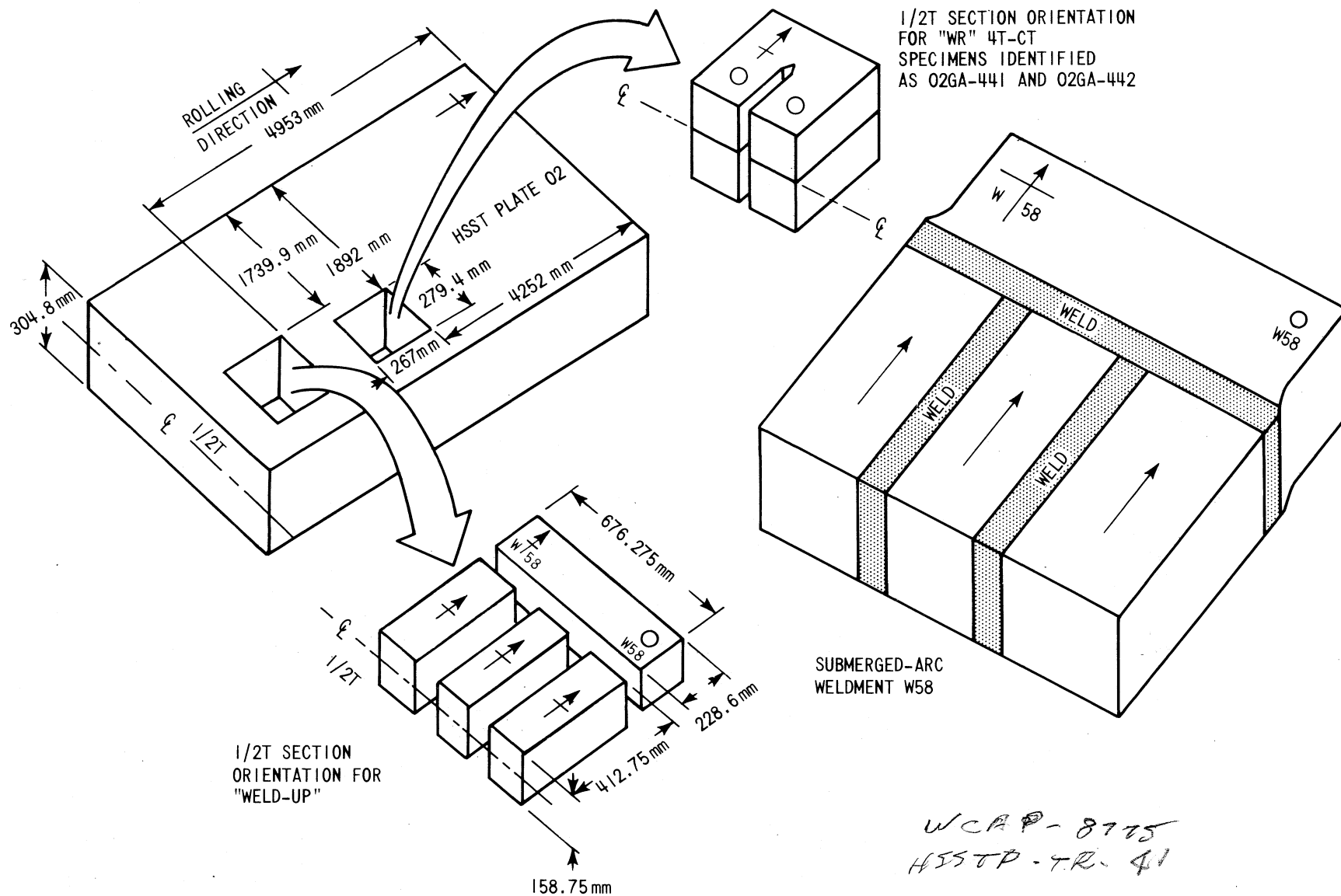


Figure 2-1. Location and Weld-Up Orientation of the Material for the RW, WR, and Weldment 4T-CT Specimens and the 0.394T-CT Small-Thickness Specimens

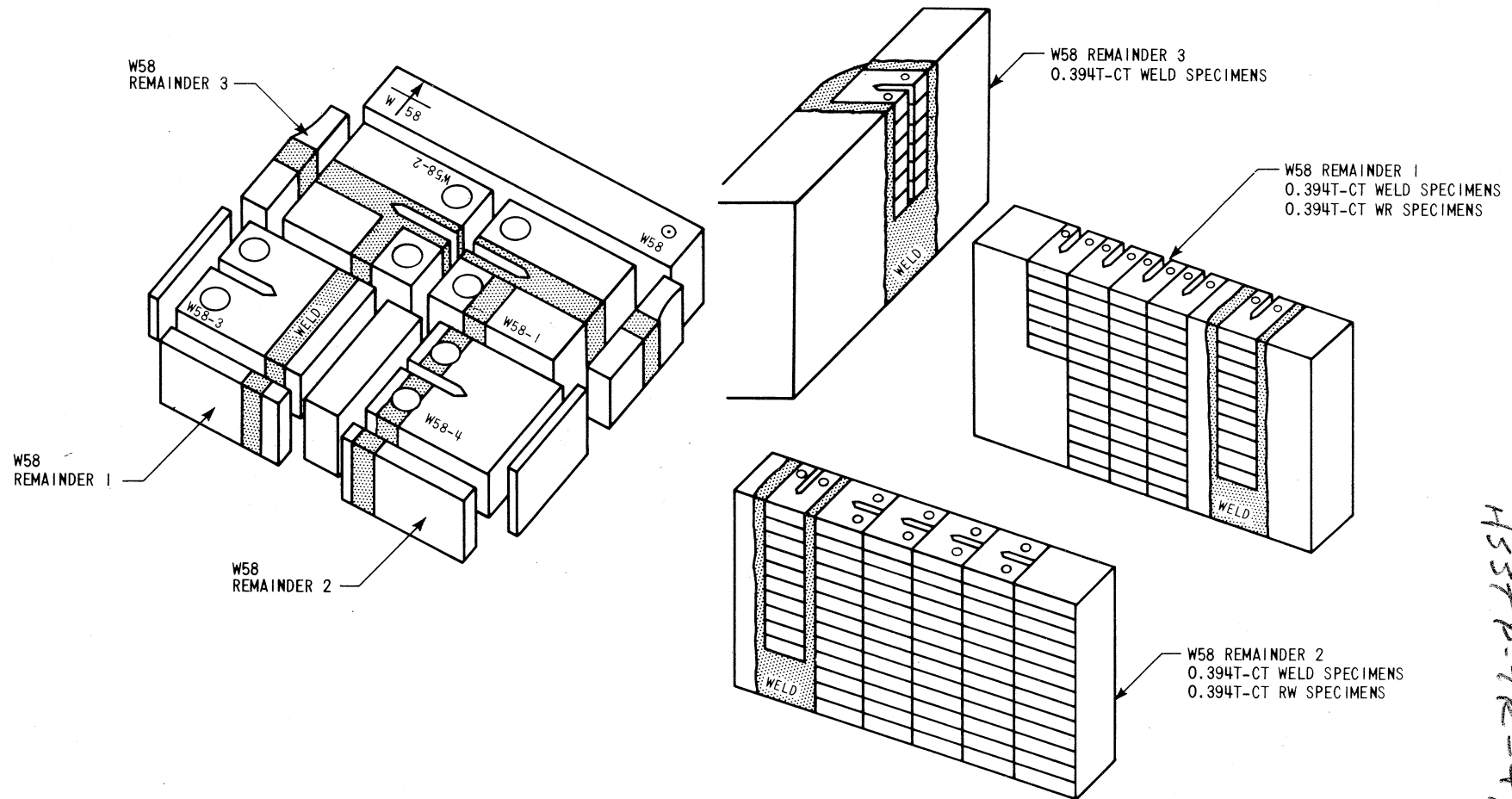


Figure 2-2. Location and Orientation of the RW and Weldment 4T-CT Specimens and the WR, RW, and Weldment 0.394T-CT Specimens.

WCAP 8775
H55TP-TR-41

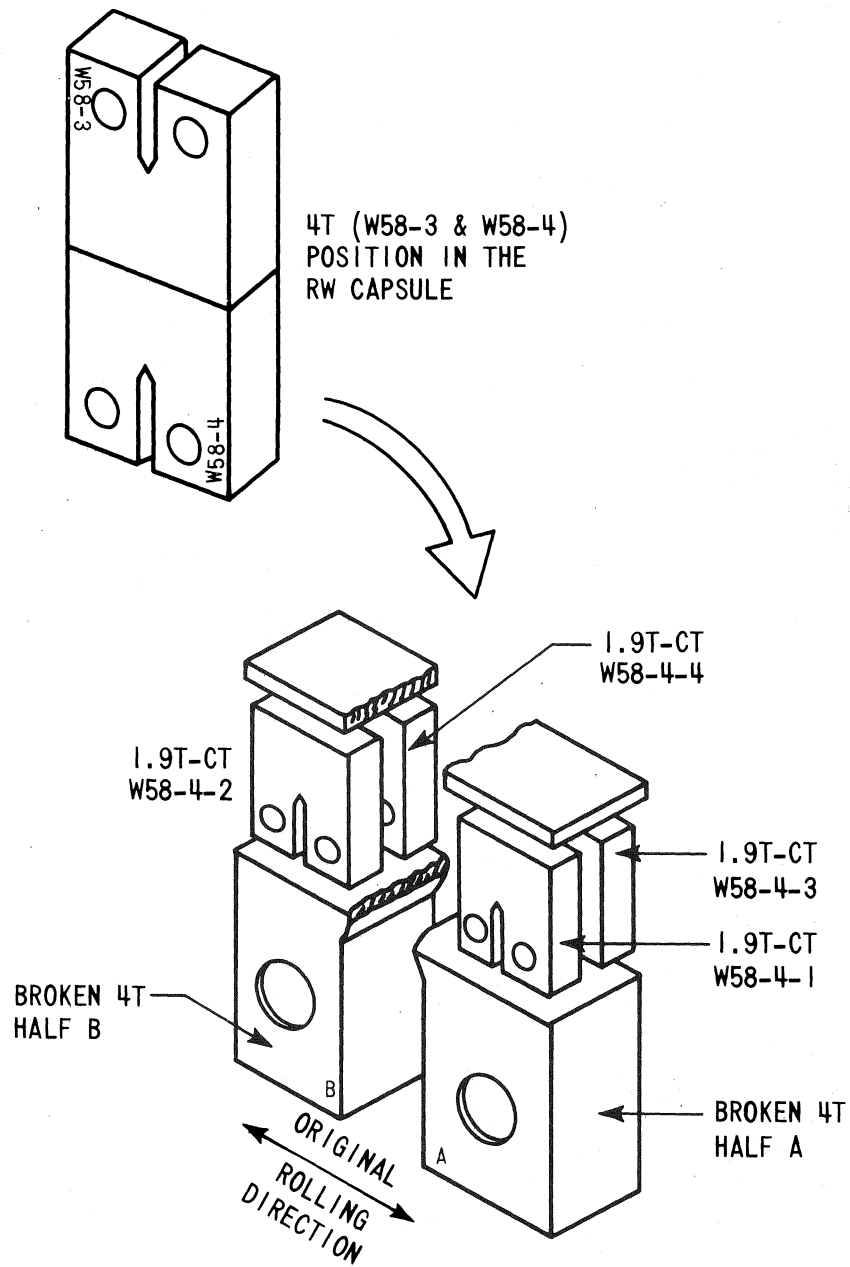
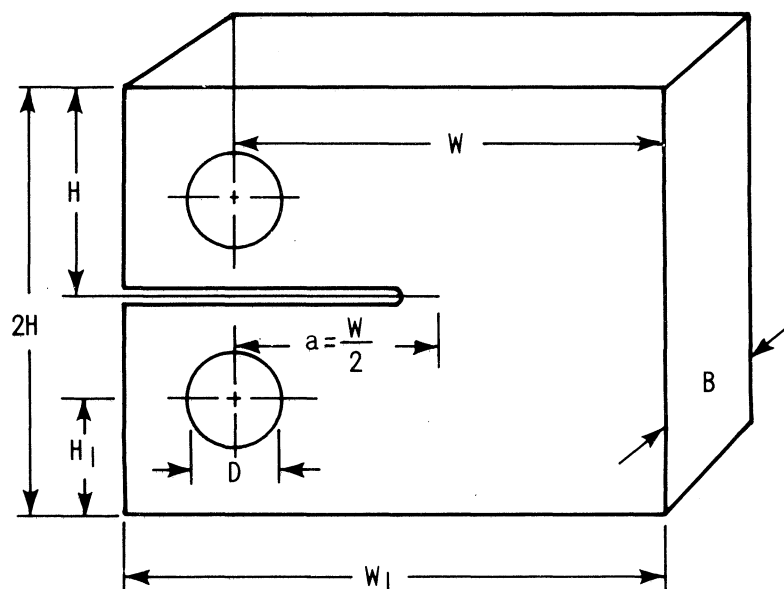


Figure 2-3. Location And Orientation Of The Four 1.9T-CT Specimens Machined From The Broken Halves Of 4T-CT Specimen W58-4.



$$\begin{aligned} W &= 2.0B \\ a &= 1.0B \\ H &= 1.2B \end{aligned}$$

$$\begin{aligned} D &= 0.5B^* \\ W_1 &= 2.5B \\ H_1 &= 0.65B \end{aligned}$$

*EXCEPT IN THE CASE OF THE 4T-CT SPECIMENS WHERE THE PIN HOLES WERE SLIGHTLY ENLARGED TO ACCOMMODATE THE CANS CONTAINING THE SMALL THICKNESS TEST SPECIMENS.

Figure 2-4. Typical Dimension Relationships For Compact Tension Specimens Used In The Irradiation Program.

TABLE 2-1
COMPOSITION OF HSST PLATE 02 AND SUBMERGED
ARC WELDMENT W58-A^[a,b]

Material	C	Mn	Ni	Mo	Si	S	P	Cu
A533, Grade B, Cl. 1, Steel 304.8-mm-Thick Plate (HSST-02)	0.22	1.48	0.68	0.52	0.25	0.018	0.012 ^[a] 0.008 ^[b]	0.12 ^[1] 0.14 ^[2]
Submerged Arc Weld Metal (HSST 58A)	0.15	1.08	0.15	0.54	0.26	0.014	0.026	0.16- ^[1] 0.22

TABLE 2-2
HEAT TREATMENT OF HSST PLATE 02 AND
SUBMERGED ARC WELDMENT W58-A^[c]

Material	Treatment		
Plate 02	912.7 ± 13.8°C	4 hrs	Normalizing
	826.6 - 882.2°C	4 hrs	Austenitizing
	Water Quench		
	648.9 - 673.9°C	4 hrs	Tempering
	Air Cool		
	621.1 ± 13.8°C	40 hrs	Stress Relief
	Furnace cool to 315.6°C		
Weldment 58A	621.1 ± 13.8°C	39 hrs	Stress Relief

- a. Whitman, G. D. "HSST Program Quarterly Progress Report on Reactor Safety Programs Sponsored by the NRC Division of Reactor Safety Research," for April-June 1975, Vol. II, ORNL-TM-5021, September 1975
- b. Witt, F. J., "HSST Program Semi-Annual Progress Report on Reactor Safety Programs Sponsored by the USAEC," for the period ending February 28, 1970.
- c. Childress, C. E. "Fabrication History of the First Two 12-Inch-Thick ASTM A533 Grade B, Class 1 Steel Plates of the Heavy Section Technology Program, Documentary 1," ORNL-4313, Feb. 1969

taken from the stress-relieved plate. The pieces used to fabricate the RW oriented 4T-CT specimens were welded together and then given a postweld stress relief of 39 hours (see table 2-2). Therefore, the base plate material used in fabricating the 0.394T-compact tension, the 4T (RW) compact tension, and later the 1.9T-compact tension (RW) specimens, received a total stress relief of 79 hours. The weldment compact tension specimens received 39 hours of stress relief. The various stress reliefs are summarized in table 2-3. As reported in figure 2.8 of the HSST Quarterly Report for April-June, 1975 (figure 2-5,^[1]) 40 additional hours of stress relief resulted in an approximate 16.7° (30°F) shift (increase) in the Charpy V-notch transition temperature for HSST Plate 02 material. If this shift of 16.7°C also occurred in the fracture toughness transition region, then this difference of 16.7°C should be apparent when comparing Shabbitt's^[2] RW results (40 hours of stress relief) to results obtained by Mager^[3], Berggren, and Canonico^[4] (using the 79 hours total stress relief material) in the unirradiated condition. Figures 2-6 and 2-7 show curves for the dynamic and static test fracture toughness results of the RW oriented material. The 16.7°C shift is not apparent for these tests and therefore will be considered negligible in this report. Perhaps larger time differences in total stress relief would result in a significant shift in the fracture toughness transition temperature, but further investigation of this area would be required.

2-2. IRRADIATION PROCEDURE

The 0.394T-CT specimens were placed into twelve steel containers along with Charpy and tensile specimens which were then inserted into the pin holes of the six 4T-CT specimens. Identification of the fracture toughness specimens loaded into each capsule follows:

Capsule Designation	Specimen Identification	Smaller Specimen Container Identification
Weld	W58-1 and W58-2	1, 2, 3, 4
RW	W58-3 and W58-4	5, 6, 7, 8
WR	02GA-441 and 02GA-442	9, 10, 11, 12

A list of specimens contained in the various containers is presented in table 2-4.

-
1. Whitman, G. D. "HSST Program Quarterly Progress Report on Reactor Safety Programs Sponsored by the NRC Division of Reactor Safety Research," for April-June 1975, Vol. II, ORNL-TM-5021, September 1975
 2. Shabbitts, W. O. "Dynamic Fracture Toughness Properties of Heavy Section A533 Grade-B, Class 1 Steel Plate," HSST Technical Report No. 13, WCAP 7623, Dec. 1970
 3. "Quarterly Progress Report on Reactor Safety Programs Sponsored by the Division of Reactor Safety Research" for April-June 1974, ORNL-TM-4655, August 1974
 4. Whitman, G. D., "HSST Program Quarterly Progress Report on Reactor Safety Programs Sponsored by the NRC Division of Reactor Safety Research for April-June 1975," Vol. II, ORNL-TM-5021, September 1975.

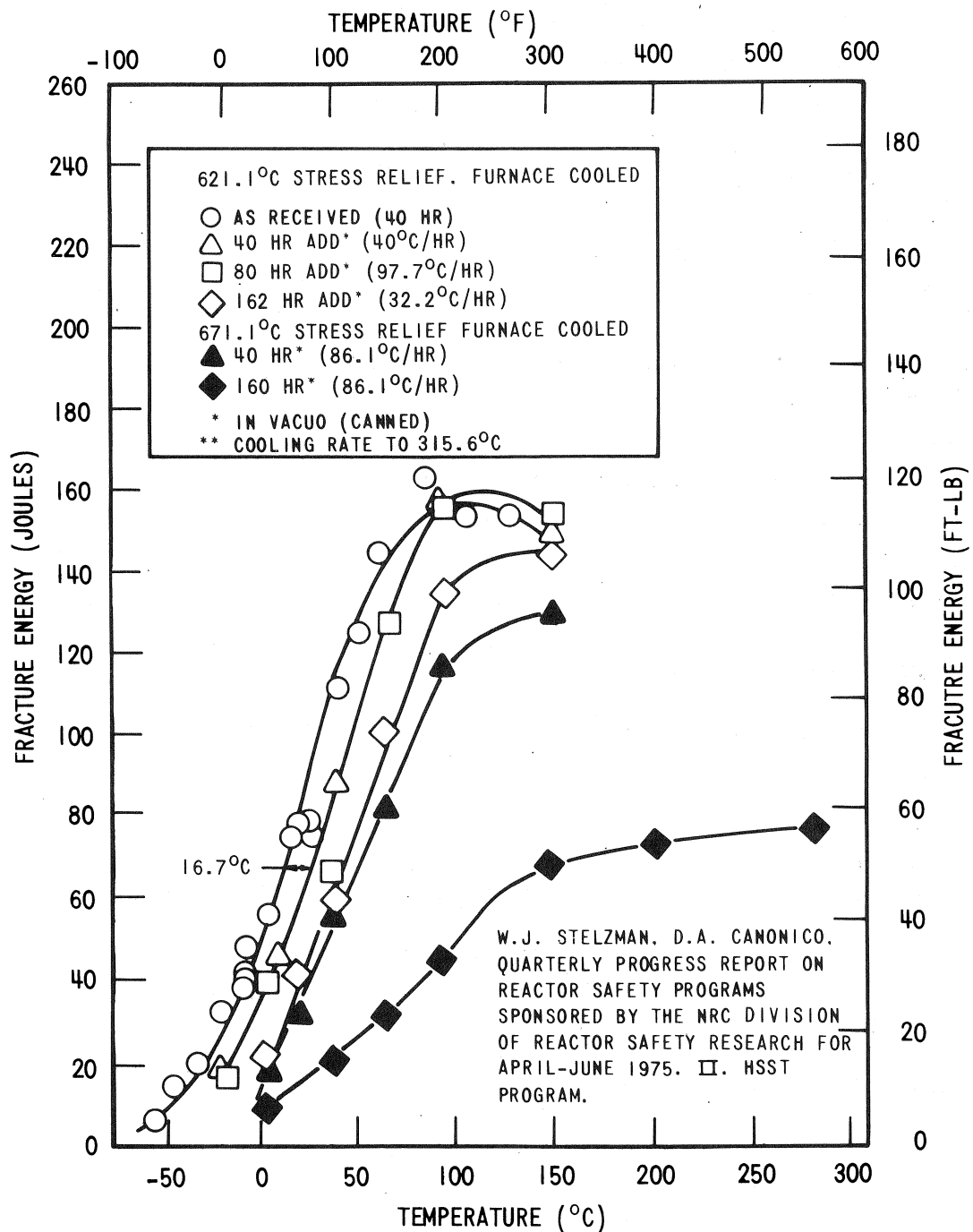


Figure 2-5. Effect of Stress-Relief Time on Charpy-V Impact Properties (RW Orientation) of HSST Plate 02 (ASTM A533, Grade B, Class 1) [1]

1. Whitman, G. D., "HSST Program Quarterly Progress Report on Reactor Safety Programs Sponsored by the NRC Division of Reactor Safety Research, for April-June 1975," Vol. II, ORNL-TM-5021, September 1975.

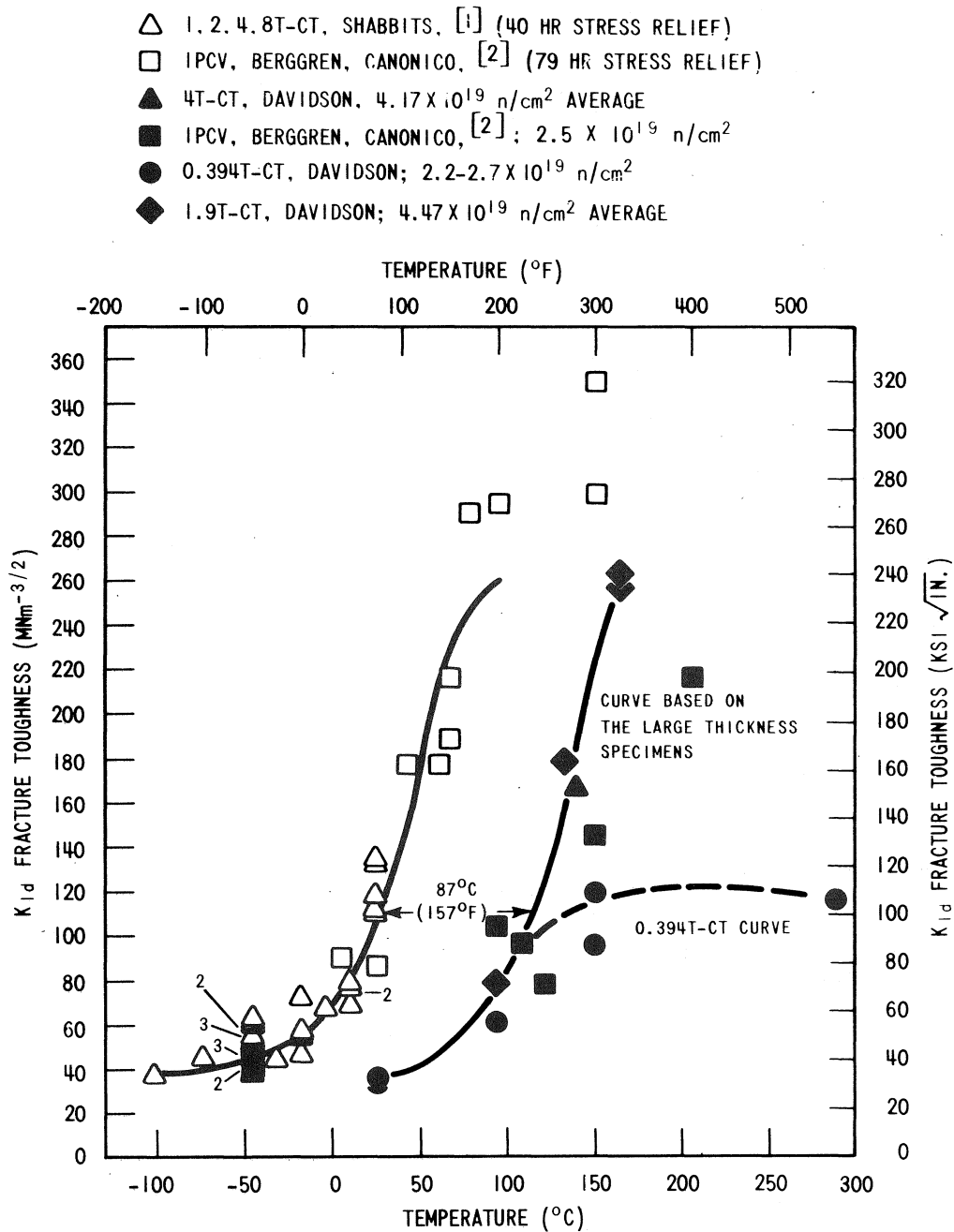


Figure 2-6. Dynamic Irradiated and Unirradiated Fracture Toughness Properties for HSST Plate 02, RW Oriented Material

1. Shabbits, W. O., "Dynamic Fracture Toughness Properties of Heavy Section A533 Grade B, Class 1 Steel Plate," HSST Technical Report No. 13, WCAP 7623, December 1970.
2. Whitman, G. D., "HSST Program Quarterly Progress Report on Reactor Safety Programs Sponsored by the NRC Division of Reactor Safety Research for April-June 1975," Vol. II, ORNL-TM-5021, September 1975.

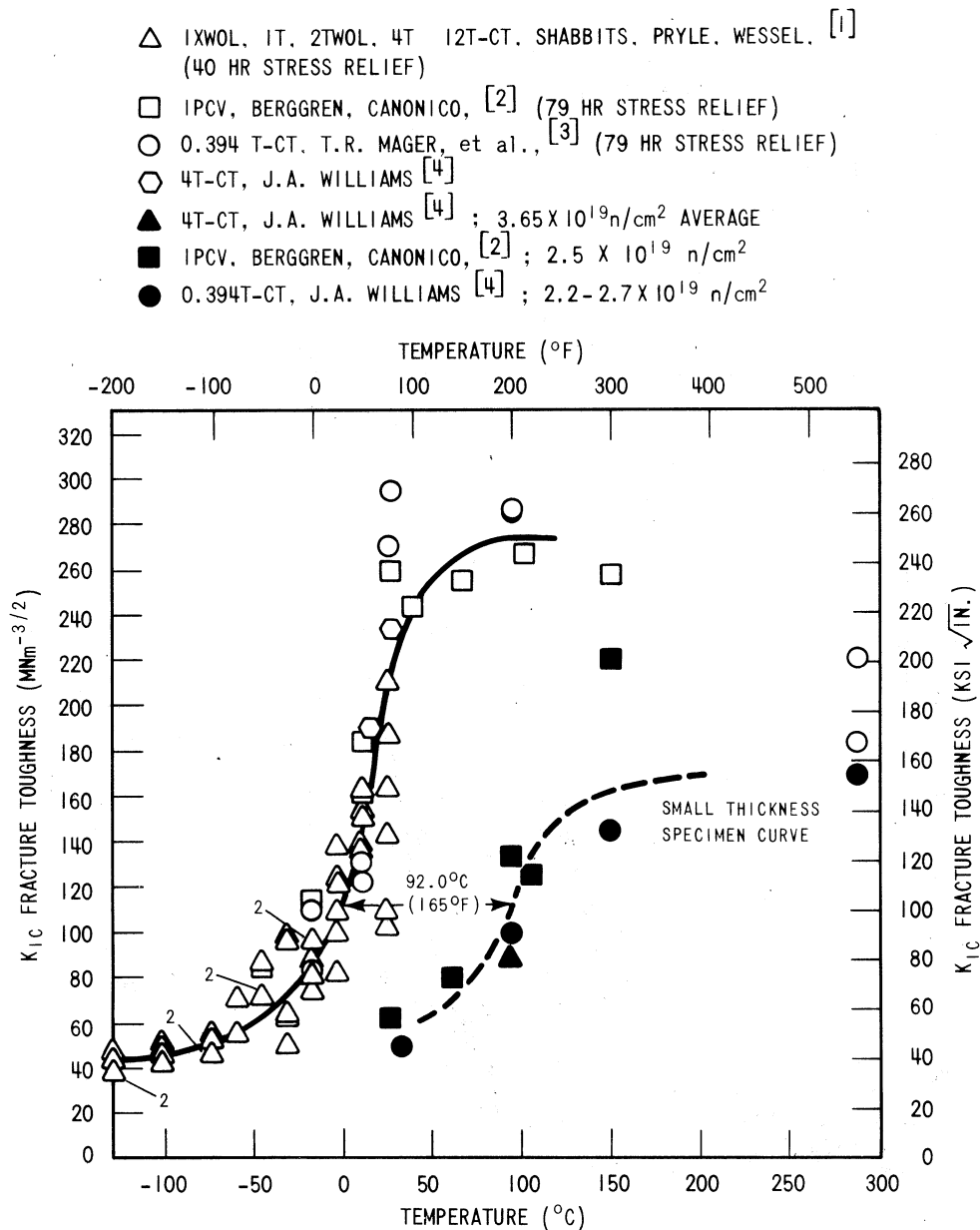


Figure 2-7. Static Irradiated and Unirradiated Fracture Toughness Properties for HSST Plate 02, RW Oriented Material

1. Shabbits, W. O., Pryle, W. H., Wessel, E. T., "Heavy Section Fracture Toughness Properties of A533 Grade B, Class 1 Steel Plate and Submerged Arc Weldment," HSST Technical Report No. 6, WCAP 7414, December 1969.
2. Whitman, G. D., "HSST Program Quarterly Progress Report on Reactor Safety Programs Sponsored by the NRC Division of Reactor Safety Research for April-June 1975," Vol. II, ORNL-TM-5021, September 1975.
3. "Quarterly Progress Report on Reactor Safety Programs Sponsored by the Division of Reactor Safety Research for April-June 1974," ORNL-TM-4655, August 1974.
4. Williams, J. A., "The Irradiated Fracture Toughness of ASTM A533, Grade B, Class 1 Steel Measured with a Four Inch Thick Compact Tension Specimen," HSST Program Technical Report No. 36, HEDL-TME 75-10, June 1975.

TABLE 2-3
SUMMARY OF TOTAL STRESS RELIEF OF THE FRACTURE
TOUGHNESS SPECIMENS

Specimen Type	Orientation	Size (T) (inches)	Total Stress Relief	Notes
CT	WR	0.394T	79 hrs	Unirradiated Results and Irradiated Results
	RW	0.394T	79 hrs	
	Weld	0.394T	39 hrs	
CT	WR	4T	40 hrs	Irradiated Results Only
	RW	4T	79 hrs	Irradiated Results Only
	Weld	4T	39 hrs	Irradiated Results Only
CT	RW	1.9T	79 hrs	Irradiated Results Only

TABLE 2-4
TYPE AND DESIGNATION OF THE 0.394T-CT SPECIMENS LOCATED
IN THE CANS IN THE 4T-CT SPECIMEN PIN HOLES^[a]

Can (Hole) Number ^[b]	Specimen Identification	Orientation
1	W21, W22, W23, W24	Weld 58A
2	30, 31, 32	RW (Center)
3	W25, W26, W27, W28	Weld 58A
4	75, 76, 77	WR (Center)
5	1 through 16	RW (Center)
6	24, 25, 26	RW (Center)
7	W13, W14 21, 22, 23	Weld 58A RW (Center)
8	72, 73, 74	WR (Center)
9	46 through 63	WR (Center)
10	69, 70, 71	WR (Center)
11	27, 28, 29	RW (Center)
12	W17, W18, W19, W20 66, 67, 68	Weld 58A WR (Center)

a. Charpy and tensile specimens were also located in the various pin holes along with the 0.394T-CT specimens.

b. See figure 2.9 for hole location.

Two 4T-CT specimens were positioned in each capsule as shown in figure 2-8.^[1] The encapsulation arrangement was designed in order to insure relative uniformity of the fluence and temperature distributions in the specimens during irradiation. The position of each capsule (figure 2-9) relative to the Battelle reactor core is shown in figure 2-10.^[1] The program goal consisted of irradiating the 4T-CT specimens as uniformly as possible to a mid-thickness fluence of 5×10^{19} nvt ($E > 1$ Mev) at a normal temperature of 288°C (550°F). These conditions were designed to most accurately simulate the type of damage incurred in a reactor pressure vessel wall at the end of plant life. Four inches of steel attenuate neutron flux rapidly. Therefore, the capsules were rotated 180° periodically to build up a fluence symmetry about the mid-thickness of the 4T specimen. The fluence distribution, Gamma attenuation and temperature control procedures are well documented^[1] as well as procedures for capsule insertion and rotation.^[2] Figure 2-11 illustrates the variation of fluence in the 4T-CT specimens as a result of irradiation in the Test Reactor.

2-3. CAPSULE DOSIMETRY

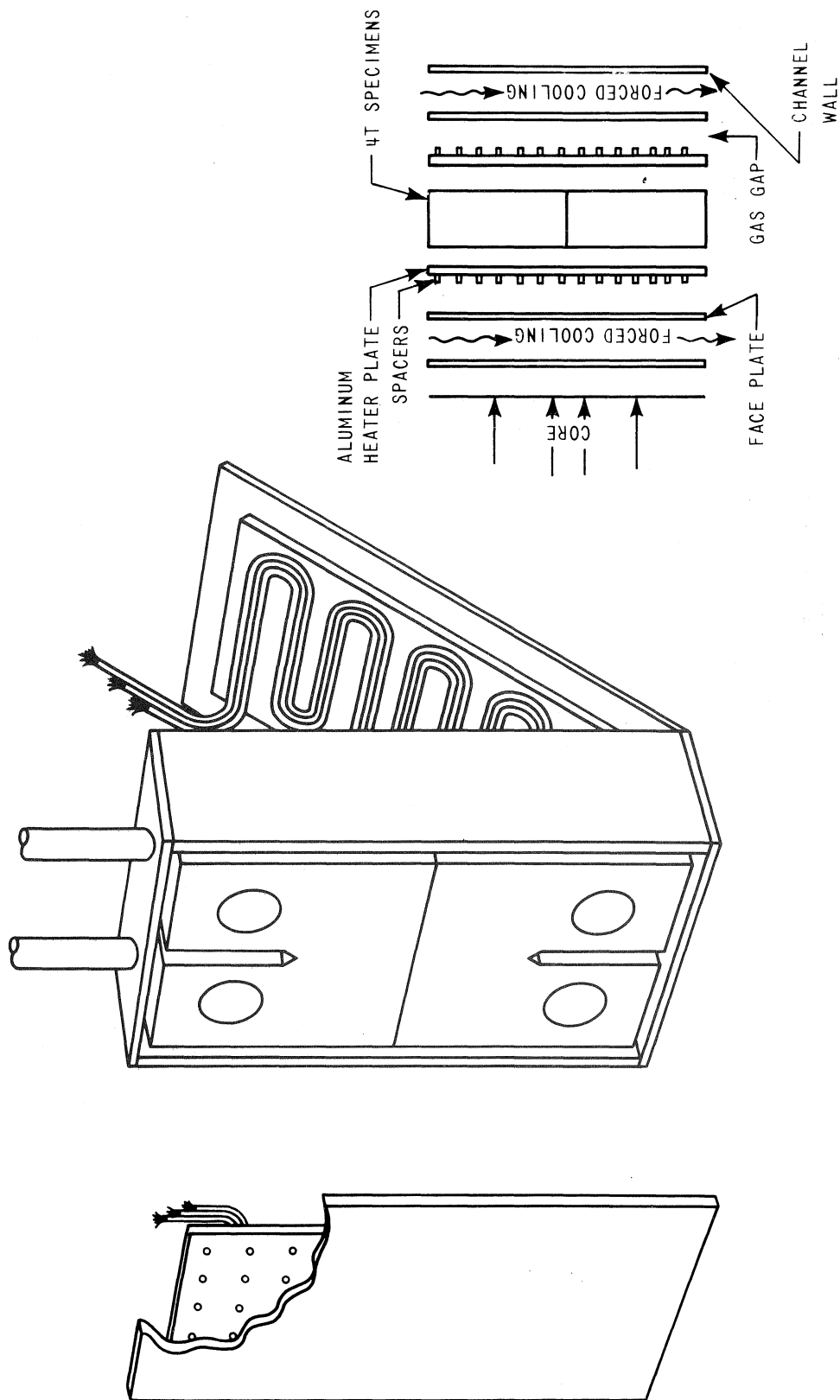
Dosimeters were placed inside the specimen irradiation capsule to measure the total amount of fluence and its spatial distribution in the post-irradiation analysis. Two types of dosimeters were used.

The first type of monitor (gradient wire) was inserted in the specimen capsule in six locations as shown in figure 2-9. Each wire was 95.25 mm long and was oriented through the thickness. Five segments of each wire were counted to obtain a range of counts through the specimen thickness. Iron and nickel wires were used in each of the six measuring points to monitor the fast neutron fluence. Also, unshielded A1 (0.15% Co) wires were used at the bottom of the notch in each capsule to obtain some measure of the thermal neutron fluence.

The second type of monitor, U^{238} , was placed in each capsule at a hole position. This monitor consists of depleted U^{238} powder encapsulated in a small brass vial, shielded by 3.2 mm of cadmium oxide powder. These monitors are for determining point measurements only and are incorporated as support data to the gradient wire activity measurements. The capsule internal dosimetry is summarized in table 2-5.^[1]

1. "HSST Program Semi-Annual Progress Report for Report Period Ending August 30, 1972," ORNL-4855, April 1973

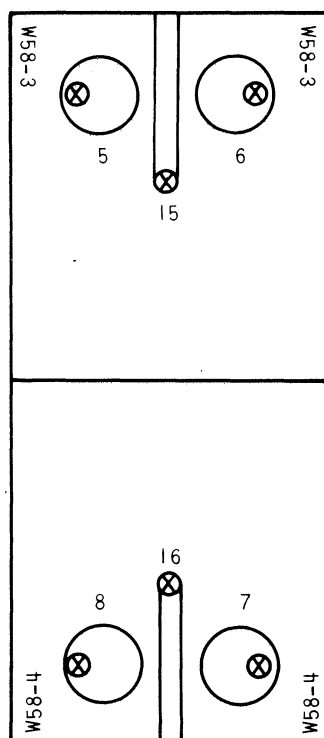
2. "HSST Program Semi-Annual Progress Report for Report Period Ending February 28, 1973," ORNL-4918, February 1974



9975-7

Figure 2-8. 4T Specimen Capsule Geometry [1]

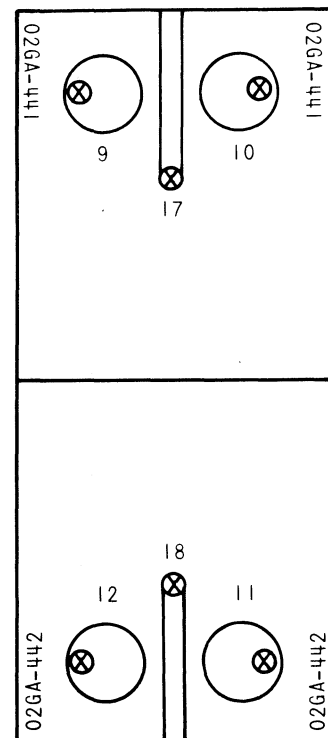
1. "HSST Program Semi-Annual Progress Report for Report Period Ending August 30, 1972," ORNL-4855, April 1973.



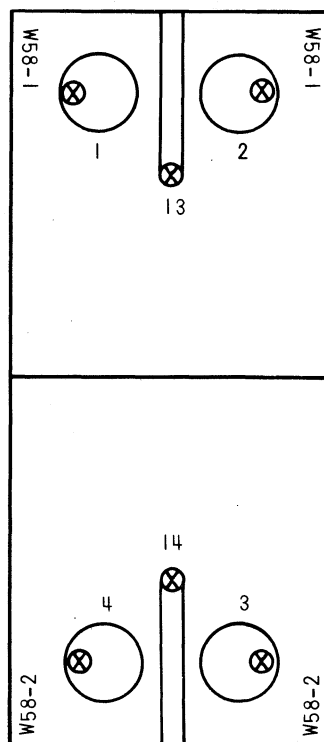
"RW" CAPSULE
(SOUTH)

NOTES:
 (X) = DOSIMETRY POSITIONS WHERE:

1. U^{238} DOSIMETER BLOCKS ARE LOCATED IN HOLES 1, 3, 5, 7, 9 AND 11
2. $Fe^{54}Ni^{58}$ GRADIENT WIRES ARE LOCATED IN POSITIONS 1 THRU 18
3. AL-0.15% Co^{59} GRADIENT WIRES ARE LOCATED IN POSITIONS 13 THRU 18



"WR" CAPSULE
(NORTH)



WELD CAPSULE
(EAST)

SPECIMEN
AND
DOSIMETRY
IDENTIFICATION
BY CAPSULE

Figure 2-9. 4T-CT Capsule Designation and Dosimetry Location

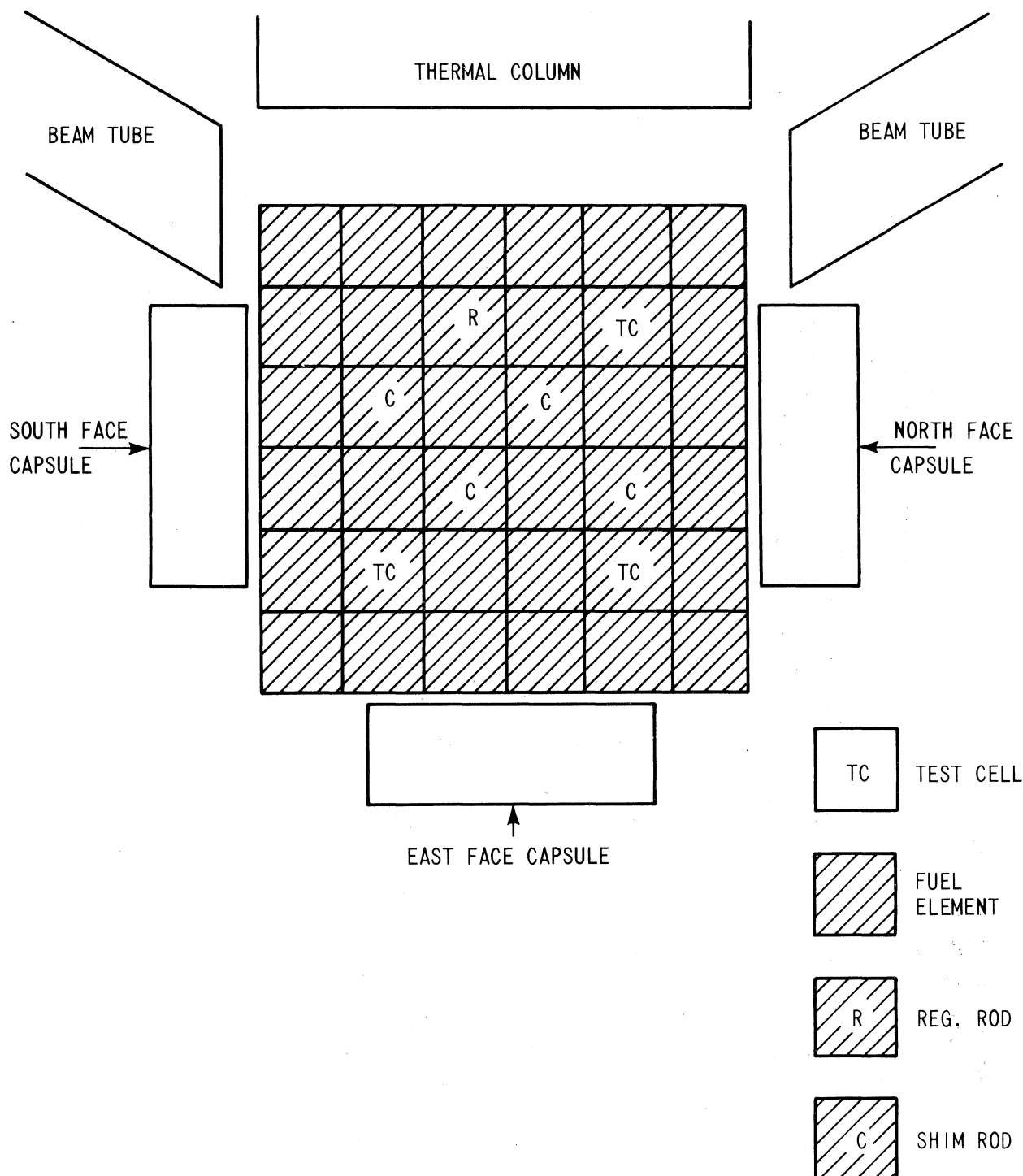


Figure 2-10. BRR Core Configuration For 4T Irradiations^[1]

1. "HSST Program Semi-Annual Progress Report For Report Period Ending August 30, 1972," ORNL-4855, April 1973.

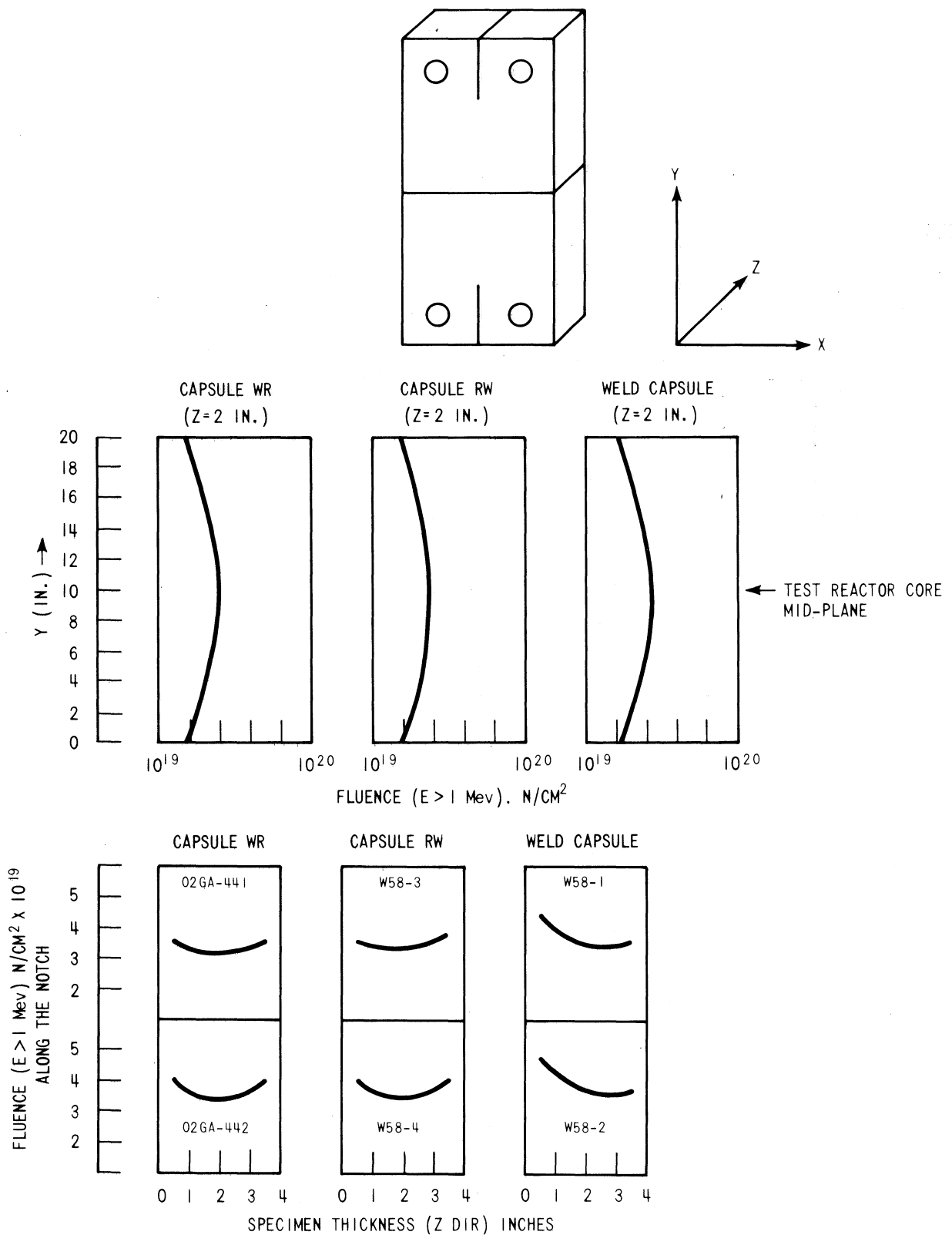


Figure 2-11. Variation in Fluence Received by the 4T-CT Specimens Located in the Three Test Capsules Based on the Dosimetry Results

TABLE 2-5
CAPSULE INTERNAL DOSIMETRY^[a]

Material & Reaction	Half Life	Threshold Energy (MEV)	Form	Number per Capsule
$\text{Co}^{59} (n,\gamma) \text{Co}^{60}$	5.2 y	Thermal	101.6 mm wire, 0.508 mm d Al (0.15% Co)	2
$\text{Fe}^{54} (n,p) \text{Mn}^{54}$	313d	2.4	101.6 mm wire, 0.2286 mm d	6
$\text{Ni}^{58} (n,p) \text{Co}^{58}$	71.4d	2.5	101.6 mm wire, 0.762 mm d	6
U^{238} Fission Cs^{137}	30y	1.7	Depleted U^{238} CdO shielded	2

a. "HSST Program Semi-Annual Progress Report for Report Period Ending August 30, 1972," ORNL-4855, April 1973

SECTION 3

DYNAMIC FRACTURE TOUGHNESS TESTING

As previously mentioned, compact tension (CT) specimens were chosen to generate the fracture toughness data for this irradiated material. The 0.394T and 4T compact tension specimens were of proportions shown in figure 2-4, except for the pin hole diameter of the 4T-CT specimens which was enlarged to 2 1/4 inches to accommodate the cans containing the 0.394T-CT specimens.

The irradiated yield strengths of both the Heavy Section Steel Technology Program (HSST) Plate 02 and submerged arc weldments have been determined^[1] and are presented graphically in figure 3-1 over a range of temperatures. Using the criterion prescribed in ASTM E-399 for static test conditions, irradiated specimens up to 4 inches thick would result in maximum valid static K_{Ic} values on the order of about $143 \text{ MNm}^{-3/2}$ ($130 \text{ ksi } \sqrt{\text{in.}}$). This K_{Ic} value for this material occurs roughly at the transition region of the static K_{Ic} versus temperature curve. Therefore, to develop fracture toughness data at temperatures greater than the transition temperature, another method of analysis was used. The method chosen was the Equivalent Energy Method (explained later). Both the Equivalent Energy and the ASTM E-399 methods use maximum load for evaluation and produce identical results for elastic (linear deflection to maximum load) fracture behavior. However, for purposes of evaluating, in a conservative manner, elastic-plastic and plastic fracture behavior where some deviation from linearity occurs in the load-deflection curve, the equivalent energy method was developed. There exist numerous cases in the literature which show, in the elastic and elastic-plastic temperature regions, that dynamic fracture test conditions (loading rate $\sim 10^4 \text{ MNm}^{-3/2} \text{ sec}^{-1}$) result in more conservative fracture toughness (K_{Id}) data at a given temperature than the static fracture test condition (load rate $\sim 5 \text{ MNm}^{-3/2} \text{ sec}^{-1}$). This is due to the higher effective yield strength^[2,3] associated

-
1. Williams, J. A., HSST Report No. 31, "The Irradiation and Temperature Dependence of Tensile and Fracture Properties of ASTM A533 Grade B, Class 1 Steel Plate and Weldment," HEDL-TME-73-75, August 1973.
 2. Kraft, J. M. and Irwin, G. R., "Crack Velocity Considerations" in *Fracture Toughness Testing and Its Application*, pp. 114-129, ASTM-STP-381, Am. Soc. for Testing and Materials, 1965
 3. Manjoine, M.J., "Influence of Rate of Strain and Temperature on Yield Stresses of Mild Steel," *Trans. Am. Soc. Mech. Engrs., J. Appl. Mech.* 66, A211-A218 (1944)

with the dynamic loading conditions. Although dynamic tests produce lower bound fracture toughness data in the elastic and elastic-plastic temperature regions, the same may not necessarily be true at upper shelf fracture toughness temperatures where fracture occurs in a fully plastic mode. Also, at temperatures in which fully plastic fracture behavior occurs, stable subcritical crack growth can occur prior to maximum load, thereby making fracture toughness calculations at these temperatures unrealistic when using maximum load for calculational purposes. The use of the J-integral analysis which accounts for stable subcritical crack growth prior to fracture should be used to evaluate the fracture toughness of the material at these temperatures.

Whereas static test conditions produce load-deflection curves which are uncharacteristic of cleavage-controlled fracture (and therefore less typical of plain-strain conditions) at elastic-plastic fracture temperatures, the dynamic test condition results in a distinct drop at maximum load up to temperatures characteristic of the initiation of the upper shelf fracture toughness (fully plastic region). This test behavior, only obtained in dynamic tests, has three major advantages. These are

- Unambiguous definition of crack initiation
- Cleavage controlled fracture and thereby closely approximated plain-strain conditions
- Obtaining valid lower bound fracture toughness data based on the equivalent energy analysis up to upper shelf fracture toughness temperatures

Details of the equivalent energy analysis and the phenomena of non-linear cleavage behavior (cleavage controlled fracture) during dynamic testing are explained in detail later in the report.

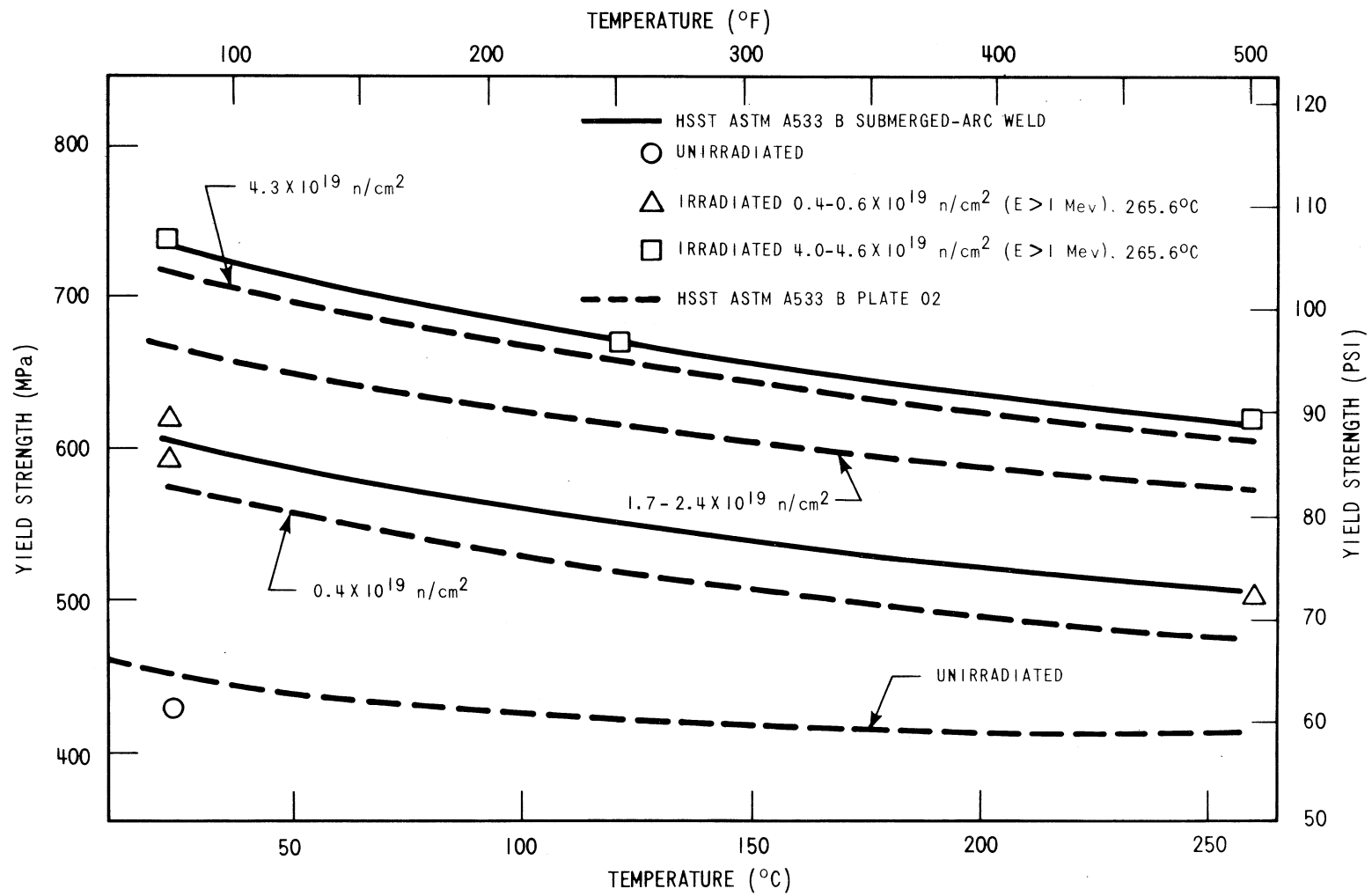


Figure 3-1. Yield Strength of Irradiated ASTM A533-B Grade B Class 1 Plate and Submerged Arc Weld^[1]

SECTION 4

TESTING EQUIPMENT AND PROCEDURE

The testing method involved testing of the compact tension (CT) specimens which had been fatigue precracked. Strong direction (RW) oriented 4T-CT specimen W58-4 was tested in the static mode by J. A. Williams at the Hanford Engineering Development Laboratory in Richland, Washington.^[1] The broken halves of this specimen were then machined into four 1.9T-CT specimens in the RW orientation. These specimens were later fatigue precracked and dynamically tested at the Westinghouse Research and Development (R&D) Center hot cell facility in Pittsburgh, Pennsylvania. The remaining five 4T-CT specimens and the 0.394T-CT specimens were fatigue precracked prior to insertion into the capsules in the test reactor. Fatigue precracking was done in accordance with ASTM E399 criteria.

4-1. TEST MACHINE^[2,3]

The test machine (figure 4-1) is an open-loop controlled hydraulic machine with loading rate of approximately 1524 mm/sec, a load capacity of 99790 Kg, and a 76.2 mm stroke. The major components, of the machine as shown in figure 4-1, are a 177.8 mm diameter and an 203.2 mm diameter cylinder connected in series, two 9.46 liter accumulators, a 0.95 liter accumulator, a 4-way solenoid valve, a 50.8 mm pilot-operated dump valve, and a high pressure air-operated hydraulic pump.

The 50.8 mm dump valve is connected to the bottom side of the 203.2 mm diameter cylinder and discharges into a small oil reservoir. The high pressure air-hydraulic pump is mounted on top of the oil reservoir. One of the 9.46 liter accumulators is connected to the top of the 203.2 mm cylinder and the other 9.46 liter accumulator is connected to the top of the 177.8 mm cylinder. The accumulators are precharged with nitrogen to approximately 14.48 MPa. The 0.95 liter accumulator is used to supply oil to operate the 50.8 mm pilot-operated dump valve.

-
1. Williams, J. A., "The Irradiated Fracture Toughness of ASTM A533, Grade B, Class 1 Steel Measured with a 4-Inch-Thick Compact Tension Specimen," HSST Program Technical Report No. 36, HEDL-TME-75-10, June 1975
 2. Spewock, M. and Ceshini, L., "Servo-Controlled Electro-Hydraulic System for Testing Fracture Toughness Specimens," Westinghouse Research Report 69-IP6-BTLFR-R3, August 1969
 3. Ceschini, L. J., Broush, W. T., "Experimental Procedure for Dynamic Testing of CT Fracture Toughness Specimens," Westinghouse Research Report 74-59296, January 1974

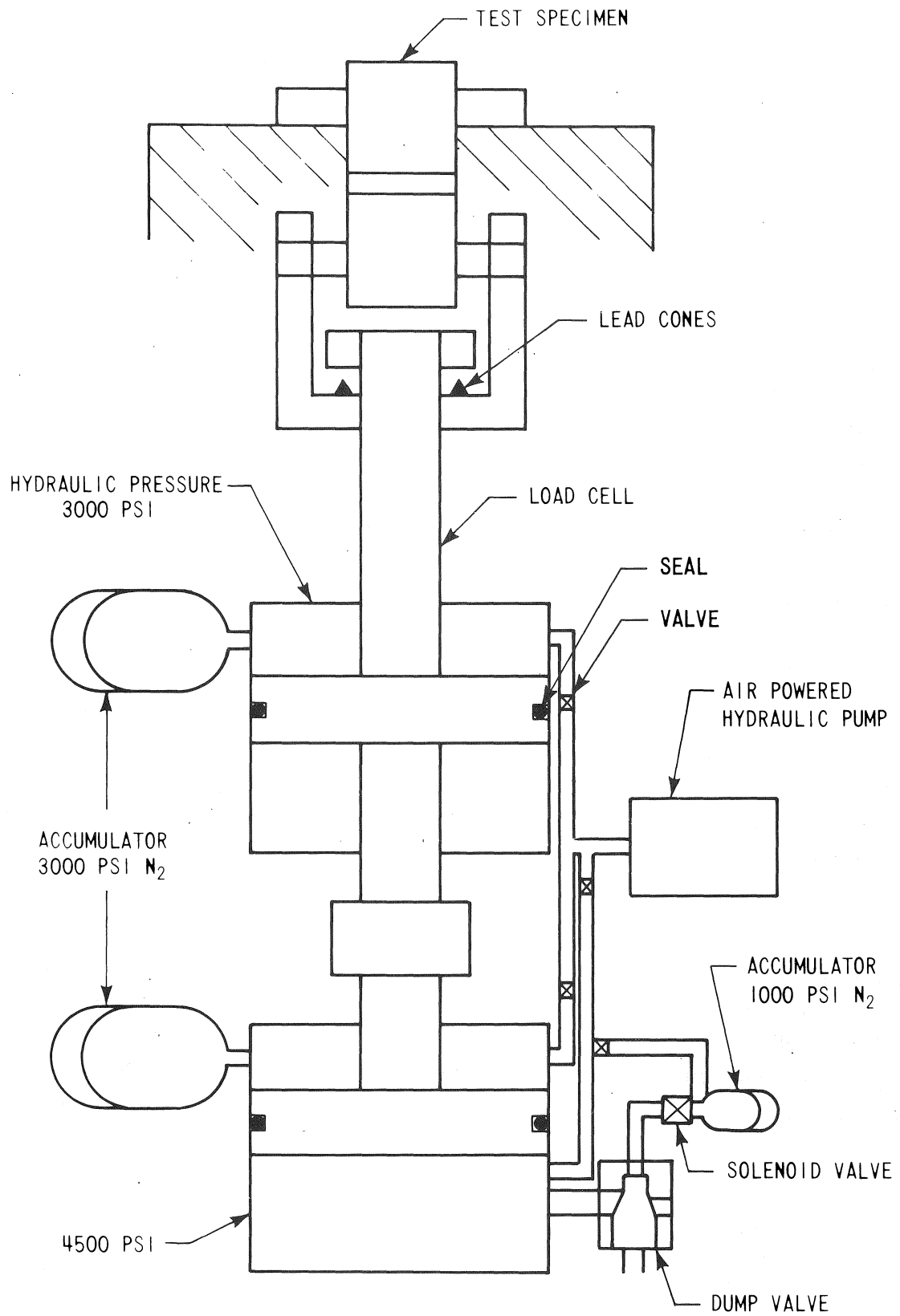


Figure 4-1. Diagram Of The Dynamic Test Machine

A series of hand operated valves are used to direct the flow from the high pressure air-operated hydraulic pump.

4-2. TEST MACHINE OPERATING PROCEDURE

- The 4-way solenoid control valve is de-energized, admitting oil pressure to the side of the pilot which closes the 50.8 mm dump valve.
- The 0.95 liter accumulator is pressurized to 20.68 MPa. This provides the hydraulic pressure to activate the pilot which operates the dump valve.
- Oil is pumped into the bottom side of the 203.2 mm cylinder through a connecting line from the air-operated hydraulic pump. This raises the series-connected pistons of both the 203.2 mm and 177.8 mm diameter cylinders to the starting position. A hand valve in the connecting line to the 203.2 mm cylinder is closed, trapping the oil in the bottom of the 203.2 mm cylinder.
- Oil is then pumped into the top of the 203.2 mm cylinder and its accumulator, and into the top of the cylinder and its accumulator. Both cylinder-accumulator pairs are pressurized to 20.68 MPa. Hand valves are closed to trap this oil in both pairs. The 20.68 MPa oil pressure in both cylinders is pushing down on the pistons with a combined force of $99 \times 10^3 \text{ kg}$. This force is opposed by the oil in the bottom of the cylinder. The oil in the bottom of the 203.2 mm cylinder is pressurized to 30.34 MPa to resist the downward force of the two cylinders. The area of the underside of the piston in the 203.2 mm cylinder is just over 322.58 square cm.

The system is then in equilibrium and ready to start a test.

- When the specimen reaches equilibrium at the selected test temperature, the 4-way solenoid valve is energized to open a 50.8 mm dump valve. The oil at 30.34 MPa in the lower side of the 203.2 mm cylinder is discharged into the oil reservoir at 3028.3 liters per minute, allowing the pressure acting on the upper sides of the pistons in the cylinders to force the load downward, and to apply load to the specimen.

4-3. SPECIMEN LOADING SYSTEM

Because of differences in specimen size (0.394, 1.9, and 4T-CT) and characteristics of the test machine, two methods were used to apply load to the specimens. When pressurized as previously described, the test machine loading accelerates for approximately 6.35 mm before constant speed is attained. Therefore, the load ram was allowed to run free during this interval before load is applied to the specimen.

This requires special features in the load train to prevent shock loading of the specimen. A through-clevis design was used to test the 1.9T and the 4T-CT specimens. The specimen was loaded in a grip arrangement which permitted a small preload to be applied to the specimen to take out slack in the clevis and pins.

The strain-gaged, stud-type load cell was slid through the clevis until the loading nut on the end of the load cell made contact with a 3.175 mm lead plate (for larger specimens) which lay between the loading rod and the load cell. Deformation of the lead dampened the impact of the loading.

The 0.394-CT specimens had a slightly different loading arrangement. The slack in the clevis, pins, and load rod was taken up with a coil compression spring which applied a preload to the loading train, above the load cell. A 0.254-mm-thick teflon washer was placed between the loading rod and the quartz load cell, which dampened the contact between the load cell and the loading rod.

4.4. LOAD CELL

Load was measured with a strain gaged load cell. Displacement was measured with a linear variable differential transformer (LVDT) in an extensometer which extended out of a resistant wound furnace for high temperature testing. The strain-gaged load cell was conditioned with a Westinghouse dc amplifier. The LVDT was conditioned with a Model 300D Daytronic amplifier. The load cell was calibrated to an accuracy of ± 1 percent by applying a known static load, and the LVDT was calibrated with a precision drum micrometer, which can resolve displacements to 0.00127 mm.

The load and displacement outputs were recorded on individual recording channels of a Consolidated Electrodynamics Corporation Frequency Modulator instrument tape recorder. Before the tests were started, calibration marks were recorded on individual recording channels. The tests were then run, and the load and displacement records recorded on the same channel with their respective calibration marks.

Load versus time and displacement versus time traces were displayed on an oscilloscope and photographed along with the calibration marks that had been prerecorded. The tape was re-played and the load and displacement signal cross-plotted to give a load versus displacement curve. To aid in data analysis, the load and displacement signal can be directly recorded on a 4-channel CMP transient recorder or rerecorded on this transient recorder from the CEC tape recorder. Then the high speed test signals can be recorded from the transient recorder at speeds slow enough to plot on an x-y recorder.

4.5. TEMPERATURE CONTROL

An air environment resistance wound furnace was used to heat the specimens. Three heating zones were used to ensure even temperature distribution throughout the specimen. The furnace was operable to temperatures of 287.7°C. The temperature of the furnace was maintained using a thermocouple imbedded in the test grip and controlling a proportioning type controller, set to give the final desired specimen temperature. The desired temperature was obtained in relatively short time, and the specimen "soaked" until the specimen reached a stable control temperature for at least 30 minutes. This method prevented overshooting of the specimen test temperature. A thermocouple embedded in the clevis was calibrated to a thermocouple attached to a dummy specimen prior to testing and indicated when the specimen reached temperature. All thermocouple outputs were recorded on a multi-point recorder. All thermocouples were calibrated in the temperature range of interest. The clevis and specimen temperatures have been found to agree within a couple °C at temperatures to 287.7°C. A small preload of 13.57 kg was put on the sample to assure good contact.

4.6. LVDT (LINEAR VARIABLE DIFFERENTIAL TRANSFORMER) EXTENSOMETER

A LVDT extensometer was used to monitor crack opening displacement at the front of the specimen. The LVDT range was calibrated according to specimen size. The LVDT was excited with a Daytronic Transducer Amplifier Model 300-D and the signal was balanced and recorded as an individual system. The calibration was accomplished with a micrometer-type drum calibrator.

All recording and indicating instruments are routinely calibrated. Internal calibrations of these instruments for the purpose of pretest setup and checkout were conducted to ensure functional instrument operation.

Due to size limitations, one LVDT extensometer was used on the Charpy Thickness Compact Tension Specimens. On the 1.9T and 4T-CT specimens, two LVDT extensometers were used to ensure a displacement-time record should one extensometer become defective during a test.

4.7. LOAD CELL CALIBRATION

The strain gage load cell was calibrated using a hydraulic cylinder and proving ring calibrated by the National Bureau of Standards.

The load signal conditioner used was a Westinghouse strain gage amplifier. The dc volt signal output of the amplifier was equal to a specified amount of load.

4-8. LVDT CALIBRATION

The LVDT was calibrated over an applicable range of mils (according to specimen size) using a Sheffield micrometer-type extensometer calibrator. The LVDT signal conditioner used was a Daytronic transducer amplifier-indicator Model 300-D.

The LVDT signal was calibrated over the respective dc volt range. All voltage measurements were taken with a Weston digital voltmeter.

After the LVDT had been calibrated, the calibrating signal in the Daytronic was recorded on the tape recorder and was used as an analog signal to calibrate the x-y recorder.

SECTION 5

EQUIVALENT ENERGY METHOD

The requirements specified by ASTM E399^[1] impose severe size restrictions on fracture toughness test specimens. Meeting these requirements is particularly difficult when testing irradiated specimens, where specimen size is limited by reactor space, fluence gradients, gamma heating, and the cost of irradiating large thickness fracture toughness specimens. Thus, there is a real need for a method of obtaining meaningful fracture toughness values using specimens smaller than required by ASTM E399.

The equivalent energy method was proposed by Witt^[2] as a solution to the size requirement problem. Witt concluded that his method would always lead to a lower bound value of the fracture toughness at a given temperature. Fracture toughness values calculated from small specimen data using the equivalent energy analysis agree well with valid test results based on ASTM E399 size requirements over a temperature range in which the fracture of the specimen is cleavage controlled. As mentioned earlier, this is because both ASTM E399 and the equivalent energy method make the assumption that crack initiation occurs at maximum load on the load-deflection traces of the fracture toughness test. During dynamic testing, the fracture mode is cleavage controlled to temperatures just prior to the onset of the fracture toughness upper shelf. At temperatures characteristic of the fracture toughness upper shelf, where large amounts of plasticity are involved with the fracture process (and therefore not cleavage controlled), crack initiation can occur prior to maximum load. Therefore evaluation of the fracture toughness using the equivalent energy method is not valid at these temperatures. Another definition of realistic upper shelf fracture toughness is possibly in order.

To more accurately characterize the upper shelf fracture toughness, J_{IC} testing and subsequent analysis should be employed. J_{IC} testing results in more conservative fracture toughness values at upper shelf temperatures because it is based on loads characteristic of the actual

-
1. "Standard Method of Test for Plane-Strain Fracture Toughness of Metallic Materials," ASTM-E399-74, Part 10, Metals - Physical, Mechanical and Corrosion Testing, pp. 432-451, Am. Soc. for Testing & Materials, 1974
 2. Witt, F. J., "Factors Influencing a Quantitative Safety Assessment of Water Reactor Pressure Vessels," CONF-730304-6, Topical Meeting on Water Reactor Safety, March 26-28, 1973, Salt Lake City, Utah

crack initiation (instead of maximum load). The values are conservative because crack initiation, although occurring prior to maximum load, is not unstable crack initiation (characteristic of temperatures lower than the upper shelf where initiation clearly occurs at maximum load) but rather stable crack growth.

J_{Ic} testing and interpretation of results is currently in progress at several research facilities. Findings of these tests will most likely change the test results at upper shelf temperatures in this report (the Charpy thickness compact tension specimen results), but for consistency in analysis of the fracture toughness of irradiated materials in this report, all test results have been evaluated utilizing the equivalent energy method.

5-1. ANALYSIS

The lower-bound fracture toughness values using Witt's equivalent energy method can be obtained from non-linear load-displacement traces, such as that shown in figures 5-1 and 5-7. Basically, two quantities are required from the load-displacement curve: the area under the curve to maximum load (A_1) and the area under the curve to any point (P_B) on the linear portion of the curve (A_2). The lower bound fracture toughness^[1] is then given by:

$$K_{Ic} = \frac{P_B \sqrt{A_1/A_2} f(a/w)}{B \sqrt{W}} \quad (5-1)$$

or equal to K_{Ic} for the dynamic fracture toughness case, where:

a is the specimen crack depth

W is the specimen width

B is the specimen thickness

$f(a/w)$ is a geometric shape factor which is commonly available in the literature.^[2,3]

The procedure for evaluating the K_{Ic} using the load-displacement curve is reasonably straight forward. However, it is important that the linear region of the curve be compared to the calculated compliance slope of the specimen, which considers the fact that the displacement

-
1. Riccardella, P. C. and Swedlow, J. L., Heavy Section Steel Technology Program Technical Report No. 33, "A Combined Analytical-Experimental Fracture Study of the Two Leading Theories of Elastic-Plastic Fracture (J-Integral and Equivalent Energy)," WCAP-8224, October 1973
 2. "Standard Method of Test for Plane-Strain Fracture Toughness of Metallic Materials," ASTM-E-399-74, Part 10, Metals - Physical, Mechanical and Corrosion Testing, pp. 432-451, Am. Soc. for Testing & Materials, 1974
 3. Brown, W. F., Jr. and Srawley, J. E. "Plane-Strain Crack Toughness Testing of High Strength Metallic Materials," ASTM-STP-410, Am. Soc. for Testing and Materials, 1966

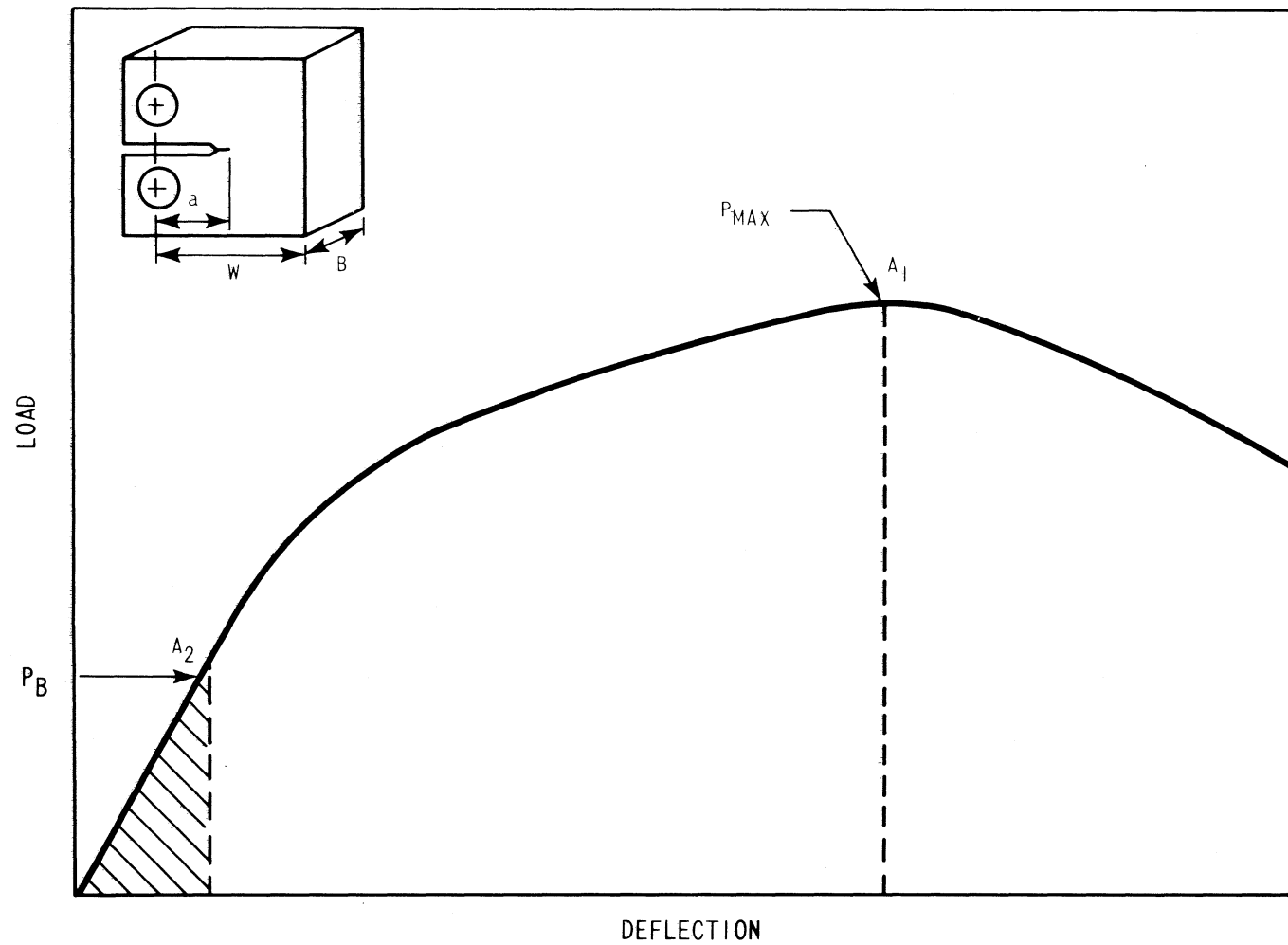


Figure 5-1. Typical Load-Displacement Curve for a Compact Tension Specimen Tested at a Temperature at which Elastic-Plastic Fracture Toughness Values are Evaluated

measurement was performed some distance from the front of the specimen. Since the appearance of this linear region may be slightly wavy at times in the dynamic load-deflection trace, it is sometimes helpful to reconstruct this region based on the calculated measurement point compliance for that specimen before calculating K_{Id} .

5-2. COMPLIANCE CONSIDERATION

When using compact tension specimens (figure 2-4) in fracture toughness testing, a knowledge of the crack edge displacements (see figure 5-2) is useful in the interpretation of test results. The elastic crack surface displacements in compact tension specimens have been determined analytically by use of the finite element method. W. K. Wilson has shown^[1] that the crack surface displacements at the line of loading (v_L) and at the crack edge (v_E) are related to the specimen crack length to W ratio (a/w). It was also shown that the error in the finite element analysis was about one percent.

TABLE 5-1
FINITE ELEMENT DISPLACEMENTS ON THE CRACK SURFACE
OF COMPACT TENSION SPECIMENS ($H/W = 0.6$)^[a]

a/w	EBv_E/P (Finite Element)	EBv_L/P (Finite Element)
0.48	50.0	33.4
0.50	54.6	36.9
0.52	59.6	40.7
0.54	65.3	45.2
0.56	71.9	50.1
0.58	79.4	56.0
0.60	88.2	62.6

a. Wilson, W. K., "Elastic Displacements for Compact Tension Specimens," Westinghouse Research Report 71-1E7-FMPWR-P5, September 1971

A polynomial representation of the finite element displacements at the crack edge for $0.48 < (a/w) < 0.6$ is given as:

$$EBv_E/P = 372.6 + 2390.2 (a/w) - 4910.0 (a/w)^2 + 3681.0 (a/w)^3 \quad (5-2)$$

This polynomial was obtained from a least square fit of the finite element data, and is presented in tabular form as a function of a/w in table 5-1.

In measuring the crack edge opening displacements, the clip gage (or other measuring instrument) is attached to a small block which is fastened to the specimen face. The contact points are not at the specimen face, but are some distance (L) beyond the face as illustrated in figure 5-2.

The additional deflection beyond that which occurs at the specimen face can be calculated by assuming that the block rotates the same as the point on the specimen to which it is attached. For a given a/w value of a particular test specimen, the finite element displacements on the crack surface for the load line (EBv_L/P) can be obtained from table 5-1, where E is the modulus of elasticity of the material (30×10^6 psi for A533 B - Cl 1 material), B is the specimen thickness (inches), P is the load, and v_L is the displacement at the load line. By rearranging this expression, the load line compliance, v_L/P , for the specimen can be expressed in terms of the finite element displacements on the crack surface as

$$v_L/P = [EBv_L/P]/(B) \ 30 \times 10^6 \quad (5-3)$$

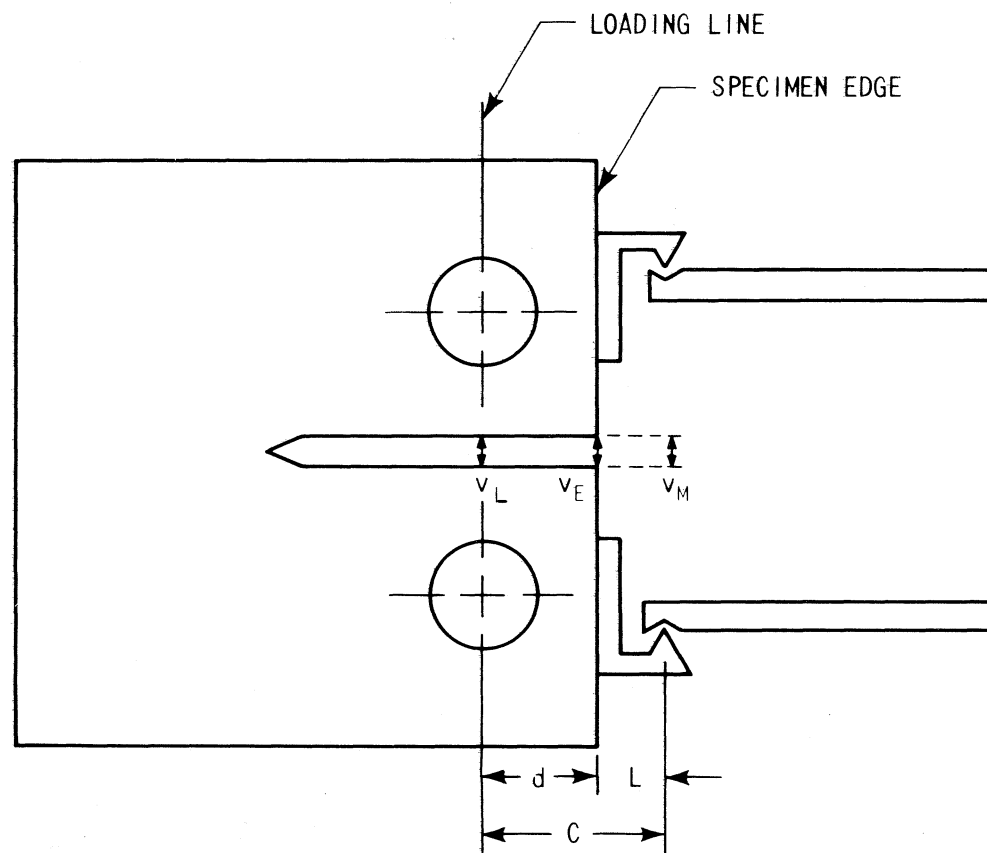
By using a straight line extrapolation to the measuring point of the displacement at some distance, L , in front of the specimen (see figure 5-2) an expression, for the measurement point compliance (v_m/P) of that particular test specimen can be written as

$$v_m/P = v_L/P \left(\frac{a + c}{a} \right) \quad (5-4)$$

This measurement point compliance is then plotted on the load-displacement curve of that particular specimen as illustrated in figure 5-3.

This measurement point compliance line is moved to the left or right to a position such that the curve is tangent to it at the point of deviation from linearity as shown in figure 5-4.

A new zero displacement point is now defined for the zero load condition. The portion of the compliance line up to P_B is now established as the slope of the linear portion of the load displacement curve. This is done because slightly irregular curves result when small-thickness ($< 1T$) compact tension specimens are tested dynamically or when a preload has



NOTES:

v_L CRACK SURFACE DISPLACEMENT AT THE LOAD LINE

v_E CRACK SURFACE DISPLACEMENT AT THE SPECIMEN EDGE

v_M CRACK SURFACE DISPLACEMENT AT THE MEASURING POINT

CRACK SURFACE DISPLACEMENT = DISPLACEMENT DUE TO LOADING ANYWHERE ALONG THE CRACK SURFACE
(e.g., v_L , v_E , v_M)

Figure 5-2. Typical Displacement Measuring Assembly Attached to a Compact Tension Specimen

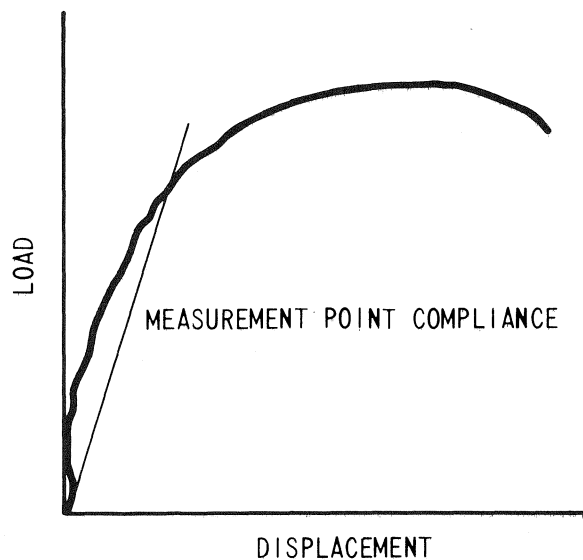


Figure 5-3. Measurement Point Compliance of a Typical Dynamic Load Displacement Curve for a Compact Tension Specimen Tested at Upper Shelf Temperatures

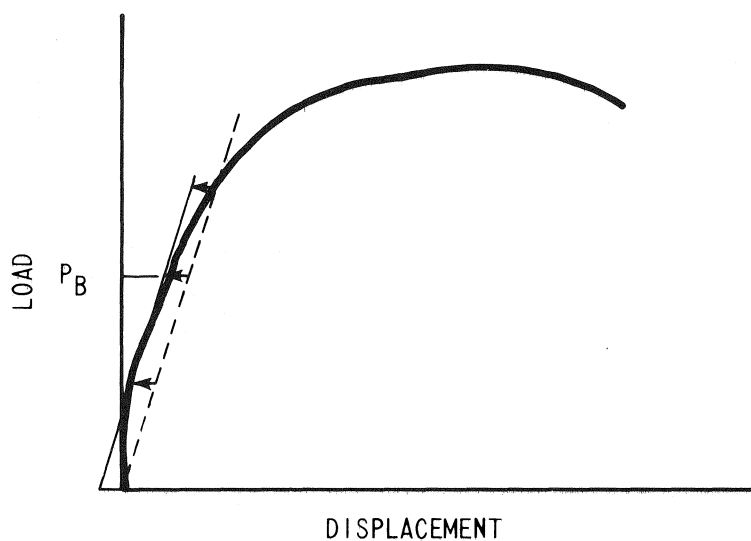


Figure 5-4. Adjustment of the Measurement Point Compliance Line to the Point where Deviation from Linearity is Presumed to Occur

been initially applied prior to testing. So, if the curve is now redrawn, it can then be analyzed to obtain a K_{1d} value for the particular specimen of interest at a given temperature as illustrated in figure 5-5.

5-3. CLEAVAGE CONTROLLED FRACTURE AND VALID K_{1d} TESTS

As mentioned earlier, the equivalent energy analysis is an acceptable analytical tool for evaluating load-deflection curves resulting from fracture toughness tests in which fracture is cleavage controlled. Fracture which is cleavage controlled exhibits a distinct drop at maximum load on the load-deflection trace. At temperatures characteristic of the lower fracture toughness shelf, the load-deflection traces are generally linear to maximum load at which time the crack initiation results in a distinct drop in load. This behavior is typical of static and dynamic testing at these temperatures.

As the testing temperature is increased from the lower shelf fracture toughness regime, more and more plasticity is associated with the fracture process during testing. This increased plasticity is reflected in the load-deflection trace of the test as nonlinear behavior.

Some linearity in the trace is maintained however even up to temperatures characteristic of the upper shelf. At these temperatures in which increased plasticity results, the load-deflection traces for the static test case eventually become more rounded and fail to show a distinct drop at maximum load (figure 5-6). Therefore, determining the onset of crack initiation for static tests at these higher temperatures becomes uncertain and a valid fracture toughness value (with respect to the equivalent energy method) is unobtainable.

Fortunately, the load-deflection traces for the dynamic tests maintain this distinct drop at maximum load up to temperatures characteristic of the onset of the upper shelf fracture toughness. The load-deflection traces are typical of that shown in figure 5-7 in which large amounts of nonlinear behavior occur prior to maximum load. At maximum load, the distinct drop in load not only implies that the fracture is cleavage controlled, but that crack initiation is occurring at maximum load, and therefore the equivalent energy analysis can be used to determine the dynamic fracture toughness at that temperature. This type of fracture behavior has been termed as nonlinear cleavage^[1] and occurs at these higher (elastic-plastic) test temperatures only in the dynamic case. Since, in this temperature range from the lower to the upper shelf fracture toughness regime, dynamic K_{1d} fracture toughness results are more conservative than the static case, the K_{1d} values obtained from these fracture toughness tests represent the most conservative values of fracture toughness at a given temperature.

1. Personal communication with W. A. Logsdon, Westinghouse Research and Development Center, Pittsburgh, Pa.

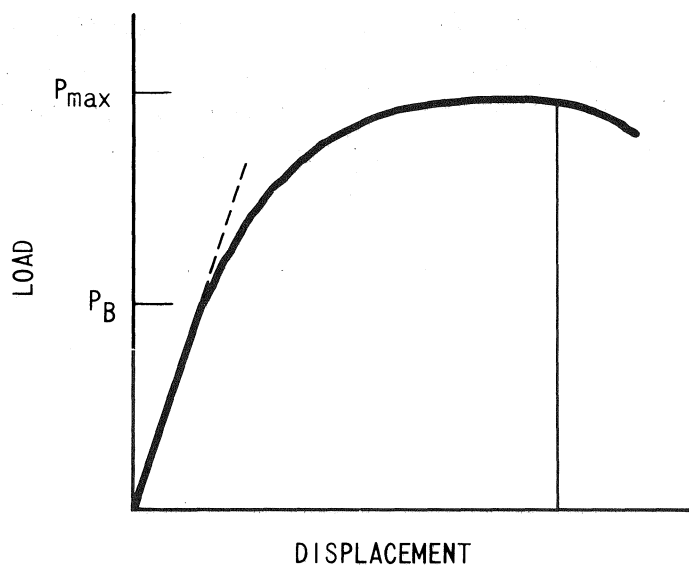


Figure 5-5. Modified Load-Displacement Curve Employing The Measurement Point Compliance As The Linear Region Of The Curve

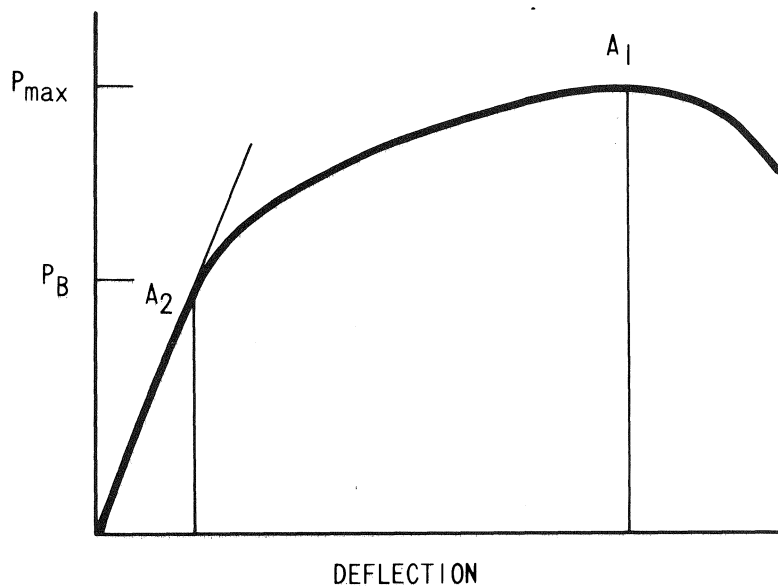


Figure 5-6. Load-Deflection Traces Typical of Upper Shelf Temperatures For Dynamically Performed Fracture Toughness Tests

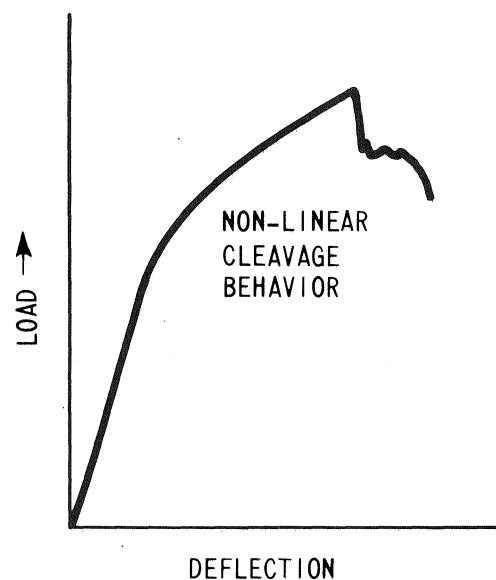


Figure 5-7. Load-Deflection Traces Typical of Shelf Initiation Temperatures For Dynamically Performed Fracture Toughness Tests

At temperatures greater than the initiation of the fracture toughness upper shelf, even the dynamic load-deflection traces fail to show a distinct drop at maximum load (figure 5-6) and hence the point of initiation of crack growth once again becomes ambiguous. This fully ductile fracture behavior cannot be characterized by linear-elastic techniques. The effects of applying linear-elastic analytical methods in a region in which fracture behavior is characterized by varying amounts of subcritical crack growth prior to instability is illustrated in figure 5-8^[1] where the upper shelf results are definitely affected by specimen size.

1. Witt, F. J. and Mager, T. R. "A Procedure for Determining Bounding Values on Fracture Toughness K_{Ic} at any Temperature," ORNL-TM-3894, October 1972

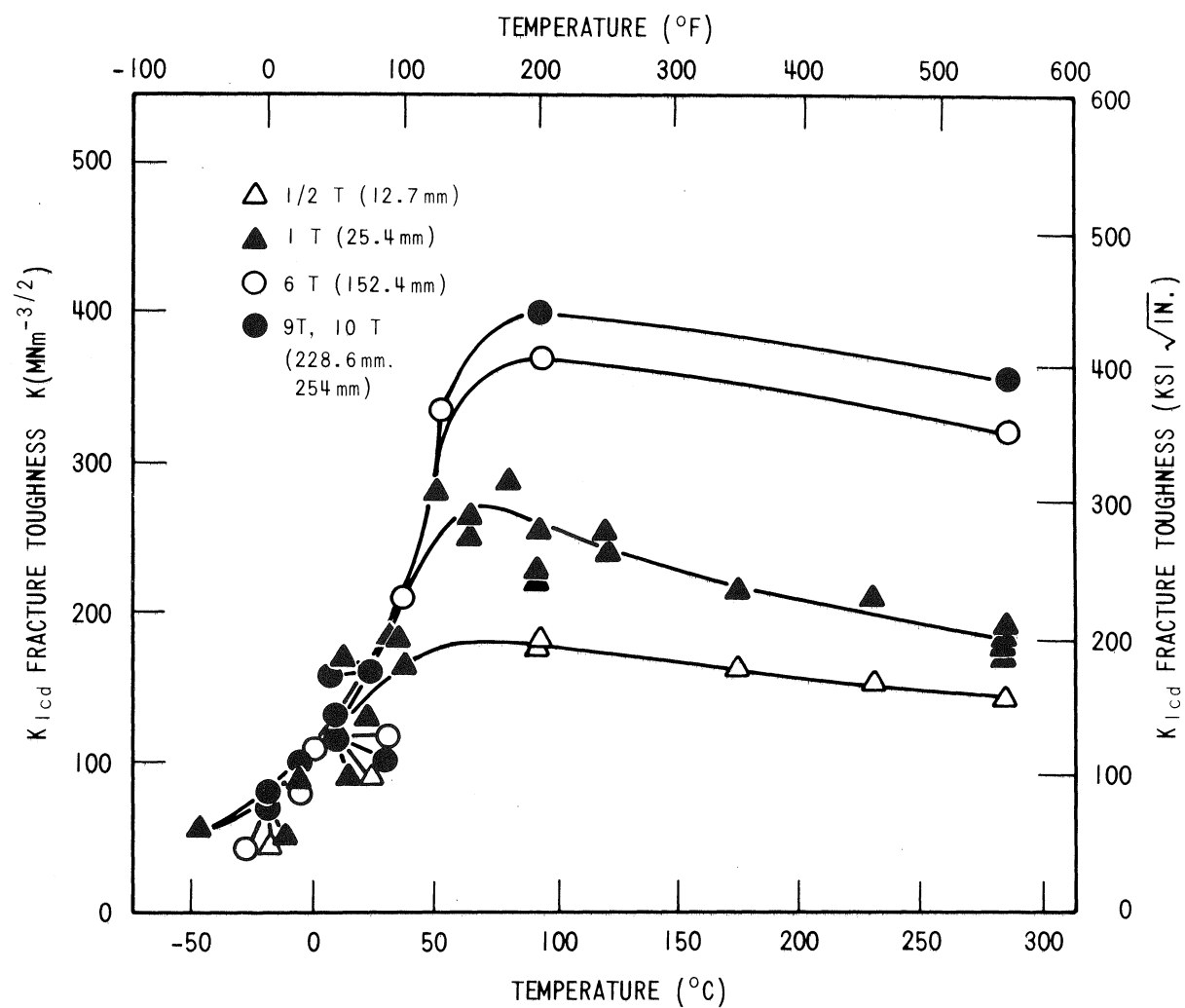


Figure 5-8. Variation of K_{Icd} as a Function of Temperature and Thickness^[1]

1. Witt, F. J. and Mager, T. R. "A Procedure for Determining Bounding Values on Fracture Toughness K_{Ic} at any Temperature," ORNL-TM-3894, October 1972

SECTION 6

TEST RESULTS

6-1. FRACTURE TOUGHNESS TEST RESULTS

The compact tension specimen test results are presented below according to specimen size.

6-2. 0.394T-Compact Tension Specimens

Table 6-1 lists the charpy thickness CT dynamic K_{1d} fracture toughness tests results for the strong direction (RW) and weak direction (WR) oriented irradiated plate material as well as for Heavy Section Steel Technology Program (HSST) Weldment W58 material. Also included in the table is the loading rate (\dot{K}), crack length, maximum load, and P_B . K_{1d} was evaluated for these specimens by using the equivalent energy concept explained earlier.

6-3. 1.9T-Compact Tension (RW) Specimens

Table 6-2 lists the dynamic K_{1d} fracture toughness test results for the RW oriented irradiated plate 02 specimens machined from the broken halves of the 4T-CT W58-4 specimen. In addition to the dynamic fracture toughness of this material, other information is included as in the 0.394T-CT test results. The lower loading rate ($\dot{K} = 10^2$ ksi $\sqrt{\text{in.}}/\text{sec}$) for specimen 5842 was a result of nitrogen leakage in the accumulator that supplies oil to the dump valve. Therefore, there was an insufficient amount of oil to move the valve at high speed.

6-4. 4T-Compact Tension Specimen Dynamic Test Results

Table 6-2 also lists the dynamic K_{1d} fracture toughness test results for the various 4T-CT irradiated specimens. Other important fracture toughness data are also included in the table. It should be noted that 4T weld specimen W58-1 did not break during testing even though the K_{1d} was $237.0 \text{ MNm}^{-3/2}$ ($215.7 \text{ ksi } \sqrt{\text{in.}}$). Specific results of this test are presented later in the report.

Initially, some concern was shown in regard to water present in the shipping cask containing the 4T-CT specimens. About 3 quarts of water were found at the bottom of the cask upon opening at the Westinghouse R&D hot cell facility. This volume of water was sufficient to immerse the two bottom 4T-CT specimens in the cask (W58-3 and 02GA-441) to slightly

TABLE 6-1
IRRADIATED DYNAMIC FRACTURE TOUGHNESS DATA RESULTS FOR THE
SMALL-THICKNESS COMPACT TENSION SPECIMENS

Specimen Designation	Orientation	Thickness mm, (in.)	Test Temp. °C, (°F)	Crack Length mm, (in.)	P_B ($\times 10^3$) kg (lb)		b	P_{max} ($\times 10^3$) kg (lb)		K_{1d} MNm ^{-3/2} , (ksi $\sqrt{\text{in.}}$)	\dot{K} ($\times 10^4$) MNm ^{-3/2} /sec, (ksi $\sqrt{\text{in.}}$ /sec)
25	RW	10 (0.394)	23.9 (75)	9.561 (0.3764)	0.53	(1.175)	1.0	0.53	(1.175)	33.1 (30.1)	1.43 (1.3)
28	RW	10 (0.394)	23.9 (75)	9.578 (0.3771)	0.57	(1.275)	1.0	0.57	(1.275)	36.0 (32.8)	0.77 (0.7)
26	RW	10 (0.394)	93.3 (200)	9.723 (0.3828)	0.95	(2.110)	1.0	0.95	(2.110)	61.6 (56.1)	0.99 (0.9)
31	RW	10 (0.394)	93.3 (200)	10.706 (0.4215)	0.51	(1.140)	2.47	1.06	(2.350)	60.4 (55.0)	1.65 (1.5)
27	RW	10 (0.394)	148.9 (300)	10.264 (0.4041)	0.97	(2.150)	2.0	1.14	(2.540)	95.9 (87.3)	1.65 (1.5)
32	RW	10 (0.394)	148.9 (300)	9.794 (0.3856)	1.04	(2.300)	3.19	1.24	(2.760)	120.3 (109.5)	1.43 (1.3)
29	RW	10 (0.394)	287.8 (550)	10.909 (0.4295)	0.79	(1.750)	3.68	1.04	(2.300)	116.5 (106.0)	1.87 (1.7)
71	WR	10 (0.394)	23.9 (75)	10.597 (0.4172)	0.53	(1.176)	1.0	0.53	(1.176)	38.9 (35.4)	0.88 (0.8)
76	WR	10 (0.394)	23.9 (75)	10.686 (0.4207)	0.48	(1.075)	1.0	0.48	(1.075)	35.8 (32.6)	1.32 (1.2)
73	WR	10 (0.394)	65.6 (150)	10.409 (0.4098)	0.63	(1.394)	1.94	0.71	(1.575)	62.6 (57.0)	1.54 (1.4)
70	WR	10 (0.394)	121.1 (250)	10.721 (0.4221)	0.60	(1.330)	7.12	0.99	(2.200)	119.8 (109.0)	0.77 (0.7)
75	WR	10 (0.394)	121.1 (250)	10.569 (0.4161)	0.96	(2.135)	1.40	1.09	(2.430)	84.1 (76.5)	
74	WR	10 (0.394)	204.4 (400)	11.044 (0.4348)	0.84	(1.875)	4.26	1.08	(2.410)	137.4 (125.0)	1.98 (1.8)
77	WR	10 (0.394)	204.4 (400)	10.483 (0.4127)	0.90	(2.000)	2.92	1.09	(2.415)	110.4 (100.5)	0.88 (0.8)
W22	Weld	10 (0.394)	23.9 (75)	9.741 (0.3835)	1.06	(2.350)	1.65	1.29	(2.860)	87.4 (79.5)	1.21 (1.1)
W23	Weld	10 (0.394)	23.9 (75)	10.526 (0.4144)	0.68	(1.500)	7.26	1.07	(2.373)	131.9 (120.0)	0.77 (0.7)
W25	Weld	10 (0.394)	93.3 (200)	10.749 (0.4232)	0.61	(1.350)	6.34	1.01	(2.240)	115.4 (105.0)	1.98 (1.8)
W26	Weld	10 (0.394)	93.3 (200)	10.747 (0.231)	0.70	(1.550)	6.28	1.13	(2.500)	131.9 (120.0)	1.76 (1.6)

TABLE 6-2
IRRADIATED FRACTURE TOUGHNESS DATA FOR THE 1.9- AND
4T-COMPACT TENSION SPECIMENS

Specimen Designation	Orientation	Thickness mm, (in.)	Test Temp. °C, (°F)	Crack Length mm, (in.)	P_B ($\times 10^3$) kg (lb)		b	P_{max} ($\times 10^3$) kg (lb)		K_{1d} MNm ^{-3/2} , (ksi $\sqrt{\text{in.}}$)	\dot{K} ($\times 10^4$) MNm ^{-3/2} /sec, (ksi $\sqrt{\text{in.}}$ /sec)
5844	RW	48.3 (1.9)	93.3 (200)	49.89 (1.964)	11.93	(26.5)	1.0	11.93	(26.5)	79.1 (72)	3.52 (3.2)
5843	RW	48.3 (1.9)	131.1 (268)	49.38 (1.944)	16.10	(35.78)	2.87	24.21	(53.8)	179.1 (163)	1.26 (1.15)
5841	RW	48.3 (1.9)	162.8 (325)	50.29 (1.980)	14.31	(31.79)	7.18	27.05	(60.1)	258.2 (235)	3.63 (3.3)
5842	RW	48.3 (1.9)	162.8 (325)	49.45 (1.947)	14.12	(31.38)	8.1	28.67	(63.7)	263.7 (240)	0.011 (0.01)
W58-3	RW	101.6 (4)	137.8 (280)	104.90 (4.130)	32.63	(72.5)	5.53	67.50	(150.0)	167.1 (152.1)	1.57 (1.43)
02GA442	WR	101.6 (4)	121.1 (250)	105.16 (4.140)	40.64	(90.3)	2.55	65.25	(145.0)	141.9 (129.1)	1.73 (1.57)
02GA441	WR	101.6 (4)	143.3 (290)	115.57 (4.550)	49.50	(110.0)	4.83	85.77	(190.6)	282.4 (257.0)	1.87 (1.70)
W58-2	Weld	101.6 (4)	37.8 (100)	105.31 (4.146)	43.65	(97.0)	1.23	46.35	(103.0)	106.3 (96.7)	0.88 (0.80)
W58-1	Weld	101.6 (4)	73.9 (165)	106.04 (4.175)	52.20	(116.0)	4.19	91.35	(203.0)	>237.0 ^[a] (>215.7)	1.21 (1.1)

a. Did not break

below the machined notch. The specimens in the water were observed to have three or four water marks on their sides in addition to extensive visible scale. Specimens out of the water appeared to only have spotted areas of slight corrosion. Figure 6-1 illustrates the condition of the specimen in and out of the water. The possibility of corrosion at the fatigue precrack tip area of the specimens was not considered severe enough to necessitate extension of the fatigue precrack tip away from the potential corrosion area. Upon breaking the first specimen (W58-3), the fatigue precrack tip area was found free of corrosion, and it was concluded that the presence of the water in the cask posed no influence due to corrosion on the dynamic K_{1d} fracture toughness test results.

As mentioned earlier, weld specimen W58-1 failed to break at 74°C (165°F) even though a $99 \times 10^3 \text{ kg}$ ($203 \times 10^3 \text{ lb}$) dynamic load was applied. The fact that this occurred offered opportunity to evaluate the amount of subcritical crack growth which presumably occurs at these temperatures prior to maximum load in 4T-CT and other large thickness specimens.

First, the crack tip area on the specimen side was polished and photographed (see figure 6-2). No branching at the crack tip was apparent, as was the case in Shabbits' [1] 8T-CT specimen which failed to break dynamically. The specimen was cooled to -18°C (0°F) and broken in the completely brittle mode. Plastic replicas of the fatigue precrack tip area were made to determine if any subcritical crack growth resulted from this test using scanning electron microscopy. The typical appearance of this region is shown in figure 6-3. Area "A" is characteristic of the fatigue precracking event prior to testing. Area "C" is typical cleavage appearance as would be expected since it was broken at -18°C (0°F). The zone between these two areas, area "B", exhibits a fracture appearance characteristic of area "A" (the fatigue precrack appearance) upon closer examination. If subcritical crack growth had occurred, a ductile type fracture zone should have resulted between areas "A" and "C" with an appearance typical of elastic-plastic or plastic fracture expected from a test conducted at 75°C (165°F) for this irradiated material. Since this ductile fracture appearance is not present, and area "B" is similar to area "A", it is concluded [2] that this small zone (area "B") is associated with the fatigue precracking event and that no subcritical crack growth has occurred.

1. Shabbits, W. O., "Dynamic Fracture Toughness Properties of Heavy Section A533 Grade B, Class 1 Steel Plate," HSST Technical Report No. 13, WCAP-7623, December 1970

2. Personal communication with D. M. Moon, Westinghouse Research and Development Center, Pittsburgh, Pa.

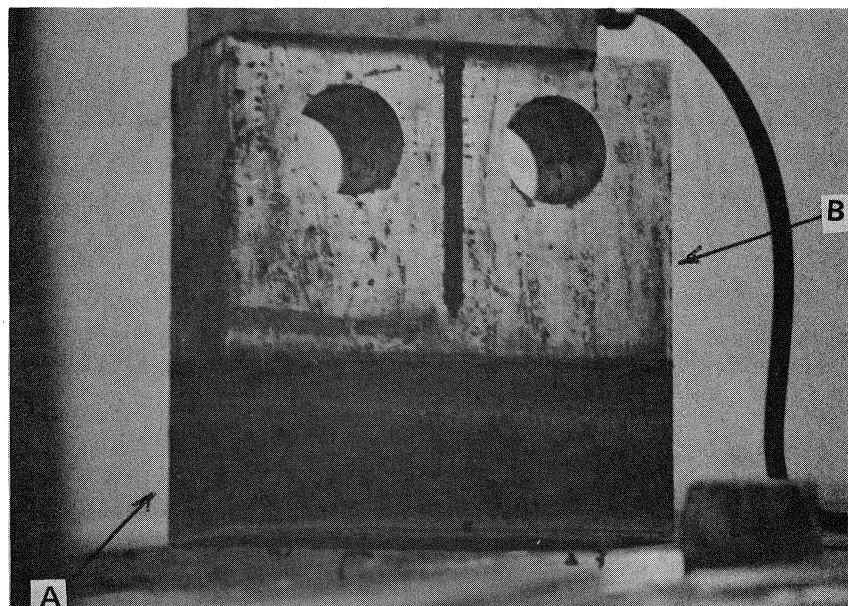


Figure 6-1. Immersed (a) and Unimmersed (b) Condition Of The HSST Irradiated 4T-CT Specimens As Received In The Shipping Cask At the Westinghouse R&D Hot Cell Facility



Figure 6-2. Close-up Photograph Of The Fatigue Precrack Tip Area On The Side Of The Unbroken Irradiated Weldment 4T-CT Specimen W58-1 Tested Dynamically At 74°C (165°F)

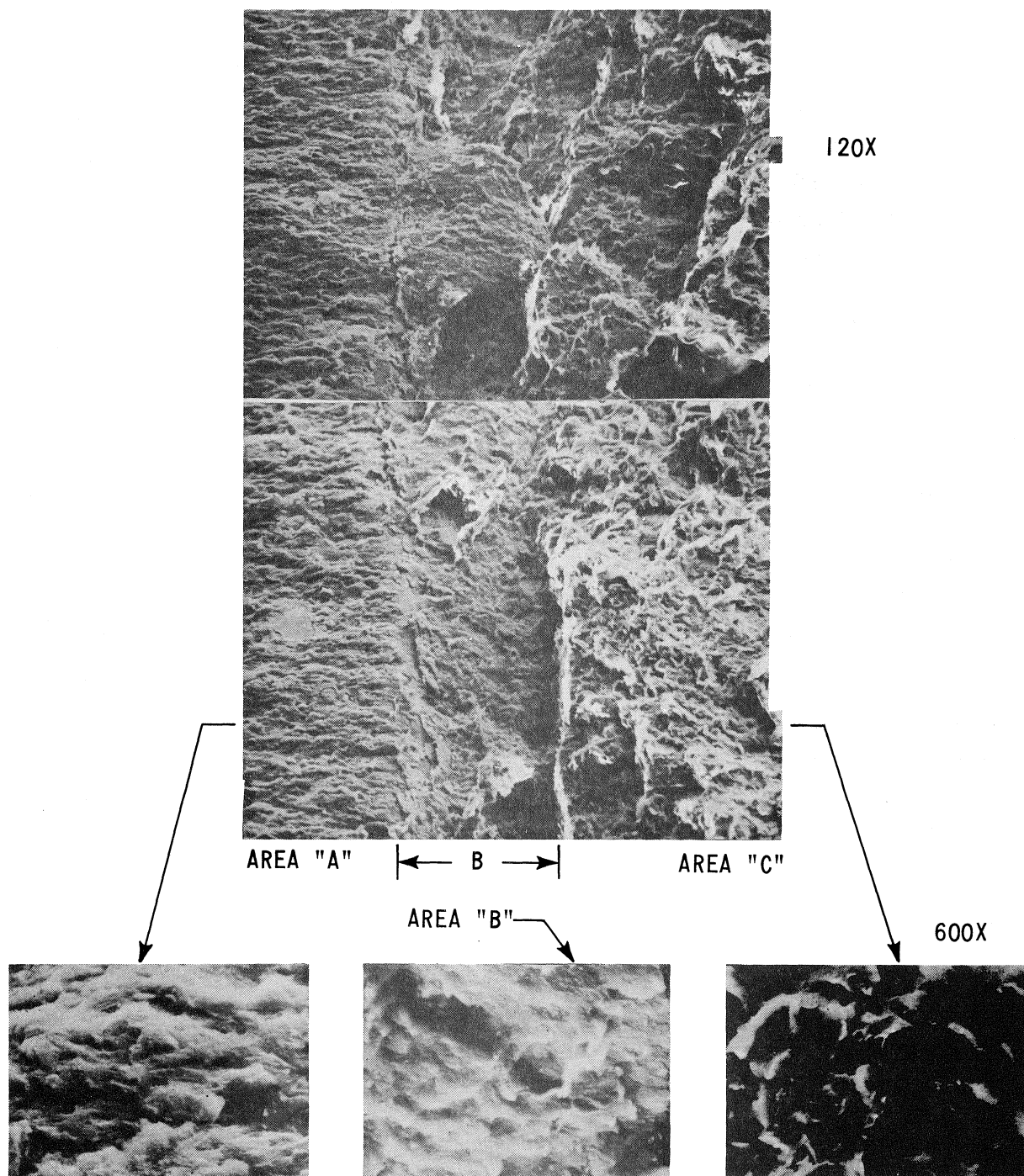


Figure 6-3. Three Fracture Areas Of W58-1 4T-CT Weldment Specimen After Break At $-18^{\circ}\text{C}(0^{\circ}\text{F})$. S.E.M. Photographs Illustrate Fracture Areas Characteristic Of: A, Fatigue Precracking; B, Fatigue Precracking; and C, Cleavage Failure

6-5. Previous Static Test Result for Irradiated 4T-CT Specimen W58-4

J. A. Williams^[1] at the Hanford Engineering Development Laboratory (HEDL) in Richland, Washington, performed the static K_{Ic} test for the irradiated HSST Plate 02 strong direction (RW) specimen W58-4. Results of this test showed that this material exhibited a K_{Ic} fracture toughness of $88 \text{ MNm}^{-3/2}$ (80 ksi $\sqrt{\text{in.}}$) at 93.3°C (200°F). The broken halves of this specimen were machined into four 1.9T-CT specimens (RW orientation) as mentioned earlier.

6-6. DOSIMETRY RESULTS

The compact tension specimen dosimetry results are presented below.

6-7. 0.394T-Compact Tension Specimens

The fluence that the 0.394T-CT specimens received was evaluated using the dosimetry wires in the pin holes of the 4T-CT specimens. The U^{238} dosimeter blocks located in 4T-CT specimen pin holes numbers 1, 3, 5, 7, 9 and 11, the Fe, Ni gradient wires located in positions 1 through 18, and the Al (0.15% Co) gradient wires located in positions 13 through 18 (see figure 2-9) were removed and sent to the Westinghouse Advanced Reactor Division's Analytical Laboratories at Waltz Mill. Tables 6-3 through 6-6 list the results of the analyses.

Analysis of these data with respect to location in the Battelle Research Reactor resulted in fluence calculations for the 0.394T-CT specimens ranging from $2.2\text{-}2.5 \times 10^{19} \text{ n/cm}^2$ ($E > 1 \text{ Mev}$). Fluences for the larger 1.9T and 4T compact tension specimens at the crack tip location were determined from drillings taken at the fatigue crack tip area. Results of these tests follow.

6-8. 1.9T-CT (RW) Specimens

Drillings were taken normal to the fatigue precrack area at the fatigue crack front at both edges (the zero and 1.9-inch thickness location) of each specimen and analyzed for fluence received during irradiation. The fluence analysis results given in table 6-7 were based on the Mn^{54} activity (DPS/mg-Fe).^[2] The average fluence incurred by these specimens was determined to be $4.47 \times 10^{19} \text{ n/cm}^2$, which would be expected since the 1.9T-CT crack tips were closer to the test reactor core midplane location than the 0.394T-CT specimens located in the 4T-CT specimen pin-holes (see figure 2-11).

-
1. Williams, J. A., "The Irradiated Fracture Toughness of ASTM A533, Grade B, Class 1 Steel Measured with a Four Inch Thick Compact Tension Specimen," HSST Program Technical Report No. 36, HEDL-TME 75-10, June 1975
 2. Yanichko, S. E., Mager, T. R., Kang, S., "Analysis of Capsule R from the Rochester Gas & Electric Corporation R. E. Ginna, Unit No. 1 Reactor Vessel Radiation Surveillance Program," WCAP 8421, December 1974

TABLE 6-3
DOSIMETRY RESULTS OF Cs¹³⁷

Dosimeter Block No.		Cs ¹³⁷ DPS/mg of U ²³⁹ (on 2/1/74); x 10 ³ ± 10%
1	74-258	1.51
3	74-259	1.99
5	74-260	0.95
7	74-261	1.46
9	74-262	0.99
11	74-263	1.48

TABLE 6-4
Co⁶⁰ DOSIMETRY RESULTS OF THE Al-Co DOSIMETER WIRES

Sample No.	Co ⁶⁰ DPS/mg of Al-Co Wire ± 10% ^[a] (on 1/31/74); x 10 ⁴				
	A	B	C	D	E
W58-1	7.10	4.03	3.28	3.84	6.57
W58-2	7.63	4.31	3.40	3.99	6.67
W58-3	6.37	3.68	3.12	3.99	7.04
W58-4	6.74	4.00	3.51	4.21	7.42
02GA441	5.95	3.33	3.06	3.73	6.55
02GA442	6.17	3.57	3.23	4.42	7.62

a. Each Al-Co wire was cut into approximately 18.8 mm segments (A through E).

TABLE 6-5
Mn⁵⁴ DOSIMETRY RESULTS OF Fe DOSIMETER WIRES

Sample		Mn ⁵⁴ DPS/mg \pm 10% ^[a] (on 1/30/74); $\times 10^4$				
		A	B	C	D	E
Shim No.	1	1.85	1.52	1.52	1.69	2.24
	2	2.08	1.59	1.39	1.44	1.72
	3	2.22	1.72	1.54	1.62	1.98
	4	2.20	1.67	1.50	1.56	1.84
	5	1.60	1.29	1.24	1.35	1.75
	6	1.80	1.45	1.35	1.48	1.82
	7	1.84	1.46	1.42	1.55	1.92
	8	1.75	1.44	1.38	1.52	1.99
	9	1.62	1.28	1.14	1.20	1.44
	10	1.48	1.22	1.14	1.22	1.50
	11	1.66	1.35	1.27	1.40	1.76
	12	1.73	1.37	1.23	1.30	1.62
W-58-1		3.10	2.39	2.04	2.00	2.40
W-58-2		3.25	2.45	2.18	2.17	2.64
W-58-3		2.45	1.97	1.89	2.01	2.59
W-58-4		2.67	2.15	2.04	2.24	2.83
02GA-441		2.17	1.75	1.60	1.71	2.19
02GA-442		2.39	1.87	1.72	1.89	2.40

a. Fe wire was cut into approximately 18.8 mm segments (A through E); all activity results are per mg of wire.

TABLE 6-6
Co⁵⁸ DOSIMETRY RESULTS OF Ni DOSIMETER WIRES

Sample		Co ⁵⁸ DPS/mg of wire \pm 10% ^[a] (on 2/5/74); $\times 10^5$				
		A	B	C	D	E
Shim No.	1	2.99	2.26	3.19	1.79	1.95
	2	2.74	2.12	1.78	1.67	1.82
	3	3.07	2.34	1.97	1.88	2.08
	4	3.02	2.33	1.93	1.79	1.99
	5	1.79	1.52	1.52	1.73	2.21
	6	1.98	1.69	1.64	1.84	2.33
	7	2.02	1.74	1.69	1.90	2.45
	8	1.90	1.68	1.66	1.94	2.52
	9	1.19	0.93	0.84	0.86	1.02
	10	1.06	0.86	0.81	0.89	1.08
	11	1.17	0.98	0.91	1.00	1.21
	12	1.26	0.99	0.90	0.94	1.12
W-58-1		3.93	2.97	2.48	2.38	2.63
W-58-2		4.14	3.17	2.64	2.52	2.82
W-58-3		2.71	2.32	2.30	2.62	3.37
W-58-4		2.90	2.48	2.46	2.84	3.68
02GA441		1.56	1.25	1.14	1.22	1.51
02GA442		1.69	1.36	1.26	1.35	1.68

a. Each Ni wire was cut into approximately 18.8 mm segments (A through E).

TABLE 6-7
FAST NEUTRON [E > 1.0 Mev] FLUENCE LEVELS DERIVED
FROM THE 1.9T-CT DRILLING ACTIVITIES

Sample No.	Mn ⁵⁴ Activity (DPM/mg-Fe) ± 10% (6/5/75 @ 15:00); x 10 ⁵	Fluence (n/cm ²) x 10 ¹⁹	Average (n/cm ²) x 10 ¹⁹
5841A	4.60	3.94	4.46
B	7.57	4.98	
5842A	6.78	4.45	4.14
B	4.48	3.84	
5843A	8.30	5.45	4.69
B	4.58	3.93	
5844A	4.44	3.80	4.61
B	8.25	5.42	

6-9. 4T-CT Specimens

Drillings were taken from both sides and the center areas of the fatigue precrack tip of these specimens. The fluence analysis results are given in table 6-8. The average fluence received by these specimens was determined to be 4.29×10^{19} n/cm². This result is consistent with fluences determined from the 0.394T-CT and 1.9T-CT specimens as the drilling location was between the other two areas. The variation in fluence across the fatigue crack front is also consistent with the fluence distribution shown in figure 2-11 based on the dosimetry results.

6-10. 4T-CT Specimen W58-4

Dosimetry analysis^[1] of this specimen was determined as shown in table 6-9. By averaging these fluence values, an average fluence of 3.65×10^{19} n/cm² is obtained, which is consistent relative to the lower fluences determined for the 0.39T-CT specimens located further from the midplane of the reactor core. The fact that the average fluence for this specimen is less than that of the other 4T specimens is due to the lack of surface fluence values in the average calculation. It should be noted that the center region fluences of all the 4T-CT specimens are in very good agreement. The variation in fluence in this specimen across the crack front is also in agreement with figure 2-11.

1. Williams, J. A., "The Irradiated Fracture Toughness of ASTM A533, Grade B, Class 1 Steel Measured with a Four Inch Thick Compact Tension Specimen," HSST Program Technical Report No. 36, HEDL-TME 75-10, June 1975

TABLE 6-8
FAST NEUTRON [E > 1.0 Mev] FLUENCE LEVELS DERIVED
FROM THE 4T-CT DRILLING ACTIVITIES

Sample No.	Mn ⁵⁴ Activity (2/2/76 @ 12:00) (DPS/mg-Fe) ± 10%	Fluence (n/cm ²) x 10 ¹⁹	Average (n/cm ²) x 10 ¹⁹
W58-1-1	5310	3.89	4.43
-2	4260	3.75	
-3	7620	5.65	
W58-2-1	5560	4.06	4.79
-2	4450	3.93	
-3	8600	6.39	
W58-3-1	7210	5.30	4.17
-2	3800	3.35	
-3	5160	3.86	
02GA441-1	5000	4.13	3.93
-2	3370	3.36	
-3	5110	4.30	
02GA442-1	4630	3.84	4.11
-2	3460	3.44	
-3	6010	5.05	

TABLE 6-9
IRRADIATION FLUENCE OF 4T-CT (101.6 mm) SPECIMEN W58-4,
IRRADIATED AT 287.8°C (550°F)^[a]

Distance from Face, mm	Fluence (n/cm ² x 10 ¹⁹) E > 1 Mev
13.2	3.98
32.0	3.48
50.8	3.38
69.6	3.46
88.4	3.94

a. Williams, J. A., "The Irradiated Fracture Toughness of ASTM A533, Grade B, Class 1 Steel Measured with a Four Inch Thick Compact Tension Specimen," HSST Program Technical Report No. 36, HEDL-TME 75-10, June 1975

SECTION 7

DISCUSSION OF RESULTS

7-1. UPPER SHELF AND TRANSITION TEMPERATURE EVALUATION OF K_{1d}

The ability of a fracture toughness test specimen to adequately measure the K_{1d} fracture toughness of a material from temperatures characteristic of the transition temperature to the upper shelf temperature has been explained in section 5. In summary, it was pointed out that a cleavage controlled fracture was necessary to obtain valid K_{1d} values using the equivalent energy analysis. Also, smaller thickness specimens tended to be limited in their measuring capacity at upper shelf temperatures (see figure 5-8), and resulted in overly conservative K_{1d} values at upper shelf temperatures. Figure 7-1 shows all the irradiated dynamic test data broken down into valid (cleavage controlled fracture) and invalid (no distinct drop at maximum load) data points.

7-2. Upper Shelf Evaluation

None of the valid irradiated dynamic test results are characteristic of the upper shelf fracture toughness. As mentioned earlier, to obtain valid results at these temperatures, J_{1c} testing would be required. It was also pointed out earlier that, when tests are performed at upper shelf temperature, the thickness of the specimen controlled the magnitude of the upper shelf results (figure 5-8). In the case of the irradiated Charpy thickness (10 mm) specimens, several tests were conducted at upper shelf temperatures. When analyzed using the equivalent energy method (using maximum load as the point of crack initiation) invalid dynamic fracture toughness (K_{1d}) values resulted. The range of the upper shelf K_{1d} values obtained from these 10 mm thick specimens was between 110 and 132 $\text{MNm}^{-3/2}$ and violated the ASME Section III K_{1R} curve. However, these values are those which would be expected with this size specimen, and when compared to the valid data obtained from the larger thickness specimen results, the unrealistic degree of conservatism which results from testing small thickness specimens at upper shelf temperatures is quite obvious. The larger specimen (valid) data show that the dynamic fracture toughness at temperatures characteristic of the onset of the upper shelf is well above 220 $\text{MNm}^{-3/2}$ which is well within the ASME Section III K_{1R} curve limits.

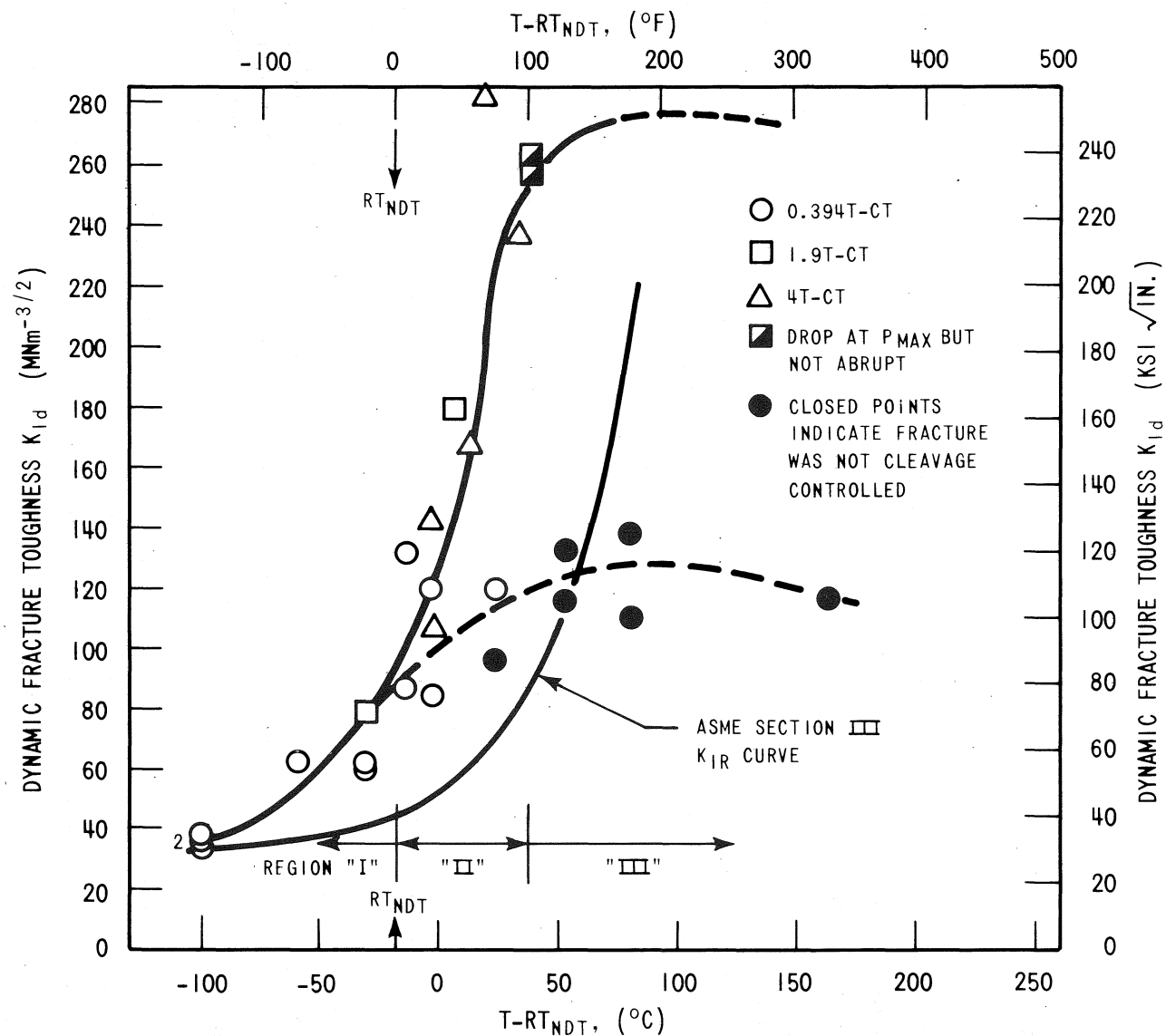


Figure 7-1. Irradiated Dynamic Fracture Toughness Results for HSST Plate 02 (WR, RW) and Weldment 58-A Material Showing the Extent of Cleavage Controlled Fracture as a Function of Temperature and Specimen Size

7-3. Transition Temperature Dynamic Toughness K_{1d}

In the transition temperature region, valid K_{1d} values for the irradiated plate and weldment material were obtained. The dynamic fracture toughness tests of the larger thickness specimens (1.9T and 4T-compact tension specimens) resulted in load-deflection curves which showed a distinct drop in load at maximum load, thereby indicating a cleavage controlled fracture. As mentioned earlier in section 5, valid K_{1d} results are obtained from this test behavior when analyzed using the equivalent energy analysis. Since these test results are valid, the specimen size should not have an influence in the K_{1d} values obtained. Figure 7-2 shows that the specimen size has no effect in this temperature region, as the 1.9T-CT data are in excellent agreement with the 4T-CT test result. Importantly, the K_{1d} data based on the larger thickness specimens shows that the upper shelf K_{1d} values are at least greater than $220 \text{ MNm}^{-3/2}$, the fracture toughness value at which the ASME section III K_{1R} curve ends. If it is assumed that the K_{1R} curve has an upper shelf of $220 \text{ MNm}^{-3/2}$, then, based on the valid, large thickness irradiated K_{1d} test results, the dynamic fracture toughnesses of plate 02 (RW, WR) and weldment W58-A are greater than the conservative K_{1R} curve.

7-4. Regions in the K_{1d} Versus Temperature Curve

As mentioned before, figure 7-1 is a composite curve of all the K_{1d} irradiated fracture toughness tests performed in this irradiation program. All the data has been adjusted with respect to the irradiated RT_{NDT} based on the irradiated Charpy data (figure 7-5, table 7-1). The curve shows which specimen tests exhibited a drop at maximum load during testing, thereby producing a valid equivalent energy K_{1d} result. The curve shows very well that the small thickness (0.394T-CT) test results become invalid at upper shelf temperatures at about the same temperature as the large thickness (1.9T-CT) results (showing a tendency for becoming invalid) do. This is not to say that the two 1.9T-CT data points on the curve are invalid, but the load-deflection traces for these two tests, although showing a drop at maximum load, showed a more gradual drop at maximum load. It is judged that if these two tests were performed several degrees higher, the load deflection would fail to show a drop at maximum load and therefore produce an invalid K_{1d} result.

Figure 7-1 also illustrates that the 1.9T and 4T-CT data were in excellent agreement with each other up to the initiation of the upper shelf. On the other hand, the Charpy thickness test specimens begin to lose their measuring capability at about $88 \text{ MNm}^{-3/2}$.

Figure 7-1 suggests a good method for determining valid lower bound dynamic K_{1d} fracture toughness values over a range of temperatures characteristic of the lower fracture toughness shelf up to the upper shelf. If the whole curve is divided into three regions (as shown on the curve in figure 7-1), the following test procedure can be applied to obtain lower bound valid K_{1d} toughness results:

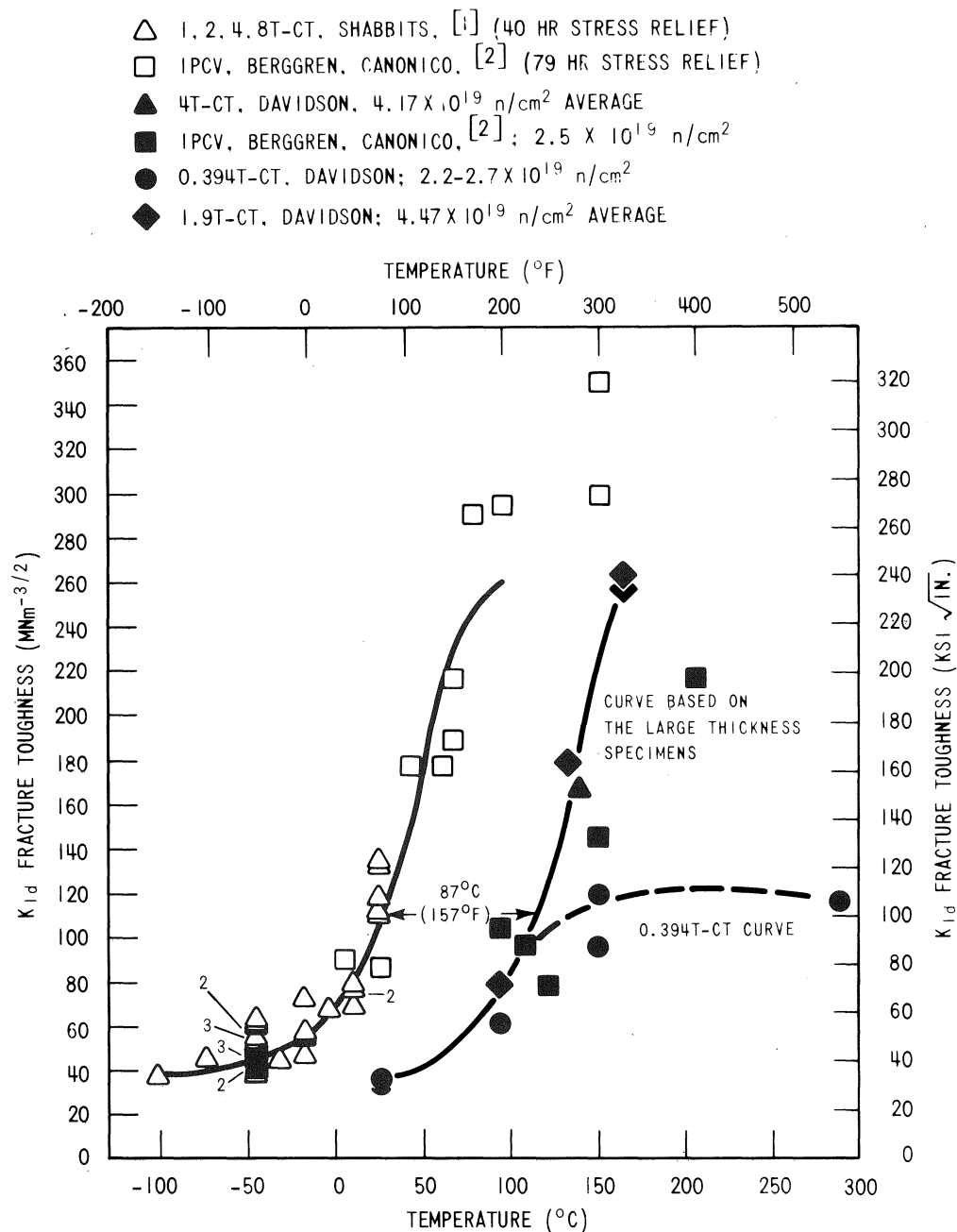


Figure 7-2. Dynamic Irradiated and Unirradiated Fracture Toughness Properties for HSST Plate 02, RW Oriented Material

1. Shabbits, W. O., "Dynamic Fracture Toughness Properties of Heavy Section A533 Grade B, Class 1 Steel Plate," HSST Technical Report No. 13, WCAP 7623, December 1970.
2. Whitman, G. D., "HSST Program Quarterly Progress Report on Reactor Safety Programs Sponsored by the NRC Division of Reactor Safety Research for April-June 1975," Vol. II, ORNL-TM-5021, September 1975.

TABLE 7-1
SHIFTS IN THE FRACTURE TOUGHNESS AND RT_{NDT} FOR THE HSST PLATE 02
AND WELDMENT W58 MATERIAL DUE TO IRRADIATION

Shift or Property	Material					
	Plate 02 (WR)		Plate 02 (RW)		Weld W58-A	
Copper	0.12 — 0.14		Same as WR		0.16 - 0.22	
Phosphorous	0.012 — 0.008		Same as WR		0.026	
Dynamic Shift ^[a]						
°C (°F)	90	(162)	87	(157)	61.1	(110)
Static Shift ^[a]						
°C (°F)	73.3	(132)	92.0	(165)	69.4	(125)
40.7 Joule (Average) Shift						
°C (°F)	99	(178)	95.5	(172)	37.8	(68)
67.8 Joule (Average) Shift						
°C (°F) Δ RT _{NDT}	102.2	(184)	96.6	(174)	39.4	(71)
Initial RT _{NDT}						
°C (°F)	4.44	(40)	—		-17.8	(0)
ΔRT _{NDT}						
°C (°F)	102.2	(184)	—		39.4	(71)
Final RT _{NDT}						
°C (°F)	106.6	(224)	—		21.6	(71)
NDT (unirradiated)						
°C (°F)	-17.8	(0)	-17.8	(0)	-17.8 ^[b]	(0)

a. Based on 110 MNm^{-3/2} (100 ksi √in.) shift.

b. NDT not performed; NDT = -17.8°C estimated using U.S. N.R.C. standard review plan sec. 5.3.2., pressure-temperature limits

- Region I** Dynamically test any size compact tension specimen or other fracture toughness specimen with mode one fracture toughness measuring capability. Region I appears to end at about the RT_{NDT} of the material.
- Region II** Dynamically test larger thickness specimens. Based on figure 5-8, 0.5T-CT specimens may be the limiting size to obtain meaningful valid K_{1d} results up to $220 \text{ MNm}^{-3/2}$. Region II appears to range between the RT_{NDT} of the material and the upper shelf initiation temperature. The upper shelf initiation temperature may be defined as that temperature at which the load-deflection trace from a dynamic fracture toughness tests fails to exhibit a distinct drop in load at maximum load.
- Region III** In Region III, obtaining meaningful, valid K_{1d} fracture toughness data is not possible from a single dynamic load-deflection trace. To obtain meaningful fracture toughness data in Region III, J_{1c} testing should be performed so that the initiation of crack growth (although stable) can be determined. In any event, the dynamic test case, which exhibits a higher effective yield strength due to the higher strain rates, may not necessarily be the most conservative. Fracture toughness results based on the equivalent energy analysis at upper shelf temperatures (Region III) are unrealistic and over conservative for small thickness specimen tests, as is evident in figure 7-1. Although Region III is a region in which the fracture toughness is presently difficult to define, the benefit of dynamic testing in Region II at least provides a means of establishing the onset of Region III and, at the same time, providing valid K_{1d} fracture toughness values up to the onset of Region III.

7-5. 4T-CT W58-1 AND SUBCRITICAL CRACK GROWTH EVALUATION

In the case of the 4T-CT weldment specimen, in which failure of the specimen did not occur after undergoing a crack tip dynamic stress intensity of $237 \text{ MNm}^{-3/2}$ ($215.7 \text{ ksi } \sqrt{\text{In.}}$), the opportunity arose to evaluate the extent, if any, of subcritical crack growth at a temperature characteristic of the onset of the K_{1d} fracture toughness upper shelf. After failing to break during testing, the specimen was broken to determine the extent of any subcritical crack growth. Upon examination (figure 6-3) of the fatigue precrack tip area, it was found that no subcritical crack growth had occurred. This implied that the upper shelf fracture toughness for the weldment material was valid and in excess of $237 \text{ MNm}^{-3/2}$. This result is important since it further shows the large degree of conservatism which results in using the Charpy thickness-CT specimens for evaluating the K_{1d} fracture toughness upper shelf.

7-6. SHIFT IN FRACTURE PROPERTIES

Presented in figures 7-2, 7-3, and 7-4 along with the irradiated dynamic fracture toughness results for the plate and weldment material are the unirradiated dynamic fracture toughness data. In all cases, the irradiation of the material resulted in pronounced shifts in the K_{1d} versus-temperature curves. This shift also occurred in the static fracture toughness (figures 7-6, 7-7, and 7-8) and in the Charpy V-notch impact energy (figure 7-5) of the same material. A summary of the various shifts in properties is presented in table 7-1.

7-7. HSST Plate 02 (RW orientation)

As mentioned earlier, the three different sized specimens received slightly different amounts of fluence. The Charpy thickness test specimens received $2.2\text{-}2.7 \times 10^{19} \text{ n/cm}^2$, the 1.9T-CT specimens received an average of about $4.5 \times 10^{19} \text{ n/cm}^2$, and the 4T-CT specimens received an average fluence of about $4.2 \times 10^{19} \text{ n/cm}^2$. Looking at the dynamic fracture toughness results for the RW oriented plate 02 specimens in figure 7-2, and considering only the valid test results (figure 7-1) for now, it can be seen that the differences in fluence received by the various sized specimens resulted in negligible differences in the shift of the dynamic fracture toughness curve. Similarly, when comparing the 4T-CT static fracture toughness test (average fluence of $3.7 \times 10^{19} \text{ n/cm}^2$) result performed by Williams to the lower fluence ($2.5 \times 10^{19} \text{ n/cm}^2$ average) small specimen results of Berggren and Williams (figure 7-6) the difference in fluence on the static irradiated fracture toughness curve appear to be no greater than the typical data scatter in the static curve as seen in the unirradiated data curve.

The shift in the dynamic fracture toughness properties (based on the average $110 \text{ MNm}^{-3/2}$ temperature) for the RW oriented plate material was 87°C (157°F) as shown in figure 7-2. For the static curve (figure 7-6) this shift was 92°C (165°F), relatively consistent with the

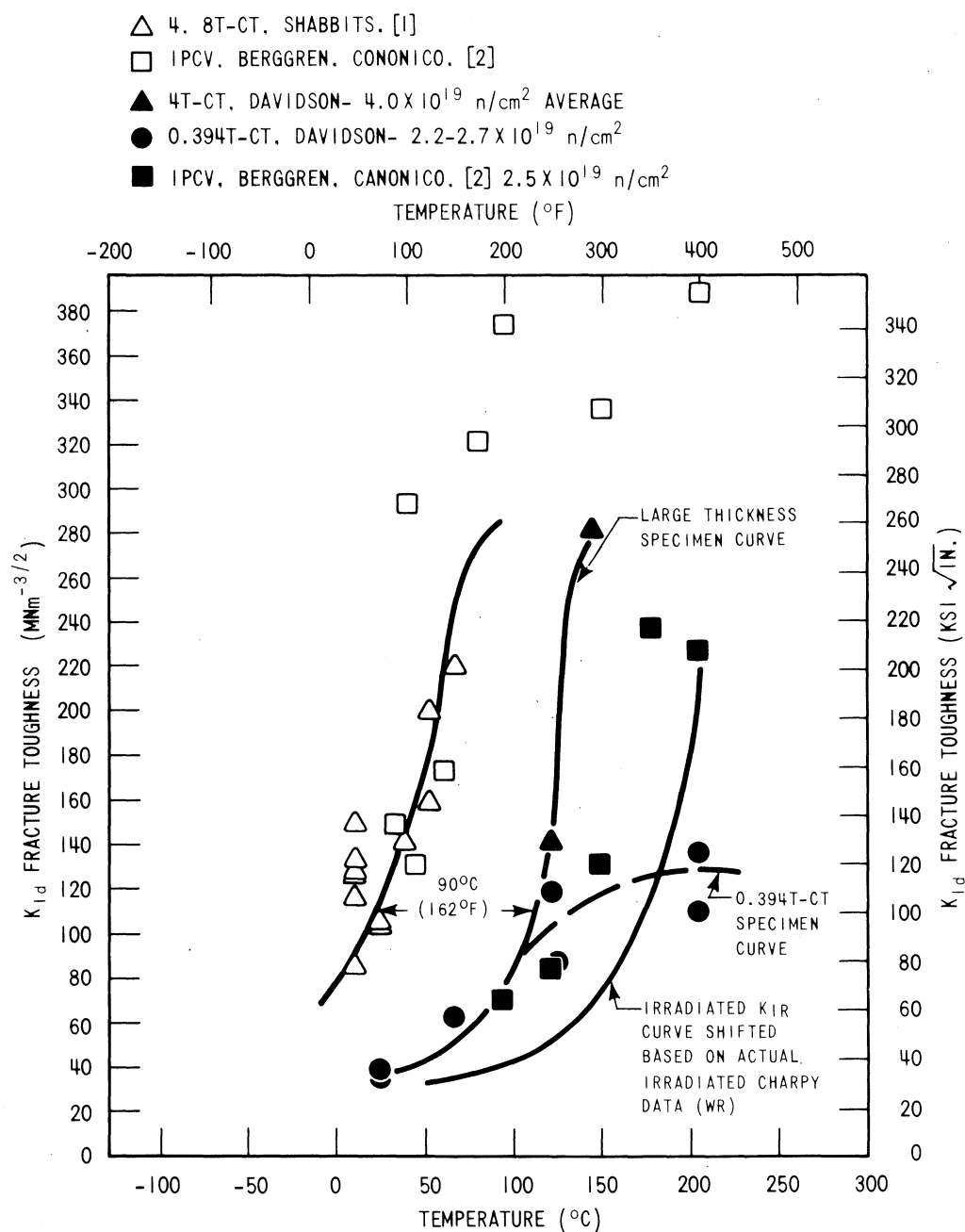


Figure 7-3. Dynamic Irradiated and Unirradiated Fracture Toughness Properties for HSST Plate 02, WR Oriented Material

1. Shabbits, W. O., "Dynamic Fracture Toughness Properties of Heavy Section A533 Grade B, Class 1 Steel Plate," HSST Technical Report No. 13, WCAP 7623, December 1970.
2. Whitman, G. D., "HSST Program Quarterly Progress Report on Reactor Safety Programs Sponsored by the NRC Division of Reactor Safety Research for April-June 1975," Vol. II, ORNL-TM-5021, September 1975.

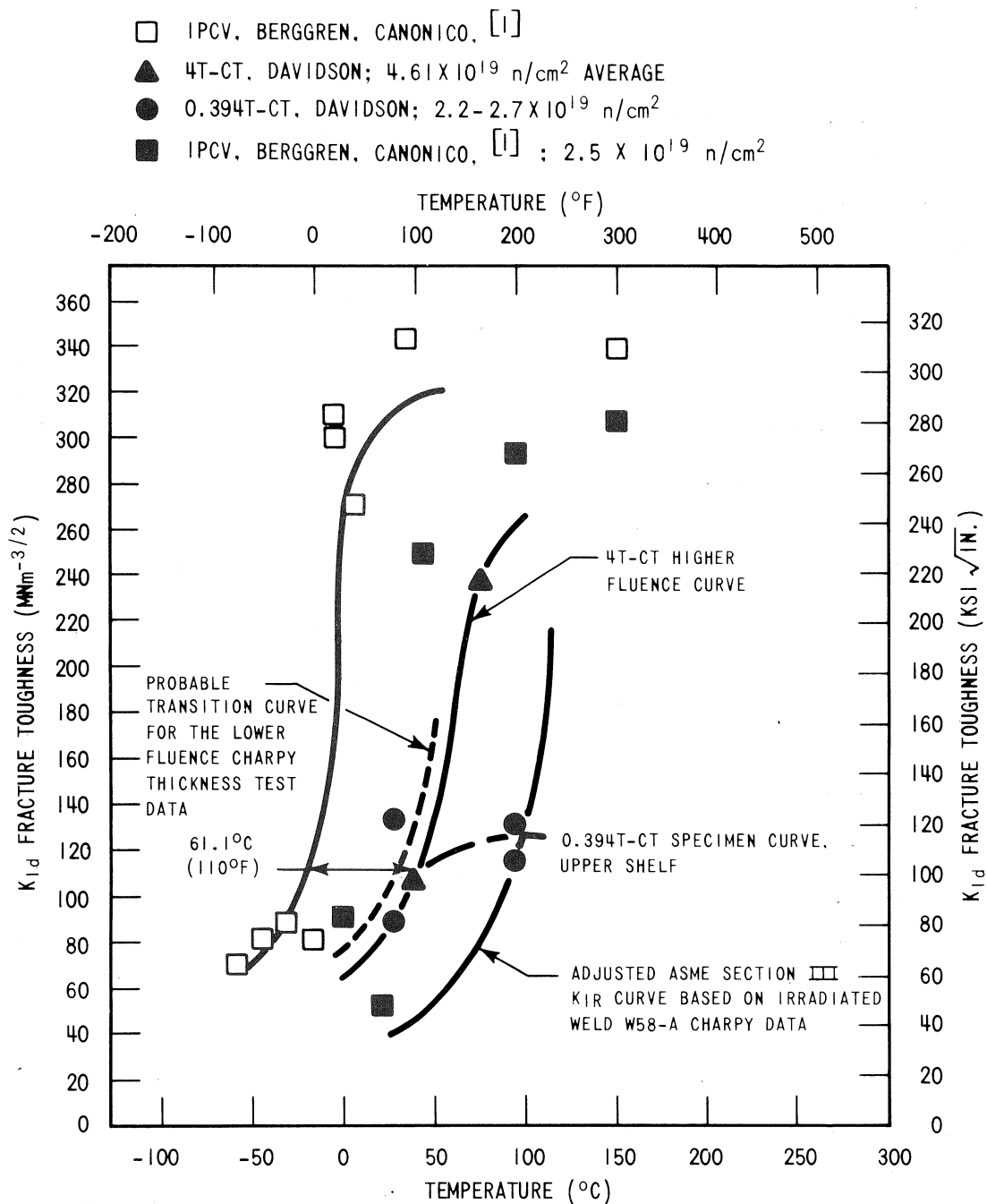


Figure 7-4. Dynamic Irradiated and Unirradiated Fracture Toughness Properties for HSST Weldment W58-A

1. Whitman, G. D., "HSST Program Quarterly Progress Report on Reactor Safety Programs Sponsored by the NRC Division of Reactor Safety Research for April-June 1975," Vol. II, ORNL-TM-5021, September 1975.

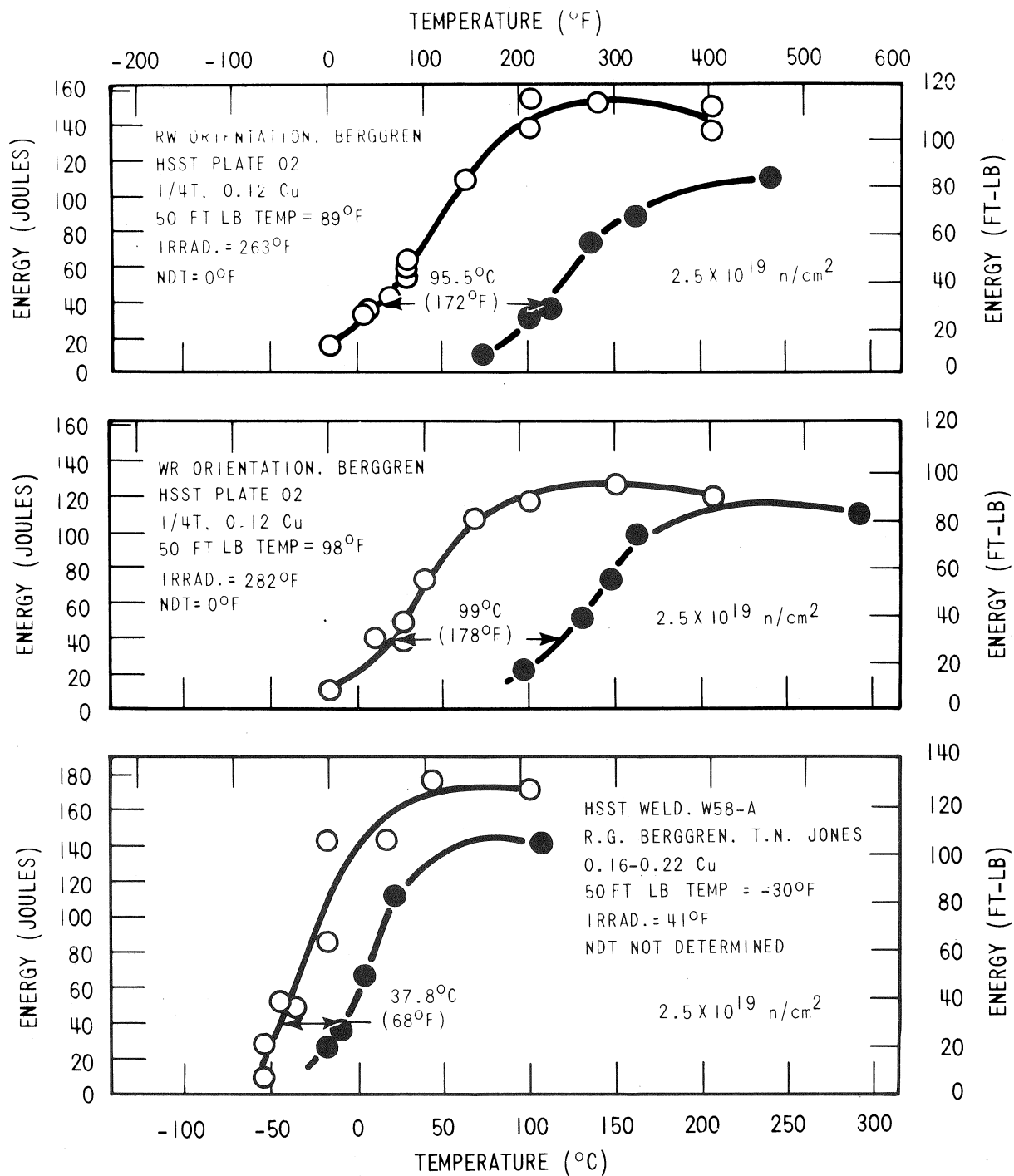


Figure 7-5. Irradiated and Unirradiated Charpy V-Notch Impact Curves for HSST Plate 02 and Submerged Arc Weldment W58-A

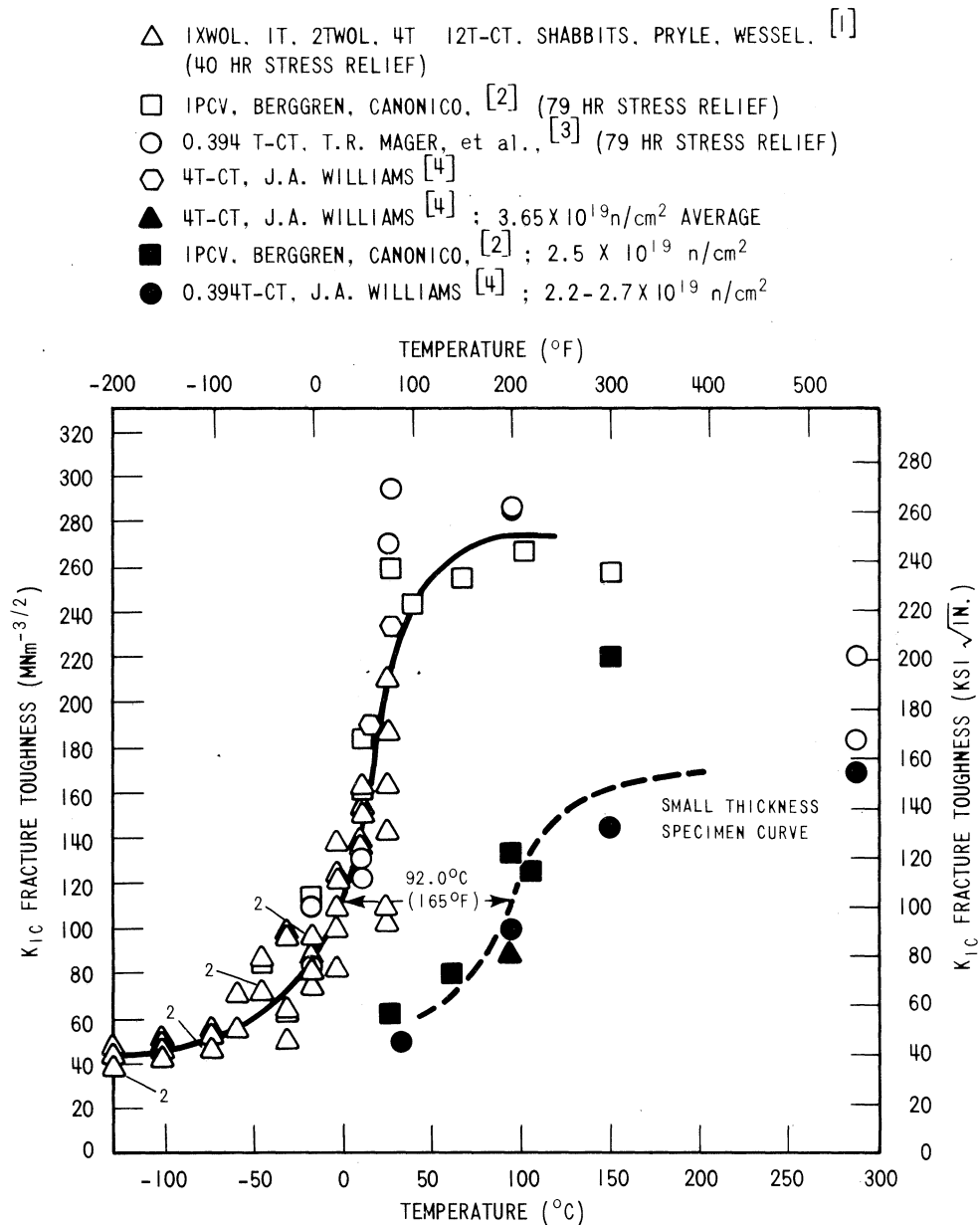


Figure 7-6. Static Irradiated and Unirradiated Fracture Toughness Properties for HSST Plate 02, RW Oriented Material

1. Shabbits, W. O., Pryle, W. H., Wessel, E. T., "Heavy Section Fracture Toughness Properties of A533 Grade B, Class 1 Steel Plate and Submerged Arc Weldment," HSST Technical Report No. 6, WCAP 7414, December 1969.
2. Whitman, G. D., "HSST Program Quarterly Progress Report on Reactor Safety Programs Sponsored by the NRC Division of Reactor Safety Research for April-June 1975," Vol. II, ORNL-TM-5021, September 1975.
3. "Quarterly Progress Report on Reactor Safety Programs Sponsored by the Division of Reactor Safety Research for April-June 1974," ORNL-TM-4655, August 1974.
4. Williams, J. A., "The Irradiated Fracture Toughness of ASTM A533, Grade B, Class 1 Steel Measured with a Four Inch Thick Compact Tension Specimen," HSST Program Technical Report No. 36, HEDL-TME 75-10, June 1975.

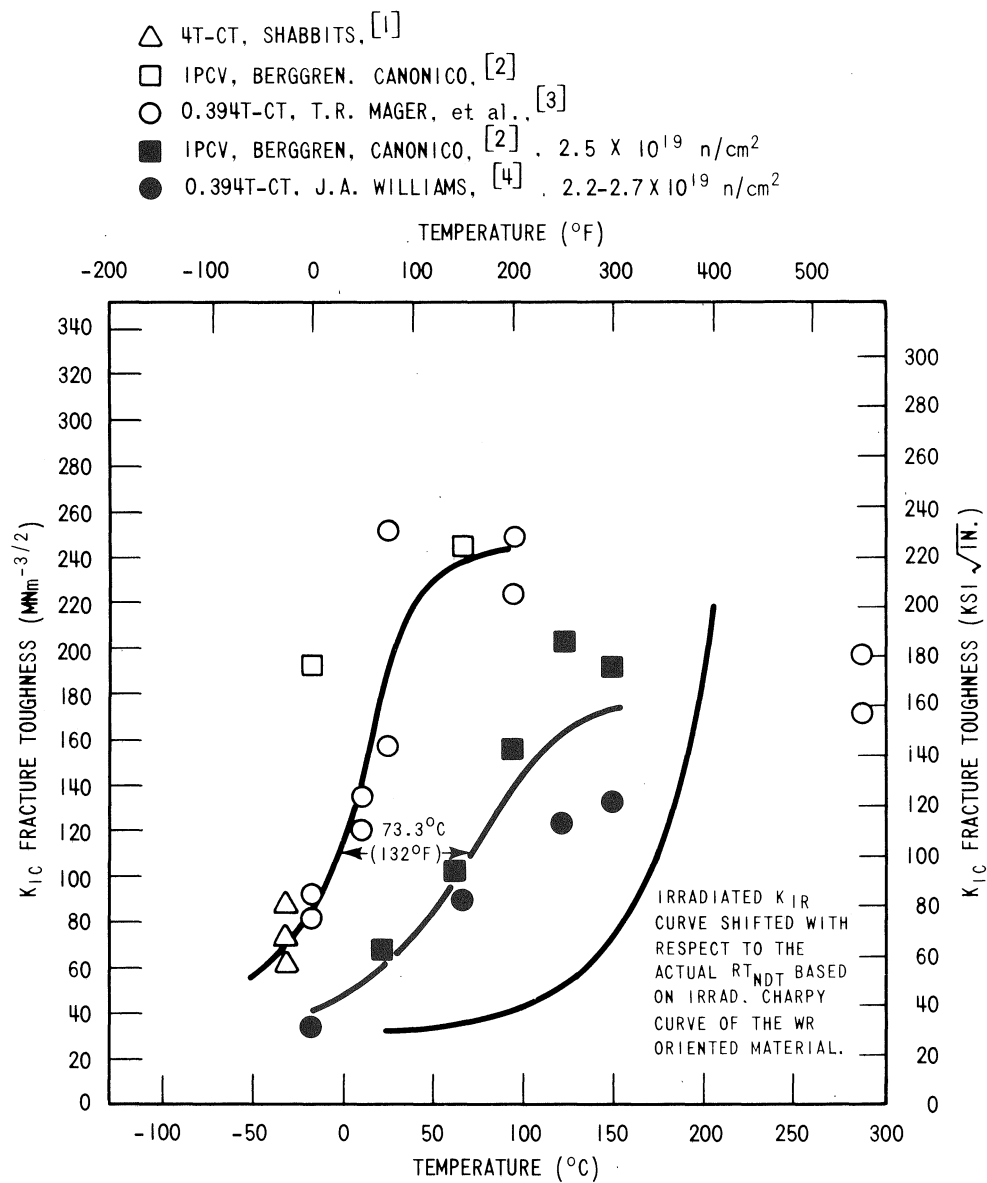


Figure 7-7. Static Irradiated and Unirradiated Fracture Toughness Properties for HSST Plate 02, WR Oriented Material

1. Shabbits, W. O., "Dynamic Fracture Toughness Properties of Heavy Section A533 Grade B, Class 1 Steel Plate," HSST Technical Report No. 13, WCAP 7623, December 1970.
2. Whitman, G. D., "HSST Program Quarterly Progress Report on Reactor Safety Programs Sponsored by the NRC Division of Reactor Safety Research for April-June 1975," Vol. II, ORNL-TM-5021, September 1975.
3. "Quarterly Progress Report on Reactor Safety Programs Sponsored by the Division of Reactor Safety Research for April-June 1974," ORNL-TM-4655, August 1974.
4. Williams, J. A., "The Irradiated Fracture Toughness of ASTM A533, Grade B, Class 1 Steel Measured with a Four Inch Thick Compact Tension Specimen," HSST Program Technical Report No. 36, HEDL-TME 75-10, June 1975.

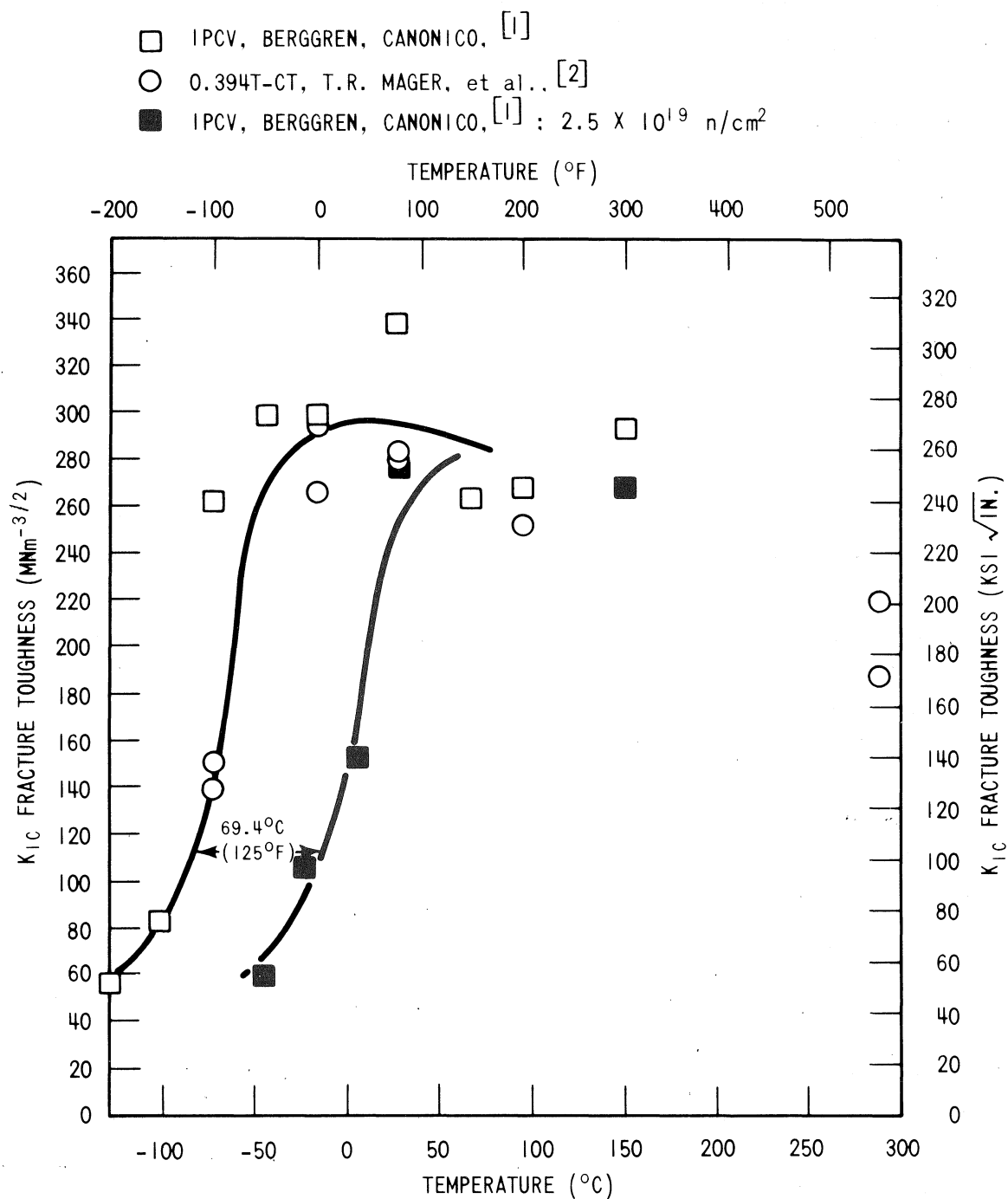


Figure 7-8. Static Irradiated and Unirradiated Fracture Toughness Properties for HSST Weldment W58-A

1. Whitman, G. D., "HSST Program Quarterly Progress Report on Reactor Safety Programs Sponsored by the NRC Division of Reactor Safety Research for April-June 1975," Vol. II, ORNL-TM-5021, September 1975.
2. "Quarterly Progress Report on Reactor Safety Programs Sponsored by the Division of Reactor Safety Research for April-June 1974," ORNL-TM-4655, August 1974.

dynamic shift. Looking at the shifts in the average 67.8 joule (50 ft lb) and 40.7 joule (30 ft lb) temperatures (table 7-1) it is seen that shifts 96.6°C (174°F) and 95.5°C (172°F) occurred respectively. This is consistent with shifts predicted by current trend curves for pressure vessel material containing 0.12 to 0.14 weight-percent copper and receiving a fluence of 2.5×10^{19} n/cm². The shift in the Charpy impact properties for the RW oriented plate material of about 96°C is slightly greater than the shift in the fracture toughness properties of 87°C (dynamic case) and 92°C (static case).

7-8. HSST Plate 02 (WR Orientation)

Figures 7-3 and 7-7 show the dynamic and static irradiated fracture toughness curves for the WR oriented plate material. Plotted on the same curves are unirradiated data of the same material and orientation. For this orientation, the shift in the dynamic average 110 MNm^{-3/2} temperature is 90°C (162°F) and the shift in the static curve is 73.3°C (132°F). The influence of additional irradiation on the dynamic fracture toughness data is negligible (figure 7-3) as was the case with the RW oriented plate material. However, in the case of the WR oriented fracture toughness results, the shift in the 110 MNm^{-3/2} temperature was 16.7°C greater for the dynamic condition than the static condition. Comparing the fracture toughness shifts of the WR oriented plate material to the shift in the Charpy V-notch impact toughness energy shifts (figure 7-5, table 7-1) at the 67.8 joule and 40.7 joule temperatures it can be seen that the 100°C (average between the 67.8 and 40.7 joule temperatures) shift in Charpy impact properties is once again greater than the shift in the fracture toughness properties but still in good agreement with the present trend curves for the copper content of plate 02. Comparing the dynamic fracture toughness results to those of the RW oriented material, it can be seen that there is little difference with respect to orientation in the fracture toughness properties of the plate (unirradiated as well as irradiated).

7-9. HSST Submerged Arc Weldment W58

The reported copper content for this weldment is very much undefined. It is reported^[1] that the copper content is between 0.16 and 0.22 weight percent. The fact is, that this copper range is not consistent with what is predicted by current trend curves. Figure 7-5 shows the shifts in the 67.8 joule and 40.7 joule temperatures for this material as 39.4°C (71°F) and 37.8°C (68°F) respectively. This degree of shift in the weldment impact properties for a fluence of 2.5×10^{19} n/cm² is characteristic of a weldment containing copper on the order of 0.08 to 0.10 weight-percent. The shift in the dynamic fracture toughness for weldment W58, as shown in figure 7-4, is 61.1°C (110°F) based on the 110 MNm^{-3/2} temperature, and about 69.4°C (125°F) for the static case based on the more limited data in figure 7-8.

1. Whitman, G. D. "HSST Program Quarterly Progress Report on Reactor Safety Programs Sponsored by the NRC Division of Reactor Safety Research," for April-June 1975, Vol. II, ORNL-TM-5021, September 1975.

Looking closer at figure 7-4, the small thickness specimen data points which represent a fluence of about 2.5×10^{19} n/cm² (same as the Charpy data in figure 7-5) appear to show a shift 11.1°C (20°F) less than the 61.1°C (110°F) shift mentioned earlier based on the 4T-CT (fluence of 4.6×10^{19} n/cm²) data. This suggests that increased irradiation resulted in further shifting of the dynamic fracture toughness of the weld material.

It is not possible to conclude, with any degree of certainty, that the weldment fracture toughness transition increased 11.1°C from additional irradiation because of three reasons. These are, first, that the RW and WR plate 02 data failed to show any significant increase in shift from additional irradiation; secondly, the large variation of the reported copper content (0.16-0.22), and may possibly be lower; and finally, scatter in data which is typical of the fracture toughness transition region.

The irradiated dynamic test results for both plate orientations and the weldment were more conservative than the irradiated static test results as was the case in the unirradiated condition.

The irradiated dynamic fracture toughness of both plate orientations and the weldment showed that the ASME Boiler and Pressure Vessel Code, Section III K_{1R} curve was, on the average, about 60°C more conservative. Figure 7-1 shows the valid dynamic fracture toughness of all three materials shifted with respect to the change in RT_{NDT} of each material based on the actual Charpy V-notch impact data in figure 7-5. Also shown on figure 7-1 is the ASME section III K_{1R} curve. It is easily noted that for this particular material, the use of the K_{1R} design curve for a fracture mechanics analysis would impose an added conservatism (in addition to the lower bound dynamic fracture results) of about 60°C in the transition region.

In summary, in determining the dynamic fracture toughness curve for irradiated and unirradiated material, the use of small-thickness (10 mm) specimens to obtain valid (based on the equivalent energy method) conservative K_{1d} data is adequate to fracture toughness values up to $88 \text{ MNm}^{-3/2}$ (80 ksi $\sqrt{\text{In.}}$). Data from the size range of specimens tested show good agreement up to this value. For characterizing the K_{1d} -versus-temperature curve from K_{1d} values of $88 \text{ MNm}^{-3/2}$ to the upper shelf initiation values, larger thickness specimens should be used. The 1.9T-CT specimen dynamic K_{1d} test results were in excellent agreement with the 4T-CT data (see figures 2-6 and 2-7) in this K_{1d} temperature region. At upper shelf temperatures, the small thickness (0.394T-CT) specimens resulted in overly conservative lower bound K_{1d} data. The use of J_{1c} testing to realistically characterize the upper shelf fracture toughness may be the solution to this problem. In all cases the valid dynamic fracture toughness results were well within the ASME Section III K_{1R} curve. In general, irradiation levels twice as high as 2.5×10^{19} n/cm² appeared to have negligible effect of the shift of the fracture toughness properties of the material.

SECTION 8

ACOUSTIC MONITORING OF 4-INCH-THICK COMPACT TENSION FRACTURE MECHANICS SPECIMENS

Westinghouse PWR Instrument Systems Development Group^[1] acoustically monitored an irradiated and a nonirradiated 4T-CT specimen during a fracture toughness test. This testing was performed as a preliminary study to determine the effect of irradiation on the acoustic emission-stress intensity factor relationships in pressure vessel grade steel. The tests were performed at the Hanford Engineering Development Laboratory in Richland, Washington, under the Heavy Section Steel Technology Program (HSST) Program.

Significantly higher levels of acoustic emission activity resulted from the irradiated sample as compared to the un-irradiated one at a given stress intensity factor (K) level. Also, the total acoustic emission counts (N) varied approximately as $K^{3.5}$ in the irradiated material while the emission from the non-irradiated one approximately follows the relationship $N \propto K^{7.3}$ (see figure 8-3), indicating a shift in the mechanism of acoustic generation during the deformation of radiation embrittled microstructure. Details of these tests and the results follow.

8-1. BACKGROUND

Since late in 1972, Westinghouse NES has been involved in a program of testing A533B pressure vessel steel under PWR conditions to determine the relationship that exists between acoustic emission (AE) activity and the magnitude of the stress intensity factor, K, of the crack emitting the sound. Acoustic emission is the stress waves generated when material undergoes deformation and/or fracture. The monitoring of acoustic emission offers a convenient means of monitoring the stress intensity factor "K" of a growing flaw since the plastic zone (the region of acoustic activity) appears to bear a direct relationship to "K." By establishing such a relationship, it is possible to determine flaw growth by monitoring the surface of the specimen with acoustic sensors and appropriate electronic instrumentation.^[2,3] This report describes preliminary studies conducted by Westinghouse to determine the effect of irradiation on the generation of acoustic emission in pressure vessel

-
1. G. V. Rao, and J. Craig, Westinghouse PWR Instrument Systems Development performed the testing and evaluation for results presented in this section.
 2. Gopal, R., "Acoustic Emission Technology for Pressure Boundary Integrity." NES Status Report, WCAP-8240, January 1974
 3. McLoughlin, V. J. and Craig, J., "An Evaluation of the Acoustic Emission Response of A533 Grade B Steel Under Fatigue Loading Conditions," W Research Report 74-7P6-EVMTL-R2, June 1974

grade steel and to determine acoustic emission-stress intensity factor relationships in radiation embrittled microstructures. Acoustic emission was used to monitor fracture toughness tests on 4T compact tension (CT) samples in the preirradiated and post-irradiated condition, at the Hanford Lab, Richland, Washington, under the Heavy Section Steel Technology (HSST) program.^[1] Earlier studies^[2] on this material indicated that a pronounced increase in yield strength occurs as a result of radiation to fluences of approximately 2×10^{19} n/cm² ($E > \text{Mev}$), above which the yield strength increases linearly with fluence at a more gradual rate. Irradiation fracture embrittlement results in a shift of the K_{1c} toughness transition curve to higher temperatures. This suggests that a higher level of emission activity could be expected at a given K level due to the embrittlement of the material. The results of this preliminary study will be discussed in this report.

8-2. INSTRUMENTATION AND TEST SETUP

Two sensors were mounted with a spring-loaded mounting fixture on the back of the specimen, one sensor 1.5 inches from the top and the other 1.5 inches from the bottom. The acoustic emission received by these sensors was sent via cable through a 3-foot lead-shielded wall to amplifiers which amplify the signal detected by the sensors to a usable level, and to discriminators where the analog signal is converted to digital pulses. These pulses were then fed to a rate-meter where the pulses could be counted and converted to a calibratable level for subsequent recording on a Hewlett Packard strip chart recorder, Hewlett Packard X-Y recorder, and a Tektronix oscilloscope (see figure 8-1).

The test setup and operation of the test was the responsibility of J. A. Williams, Senior Research Engineer, Westinghouse Hanford Co. The test stand was enclosed in a lead shield hot cell to protect personnel from the radiation hazard caused by the irradiated specimen. The specimen was housed in a furnace mounted on the test stand and heated to 93.3°C (200°F). To monitor the temperature, thermocouples were placed at various locations on the specimen, readout on a Digital Thermocouple Meter and recorded on a Honewell Strip Chart Recorder. The output of the mounted clip gages, mounted on the opening face of the specimen, was recorded along the y-axis. Load time and stroke time were also recorded on a two-channel

-
1. Davidson, J. A., "Fracture Toughness Characterization of Irradiated ASTM A533, Grade B, Class 1 Steel Using Compact-Tension Specimens," *Quarterly Progress Report on Reactor Safety Programs Sponsored by the NRC Division of Reactor Safety Research for April-June 1975*, ORNL-TM-5021, Vol. II, pp 22-24, September 1975
 2. Williams, J. A. and Hunter, C. W., "Irradiation Strengthening and Fracture Embrittlement of A533-B Pressure Vessel Steel Plate and Submerged-Arc Weld," in *Effects of Radiation on Substructure and Mechanical Properties of Metals and Alloys*, ASTM STP 529, pp 5-16, Am. Soc. for Testing and Materials; 1973

strip chart recorder. General test data information on the irradiated sample is included in table 8-1, while a detailed account of the past test data can be obtained from reference 1.

8-3. TEST RESULTS AND DISCUSSION

Both tests used the same instrumentation and setup, and care was taken to ensure that the same discriminator and amplifier gain settings were used in both cases. The first test utilizing a non-irradiated 4T-CT sample was run at 20°C (68°F) to serve as a base line in determining the changes in the fracture toughness and acoustic emission data relative to the data from irradiated sample. The non-irradiated specimen failed at $81 \times 10^3 \text{ kg}$ ($190.0 \text{ MNm}^{-3/2}$)^[1] at a displacement of about 2.03 mm. Figure 8-2 illustrates the acoustic emission from the two transducers (channels 1 and 2) as a function of stress intensity factor, on a linear scale while figure 8-3 represents the same data on a logarithmic plot. Counts during this unirradiated test were generally low and the amplitude of the acoustic bursts was only about 1 volt peak to peak. The test was quiet up to a K value of about $44 \text{ MNm}^{-3/2}$. The second test, which was run on an irradiated 4T-CT specimen, provided vital data since very little work has been reported in the past on the acoustic emission response from the deformation in radiation embrittled micro-structures.

The variation of acoustic emission counts as a function of stress intensity factor for the irradiated sample is also shown in figures 8-2 and 8-3. The specimen failed at a K value of $88.0 \text{ MNm}^{-3/2}$ ($80 \text{ ksi } \sqrt{\text{In.}}$) indicating pronounced decrease in fracture toughness due to the effect of radiation embrittlement. Significantly higher levels of acoustic activity both in total count level and in amplitude in comparison with the emission from the non-irradiated sample have been observed. This is apparent in the comparative plots in figures 8-2 and 8-3. The change in the mode of deformation accompanying flaw growth in the radiation embrittled sample is indicated by the difference in the slopes of the data lines from the two samples as shown in figure 8-3. The total acoustic counts (N) varied approximately as $K^{3.5}$ during flaw growth in the irradiated sample while the emission from the non-irradiated one followed a $N \propto K^{7.3}$ relationship. It should be noted that the irradiated specimen was tested at 93.3°C (200°F), a temperature characteristic of the pre- K_{1c} vs temperature transition temperature where cleavage controlled fracture occurred. The unirradiated specimen was tested at a post transition temperature where larger amounts of plasticity are involved with the fracture process.

1. Williams, J. A., "The Irradiated Fracture Toughness of ASME A533, Grade B, Class 1 Steel Measured With a Four Inch Thick Compact Tension Specimen," HSST Program Technical Report No. 36, HEDL-TME-7S-10, June 1975

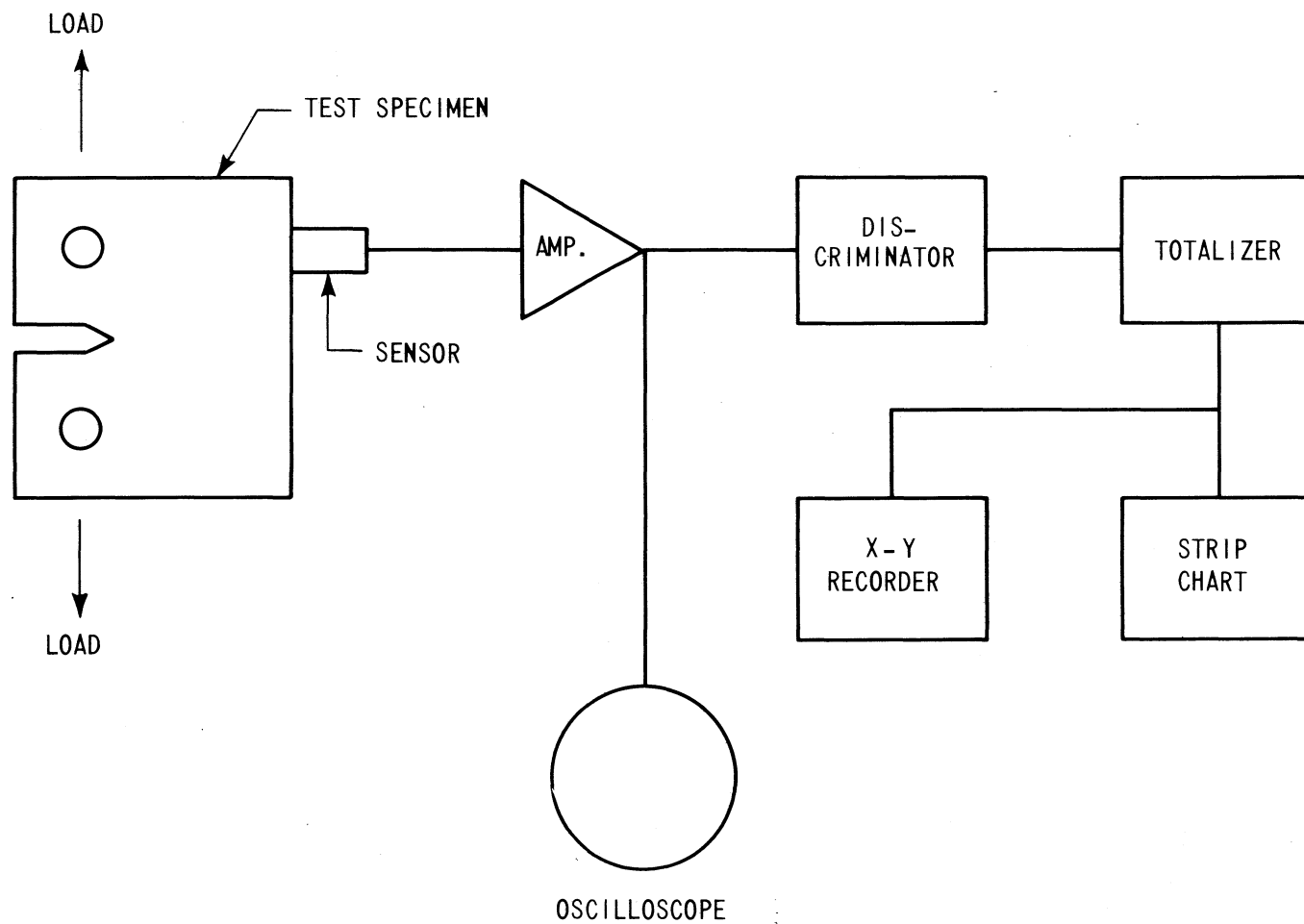


Figure 8-1. Acoustic Test Instrumentation

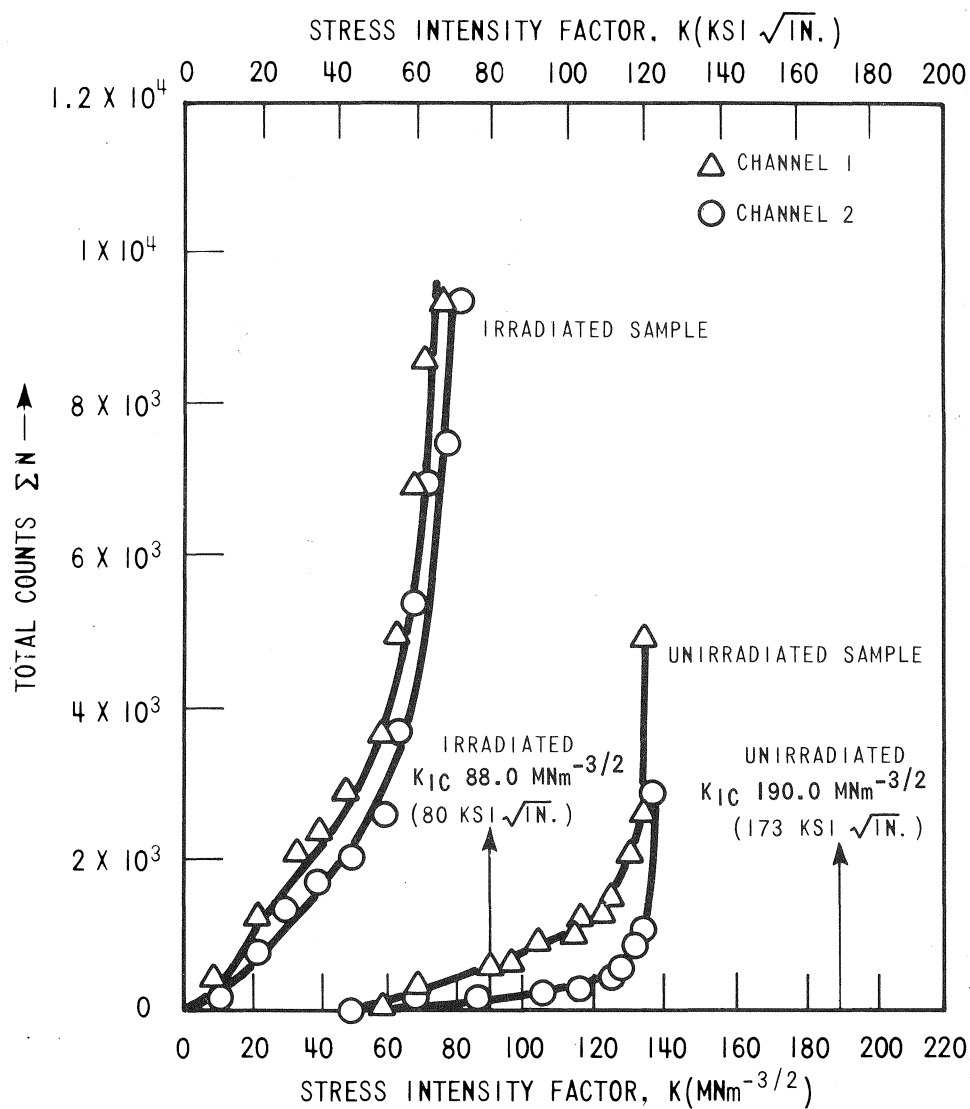


Figure 8-2. Acoustic Emission from Flaw Growth in Irradiated and Unirradiated 4T-CT Samples. Plotted as a Function of Stress Intensity Factor "K" (Linear Plot)

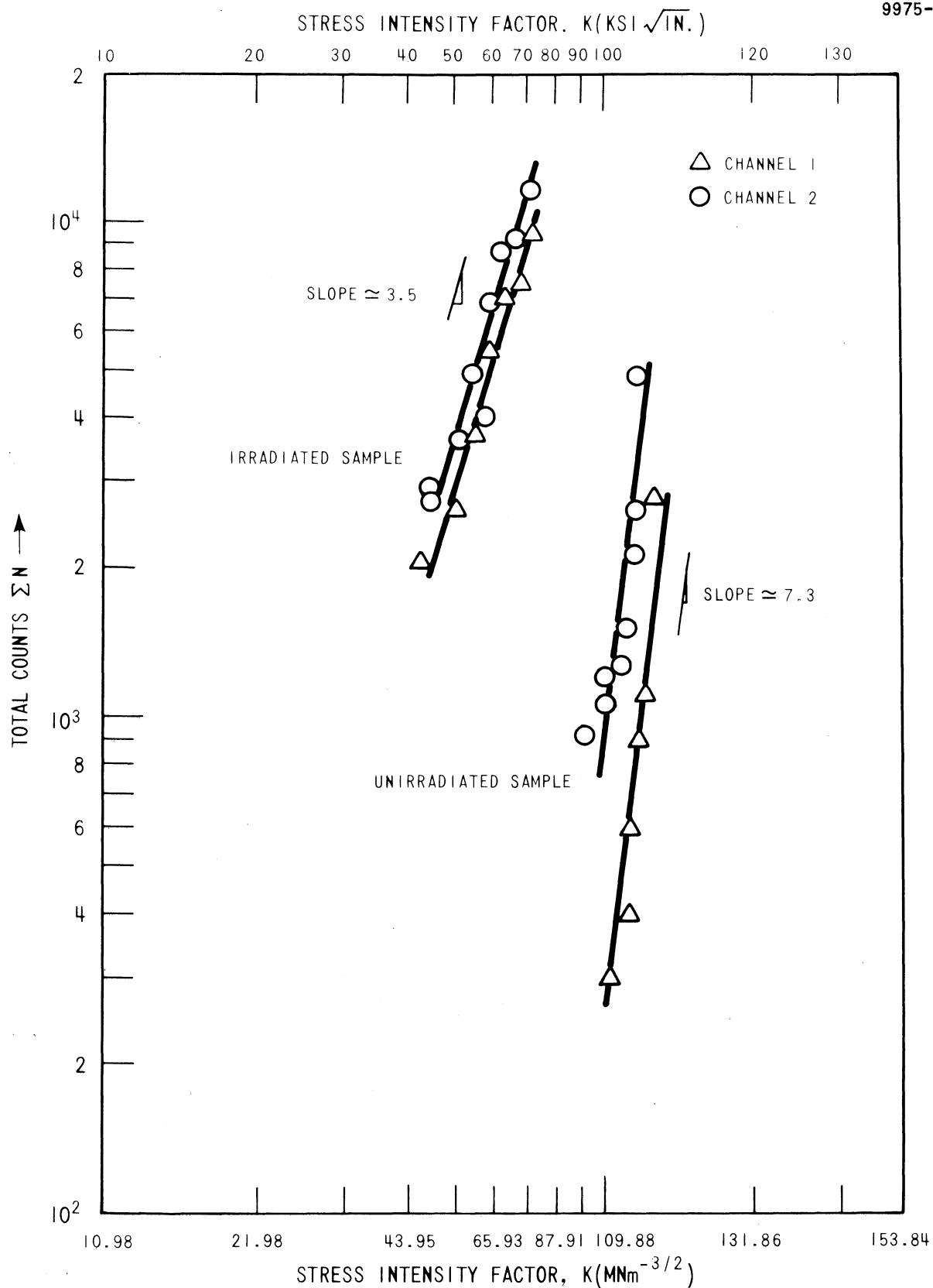


Figure 8-3. Acoustic Emission from Flaw Growth in Irradiated and Unirradiated 4T-CT Samples. Plotted as Function of Stress Intensity Factor "K" (Logarithmic Plot)

TABLE 8-1
GENERAL TEST DATA
FOR THE IRRADIATED ACOUSTIC TEST

Specimen No.	W58-4
Fluence ^[a] (E > 1 Mev)	
Distance from face, mm:	
13.2	3.98×10^{19} n/cm ²
32.0	3.48×10^{19} n/cm ²
50.8	3.38×10^{19} n/cm ²
69.6	3.46×10^{19} n/cm ²
88.4	3.94×10^{19} n/cm ²
Irradiation Temperature	287.8°C ^[b] (550°F)
Test Temperature	93.3°C (200°F)
Rate of Loading, K	0.93 MNm ^{-3/2} /sec.
Load at Fracture:	41101 kg
Clip Gage Displacement at Fracture	1.179 mm
Crack Length:	104.37 mm
Fracture Toughness	88.0 MNm ^{-3/2} 80 ksi $\sqrt{\text{In.}}$

- a. Williams, J. A., "The Irradiated Fracture Toughness of ASTM A533, Grade B, Class 1 Steel Measured With a Four Inch Thick Compact Tension Specimen," HSST Program Technical Report No. 36, HEDL-TME-75-10, June 1975.
- b. Williams, J. A. and Hunter, C. W., "Irradiation Strengthening and Fracture Embrittlement of A533-B Pressure Vessel Steel Plate and Submerged-Arc Weld," in *Effects of Radiation on Substructure and Mechanical Properties of Metals and Alloys*, ASTM STP 529, pp 5-16 American Society for Testing and Materials; 1973

Acoustic activity from the irradiated specimen was persistent with stress intensity (K) up to K_{1c} . The activity from the unirradiated specimen, although increasing steadily with K , quieted down before reaching K_{1c} .

Acoustic generation in this type material has been observed previously^[1] to be predominately characteristic of yielding rather than work hardening. Therefore, the difference in acoustic emission between the irradiated and unirradiated tests can be attributed in part to less fresh yielding being associated with the plasticity at $K = K_{1c}$ of the unirradiated specimen. The irradiated specimen was tested at a temperature, 20°C , where much less plasticity but more fresh yielding is involved with the fracture process, thereby resulting in a higher total acoustic count (figure 8-2) as would be expected.

It should be noted that the irradiated specimen was tested at 93.3°C (200°F), a temperature where cleavage controlled fracture occurred, while the unirradiated specimen was tested at 20°C (68°F), a temperature where larger amounts of plasticity are involved in the fracture process.

1. T. Ingham, et al, "Acoustic Emission Characteristics of Steels," Int. J. Pres. Ves. and Piping (2) 1974 p.31-50.

SECTION 9

CONCLUSIONS

From results of this test program, it was concluded that:

- Dynamic K_{1d} fracture toughness test results on the irradiated HSST plate 02 and Weldment W58A material were more conservative than the irradiated static K_{1c} data in the fracture toughness transition temperature range.
- There is a negligible effect of specimen orientation on the irradiated K_{1d} fracture toughness for HSST plate 02 material.
- Irradiation levels up to twice as great as 2.5×10^{19} n/cm² ($E > 1$ Mev) resulted in a negligible increase in the shift of the dynamic fracture toughness properties of both the plate and weldment material.
- The larger thickness K_{1d} fracture toughness test results, valid with respect to the equivalent energy analysis, showed that the upper shelf K_{1d} values for the plate 02 and weldment W58A material were in excess of $220 \text{ MNm}^{-3/2}$ ($200 \text{ ksi } \sqrt{\text{in.}}$) and therefore in compliance with the ASME section III K_{1R} curve.
- The Charpy thickness specimen upper shelf K_{1d} tests resulted in overly conservative upper shelf K_{1d} values due to the limited measuring capacity of this size specimen and ambiguities associated with crack initiation at upper shelf temperatures.
- Charpy thickness K_{1d} data were in good agreement with the larger specimen K_{1d} results up to about $88 \text{ MNm}^{-3/2}$ ($80 \text{ ksi } \sqrt{\text{in.}}$).
- Due to ambiguities associated with crack initiation at upper shelf K_{1d} temperatures, J_{1c} testing should be performed to establish the upper shelf fracture toughness of the material since the use of the equivalent energy analysis fails to account for subcritical crack growth prior to maximum load at these temperatures.
- Evaluation of the valid and invalid K_{1d} data suggests that the K_{1d} -versus-temperature curve can be divided into three regions, each region having its own requirements

as to what type of test specimen and size should be used to realistically produce a valid, conservative fracture-toughness-versus-temperature curve.

- Significantly higher levels of acoustic emission activity resulted from the irradiated sample (tested at 93.3°C) as compared to the unirradiated one (tested at 20°C) at a given stress intensity factor (K) level.
- The total acoustic counts (N) as a function of stress intensity (K) appear to be related to the nature of plasticity involved in the fracture process.